UNIVERSITY OF STRATHCLYDE

"STAGE-STRUCTURED INSECT POPULATION MODELS OF LARVAL COMPETITION"

by

A E JONES

DEPARTMENT OF APPLIED PHYSICS

Thesis submitted in partial fulfilment of the

Degree of Doctor of Philosophy

ABSTRACT.

The work presented in this thesis is in two sections. In Section I a detailed stage-structured model of Lawton's Plodia (Gurney,Nisebt and Lawton, 1983) is presented. This work suggests the follow-up study of Section II in which stability and cycle periodicity are investigated for a class of strategic models of larval competition.

The model of the dynamics of Plodia is based on a set of pre-publication data made available by Dr.J.H.Lawton. Factors responsible for regulation of the experimental populations are considered, these are shown to be larval competition (both for food and by interference) which acts to vary larval survival, and cannibalism of eggs by larvae. It is shown that as a first approximation, female fecundity may be taken to be constant.

The dynamics of all stages with the exception of the larval stage are specified. Within the larval stage, two indices of development and two functional forms of the per capita death rate are considered, yielding a suite of four models. Numerical solutions show the functional form of the per capita death rate may dramatically affect the dynamic behaviour. While two models which consider a per capita death rate incorporating the idea of larval 'food reserves' yield fluctuations braodly similar to those of Plodia, the period to delay ratios consistently exceed those of the experimental populations over a whole range of parameter values. As it is known that female fecundity is dependent upon emergence weight, a further model incorporating this mechanism is considered. It is shown that weight-dependent fecundity can have no significant effect on the long-term dynamics, and does not reduce the period to delay ratio. Further analysis of the data shows that Plodia larvae also compete by depositing 'junk' (faeces, silk) whose presence acts to increase the larval development period.

As the suite of Plodia models do not include this type of competition, and fail to properly reflect the development of Plodia larvae, a class of strategic models are considered in Section II to determine how the type of competition or choice of larval development index may influence stability and the period to generation time ratio. Models are considered in which the sole means of population regulation is via variations in the larval maturation period due to competition. To investigate cycle periodicity, a technique is developed to evaluate period to delay ratios near stability boundaries for systems of delay-differential equations. This technique is applied to two general classes of model; it is shown that the period to generation time ratio is always smallest for interference competition, and that the choice of larval development index cannot significantly affect this ratio.

Three specific competition models are considered; in each competition is assumed to occur in one of the three ways found in Plodia larvae. It is shown that neither the manner nor the intensity of competition can have any significant effect on stability or the size of the period to generation time ratio.

Acknowledgements.

I would like to take this opportunity to thank the following people : Dr. Bill Gurney and Professor Roger Nisbet for their encouragement and faultless supervision during my studentship, Steve Blythe for friendship and many helpful conversations, Pete Maas for much appreciated help with the computers, Professors Edward Eisner and Gordon Donaldson for providing a favourable working environment, the Science and Engineering Council for my grant, and my family for their support. Last but not least, I would like to thank the staff and students of the Department of Applied Physics, in particular Steve Blythe, Steve Evanson and Rhoddy Bain, for help, advice and mral support when I needed it.

CONTENTS

CHAPTER ONE

Chapter 1 : Introduction.

1.1 Preamble

In many species, reproductive adults commonly replace themselves with large numbers of offspring, and the potential capacity for increase of a population is enormous (e.g. Darwin (1859) estimated that 2 elephants could give rise to 19 million in 750 years). Such increases are seldom achieved in nature, but are resisted by many factors (unfavourable climate, predation, parasitism, disease, or shortage of essential resources). In many species, the high potential rate of increase is counterbalanced by high mortality in the pre-adult stages of the life-cycle - for example, frogs and toads lay thousands of eggs, many fish produce millions, yet few of these will survive to adulthood.

The study of natural populations is confounded by interactions with a variable and complex environment. In contrast, laboratory populations may be studied in isolation where disease, predation and climatic variations may be eliminated and ideal food provided. However, it is clear that even under such favourable conditions, unlimited growth of the population is not possible and must eventually be countered by competition amongst individuals for food or space. In such populations, regulation is density-dependent, that is, it

it is the size of the population in a given area which is the underlying cause of the reduction and ultimate prevention of further population growth. It is clear that regulation must occur by a reduction in fecundity or an increase in pre-adult mortality or some combination thereof at high densities.

Insects are commonly used in laboratory population studies where they may be cultured cheaply and, as many have short lifetimes, studied over several generations. In one particular class of insects, those with non-feeding adults, it is clear that any variations in fecundity must have occurred as a result of variations in the quantity or quality of food consumed as a larva. Thus, in such laboratory populations which are maintained by a regular supply of food, it is what happens to individuals in the pre-adult stages of the life-cycle which prevents unlimited growth of the population - a process which, as remarked earlier, commonly occurs in nature.

The most direct effect of density is the death of individuals in the crowded stage. A common source of mortality in many insect species is the reduction of larval survival in response to a decrease in the amount of food available (Peters & Barbosa, 1977). It is the consideration of how larval competition for food may act to regulate the population and its effect on the dynamics

of insects in culture which is the subject of this thesis.

1.2 Modelling insect populations

Many insect populations in which regulation is maintained by density-dependence in the pre-adult stages of the life-cycle may exhibit quasi-cyclic behaviour with cycle periods of a length comparable to the generation time (e.g. Nicholson's (1954) larval food limited blowfly cultures, with population 'peaks' every 2-3 generations, Lawton's Plodia (Gurney, Nisbet and Lawton, 1983), which exhibit quasi-cyclic population fluctuations with a period 'one and a bit' times the maturation delay). Understanding how such cycles may arise deterministically requires knowledge of the age-structure of the population and in particular of how vital rates may depend upon age. Indeed, any population model in which regulation occurs at one or more stage of the life-cycle must necessarily take account of age-structure.

A recent development in the modelling of age-structured populations is the use of 'stage-structured' models. The formulation and use of such models has been frequently described (Nisbet & Gurney 1983, Gurney, Nisbet and Lawton 1983, Gurney & Nisbet 1985, Nisbet & Gurney 1985, Nisbet, Blythe, Gurney and Metz 1985, Nisbet & Gurney 1985, Gurney, Nisbet and Blythe 1986,

Crowley, Nisbet, Gurney and Lawton 1987), here we give a brief description.

Stage-structured models rely on the assumption that the life-history may be divided into a number of separate stages of chosen duration, within which all individuals may be regarded as identical. Such an assumption is particularly appropriate when considering insect populations; during development from eggs into adults, insects progress through a number of distinct easily recognizable stages (e.g. Borror & De Long, 1954) and although identification of the age of an individual within a given stage is sometimes possible, the technique used usually requires the death of that individual (Southwood, 1966). The advantage of being able to choose stages of arbitrary duration is important in practical modelling; this permits model stages to be closely identified with the various stages of insect development, which are rarely of equal duration.

A second requirement of stage-structured models is the definition, for each stage, of a stage development index (Gurney et al, 1985), which is a unique measure of the state of development (or 'physiological age') of an individual within the stage. The transition of an individual from one stage to the subsequent stage will commonly occur upon the attainment of a given increment in development index (e.g. upon attaining a given age or

weight increase). [Natural variation between individuals frequently results in an observed distribution of maturation periods; such an effect may, under suitable conditions, be incorporated into the model by assuming that there is a distribution of indices at which maturation is possible (Blythe et al 1984, Gurney et al, 1986), also Appendix A.]

As a result of these assumptions the underlying continuity equation for the stage development index distribution (a partial differential equation) which governs the dynamics of a given stage may be reduced to ordinary delay differential equations in easily measured quantities such as stage population, duration and survival.

Equations describing the dynamics of the population as a whole consist of a set of coupled delay differential equations; the delays represent stage durations and may themselves, in the case of a development index other than age, be time-varying. Such equations are parameter sparse and may be easily solved numerically (Gurney et al, 1983). Careful "lumping together" where appropriate of insect developmental stages and treating these as a single model stage (e.g. Crowley et al (1987) use three model stages to represent the egg and 9-15 larval instar stages of damselflies) enables the complexity of the model to be adjusted to a level comparable with the

quantity of data available.

Stage-structured models have already been successfully used both to model laboratory and field populations and as "strategic" models. As discussed earlier, they prove particularly suitable when modelling insect populations; it is this type of model which we shall be using throughout this thesis.

1.3 Overview of the thesis

We propose, through the construction and analysis of stage-structured models, to study the ways in which density-effects in the pre-adult stage of insect laboratory cultures (in particular competition for limited food) act to regulate such populations. We consider populations with non-feeding adults in which food (utilized only by larvae) is supplied at a constant rate. In particular, we wish to identify any factors which may influence the dynamics of the population.

Regulation of such populations occurs as a result of changes in fecundity/mortality in response to variations in density. A recent review (Peters & Barbosa, 1977) of density effects on insects in culture shows that such processes may occur in a wide variety of often species-specific ways; moreover it is likely that for any given species a number of separate mechanisms combine to

regulate the population. Even were larval competition for food to be solely responsible for regulation, the mechanism(s) whereby food shortage may influence the overall population growth are many.

It is clear that no single model, or even a class of models, could possibly incorporate either the variety of ways or the mechanisms in which regulation may occur. It is for this reason that we begin by considering one particular population - that of the Plodia cultures mentioned earlier. The sole 'external' limiting factor during these experiments is the supply of food, so that larval competition for food will certainly contribute towards regulation of the population.

These populations have a large capacity for increase and regulation is rapidly established (an initial adult population of 30 gives rise to a population 'peak' numbering ≈ 300 adults a generation later; thereafter the population fluctuates between ≈ 10 and 80 adults). We present, in Section I (Chapters 2-6) a detailed model of these populations.

Through this study of Plodia we are able to identify a number of factors which may influence the dynamics (of Plodia) and also find a number of problems which may commonly arise in the modelling of laboratory insect populations. As a direct result of the study of Plodia,

we are lead to question how the larval development rate and the manner of competition, (we shall for example distinguish between competition for food and interference competition) may in general influence the dynamical behaviour of models of larval competition; this forms the basis for the work presented in Section II.

1.4 Introduction to Section I.

Plodia interpunctella (Hubner) acquired its common name, the Indian meal moth, as it is a common pest of meal made from Indian corn, or maize. It was first recorded as a pest of economic importance by Chittenden (1894). Plodia occurs worldwide and infests a variety of stored products; it occurs sporadically in warehouses in Britain (Williams, 1964). Plodia has also been used in the laboratory as a host for breeding the parasite Microbracon brevicornis Wesm (Ullyett, 1933). Thus, understanding the population dynamics of Plodia in a controlled environment is of itself important - both in order to enable laboratory stocks to be maintained at optimum density and necessary before embarking on any study of naturally occurring populations with the inevitable interactions between Plodia and environmental variation.

The life-cycle of Plodia has been described in detail by Reyes (1969), Williams (1964), Tzanakakis (1959);

Benson (1973) reviews its biology along with that of three of the commoner Lepidoptera infesting stored products with particular reference to those aspects which may influence its population dynamics. Here, we give a brief summary.

Adult moths mate soon after emergence, oviposition begins almost immediately and is usually completed within about 5 days. Adult moths do not feed, and live for about a week. Eggs hatch within about 3-4 days, although this does depend on temperature (Adler 1960, Cline 1970). First instar larvae begin to feed immediately upon hatching; fully grown larvae may enter a wandering stage to search for pupation sites (Podoler 1974). The pupa is usually enclosed in a slight cocoon, from which adult moths emerge.

There are several density-dependent factors which can affect the development and mortality of these moths. Egg mortality may be enhanced by cannibalism by larvae (Benson, 1973). Larval mortality arises predominantly from increasing larval numbers per unit food available (Snyman, 1949, Podoler, 1974); crowding may also reduce larval size (Benson, 1973) and extend the development period (Williams, 1964). A shortage of suitable pupation sites may also affect the body weight of wandering larvae (Podoler, 1974). Female fecundity may be affected by several factors. Snyman (1949) showed

that the adult population density can affect the number of eggs laid, probably due to mechanical interference, although this was only shown for extremely high adult densities. It has also been shown that the fecundity of a female increases with her size (Snyman, 1949) or weight (Podoler, 1974) at emergence. Density-dependent regulation will be discussed further in Chapters 3 and 4.

1.4.1 The Model

We shall base our model of a laboratory population of Plodia on a set of pre-publication data made available by Dr J.H. Lawton, York University. These experiments consist of a number of 'cohort experiments' designed to measure specific aspects of the life-cycle, and long-term cultures of Plodia in which the supply of food is limited. These experiments and data are described fully in Chapter 2.

Adult moths do not feed, so that during the long-term "continuous" (CTS) experiment, competition for food will occur between larvae. The data show that after an initial transient, the population size fluctuates with a period which is slightly in excess of the generation time, but which is significantly smaller than the minimum possible under delayed regulation. Gurney, Nisbet & Lawton (1983) considered a strategic model of larval competition with parameters appropriate to these

CTS experiments, and found that a uniform competition model yielded fluctuations with a period roughly that of Plodia populations, whereas a cohort competition model yielded cycle periods far greater than those observed. As a result of these studies, we shall assume in our model that each larva competes equally with all other larvae.

As discussed earlier, we shall be using a stage-structured model. Any model which is to reveal factors responsible for population fluctuation and regulation must necessarily consider the whole life-cycle. Thus, our model must take account of the four distinct developmental stages (egg, larva, pupa, adult) of Plodia.

In Chapter 2, we make a number of modelling approximations which capture general features of the data of many of the cohort experiments, while ignoring natural variability. These approximations, which we shall include in our model, show that certain characteristics of individuals in given stages are time- and density-independent.

1.4.2 Population Regulation

It is essential to identify factors responsible for regulation of the population, as these must be included in our model. This is the subject of Chapters 3 and 4:

in Chapter 3 we discuss factors responsible for population regulation, in Chapter 4 we deal with the mechanisms whereby such factors act to regulate the population.

Population regulation implies that vital rates in one or more of the stages must be time-dependent. The Outline Model developed in Chapter 2, (based on data of many of the cohort experiments) shows that the only quantities which may be time dependent are the egg-survival, larval survival and adult fecundity. Evidently a major source of regulation will be the limited supply of larval food. In Chapter 3 we show, by considering the likely sizes of the three quantities which may be time-dependent under conditions of the CTS experiment, that competition for food amongst larvae is not sufficient to account for regulation of the CTS experiment populations. We show that there must also be a significant amount of 'self-regulation' via cannibalism of eggs by larvae and by direct interference between larvae (which will result in reduced larval survival), and that as a first approximation we may take adult fecundity as constant.

The detail of the mechanisms whereby egg cannibalism, larval competition for food and by direct interference act to regulate the population are discussed in Chapter 4. We present numerical solutions to equations governing the behaviour appropriate to our models in Chapter 5;

these numerical solutions correspond to initial conditions appropriate to the CTS experiment. In Chapter 6, we consider the effect of introducing weight-dependent fecundity into our model.

SECTION I

STAGE-STRUCTURED MODELS OF THE POPULATION DYNAMICS OF *PLODIA INTERPUNCTELLA*

CHAPTER TWO

Chapter 2: The Plodia Experiments and an 'Outline Model'

Experiments carried out by Dr John Lawton at York University comprise a set of cohort experiments which investigate specific aspects of the life-cycle of the Indian meal moth *Plodia interpunctella* (Hubner), and a set of 'continuous experiments' which measure the size of the adult population of a closed community of moths over a period of 2 years. These experiments form the basis of our model of the population dynamics of *Plodia*.

We use a stage-structured model, which we wish to be as simple and parameter sparse as is feasible. This necessitates interpreting the experimental data with a view to making suitable modelling approximations, which will incorporate general features of the population dynamics while simplifying the (model) detail.

In this Chapter, we describe the *Plodia* experiments; data from these experiments suggest a number of such modelling approximations, from which we derive an 'Outline Model'.

2.1 The Experiments

All experiments were carried out at a temperature of 28^{0}C and 80% RH in continuous illumination. Experiments in which larvae were present (adult moths do not feed) were duplicated:- one experiment provided larvae with a food

mixture made up of 70g bran per 25ml glycerine, the second provided larvae with a mixture made up of 27g bran, 25ml glycerine, 20g yeast and 6g flour. We refer to these food media as BG and BGYF respectively. Weights of adult moths are in dry mg.

(1) Adult Survival (AS)

To measure adult survival, batches of newly-emerged adults were isolated. Each day, any dead adult moths were collected, weighed and sexed. Figs. 2.1 shows the survival curves; adults are classed according to sex and weight. It can be seen that adult weight does not appear to affect survival, while adult females live slightly longer than adult males.

(2) Adult Fecundity (AF)

Experiments to determine the egg-laying capacity of adult females isolated pairs (1 male, 1 female) of newly-emerged adults. The number of eggs laid each day by each female were noted. Fig. 2.2 shows the total number of eggs laid by a female plotted against her weight after death; Fig. 2.3 shows the number laid plotted against female age at oviposition. It can be seen that egg-laying behaviour varies greatly between individuals, with adult females laying between 2 and 193 eggs; the number of eggs laid is not correlated with female weight.

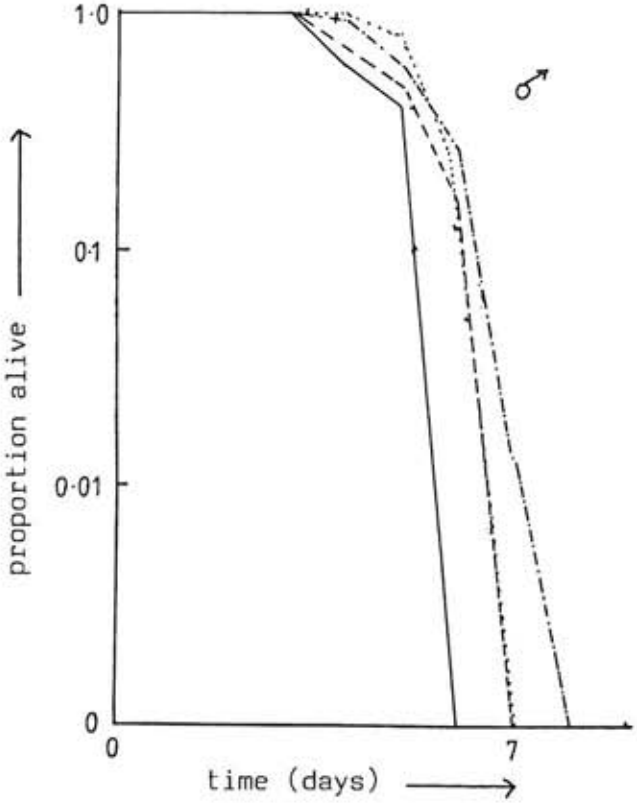
1·0
0·1
0·01
0
proportion alive
0
7
time (days)
♂

(a)

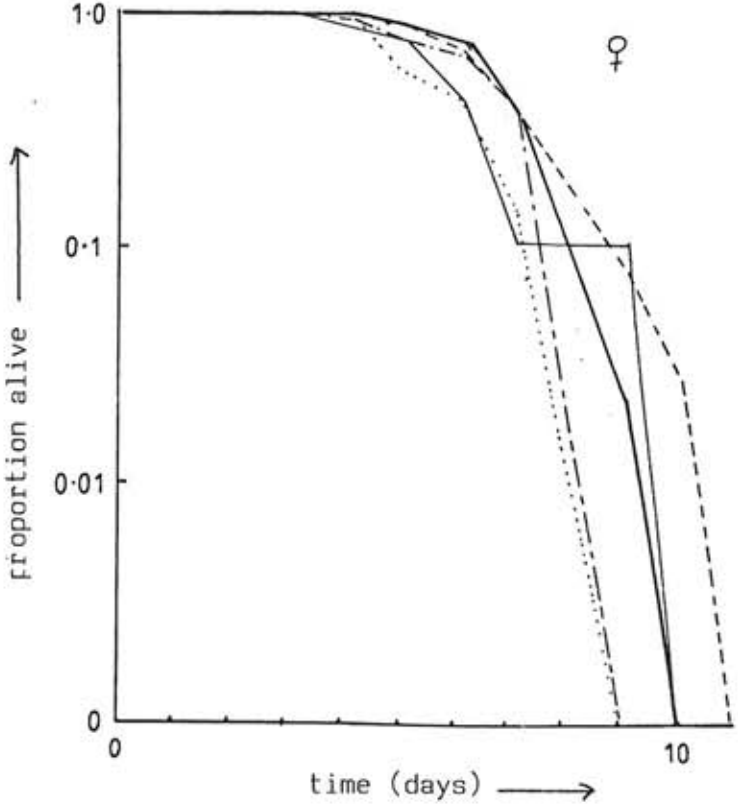
1·0
0·1
0·01
0
proportion alive
0
10
time (days)
♀

(b)

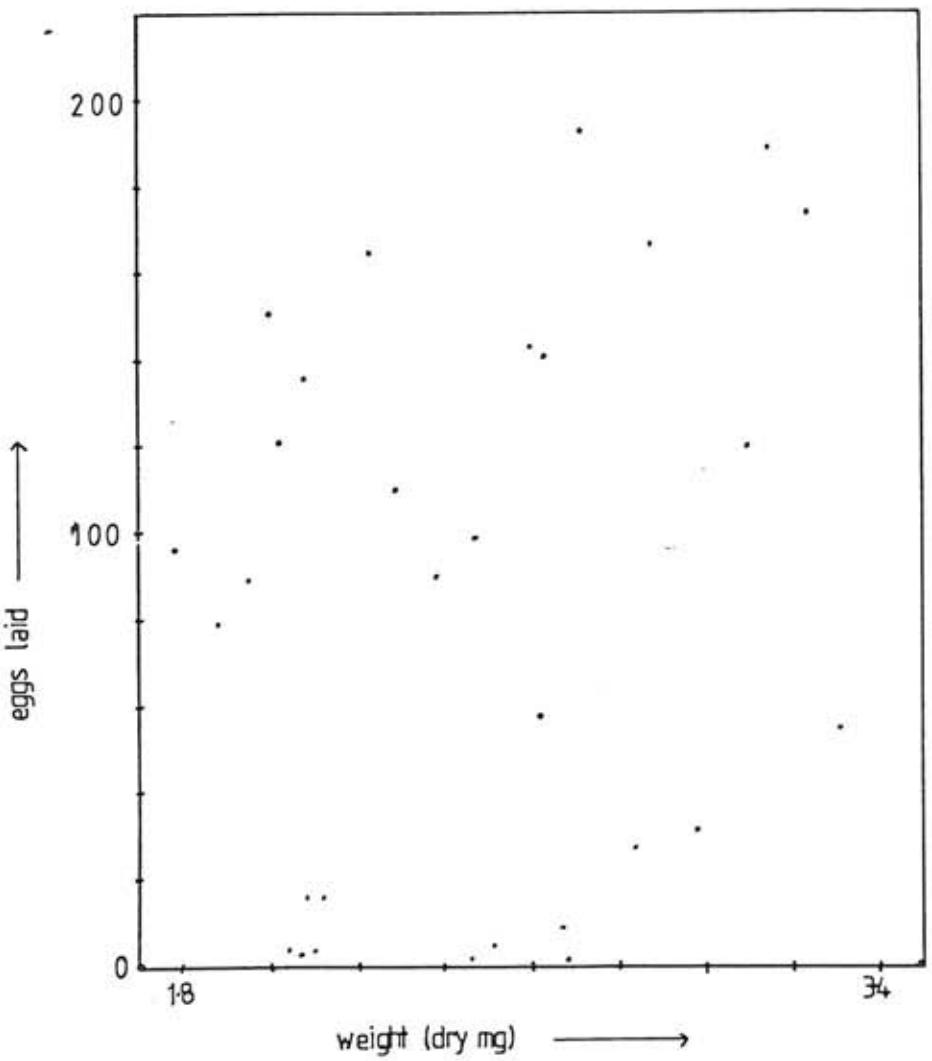

Figure 2.2 (AF experiment).

Number of eggs laid by an adult female plotted against her weight after death.

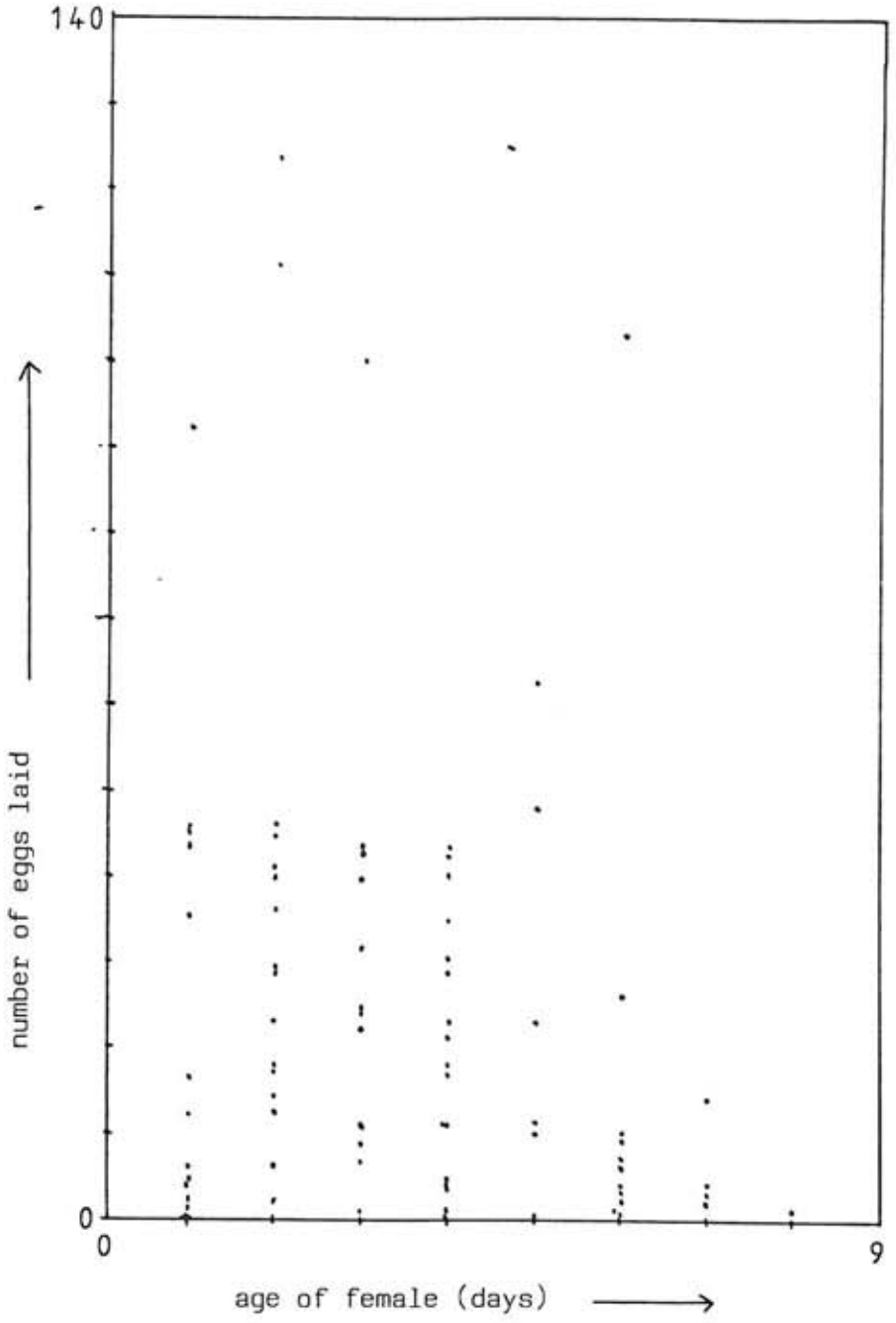

Figure 2.3. (AF experiment).

Number of eggs laid plotted against female age at oviposition.

Fig. 2.3 shows that all eggs had been laid by day 8, with most females producing most of their eggs by day 6.

(3) Egg Hatch (EH)

To measure the effect of female age on the percentage of eggs to hatch, a batch of newly-emerged adults were isolated; eggs were collected each day and allowed to hatch. Fig. 2.4 shows the proportion of eggs which hatch plotted against female age at oviposition. Again, there is a great deal of variation in the proportion of eggs which hatch; we note that approximately half the eggs laid by day 6 hatch.

(4) Adult Emergence (AE)

This experiment measures the egg to adult development time. Newly-laid eggs were collected and placed in a large container of food - the experiment was conducted for each of the food media BG and BGYF. Emerging adults were removed and counted each day. Fig. 2.5 shows the proportion (of the total) to emerge each day for each experiment. It can be seen that adults emerge after a development period of 22-40 days (BGYF) or 24-40 days (BG). There is no given (constant) development period, evidently natural variation between individuals causes an observed distribution of maturation periods in one or more stages of the life-cycle. It can be seen that the

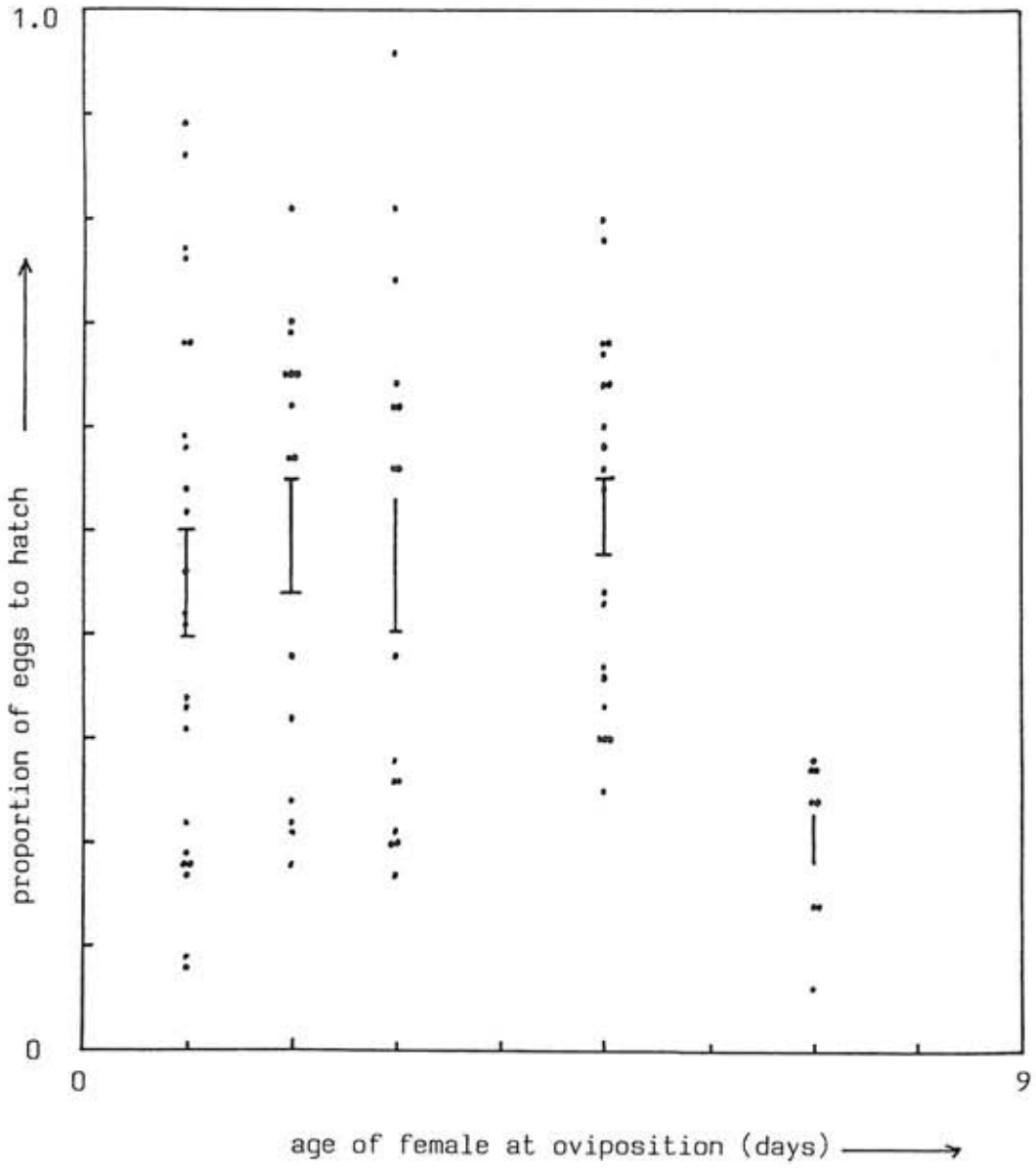

Figure 2.4. (EH experiment).

Proportion of eggs to hatch which were laid by an adult female of given age.

Error bars indicate excursins of 1 standard error from mean.

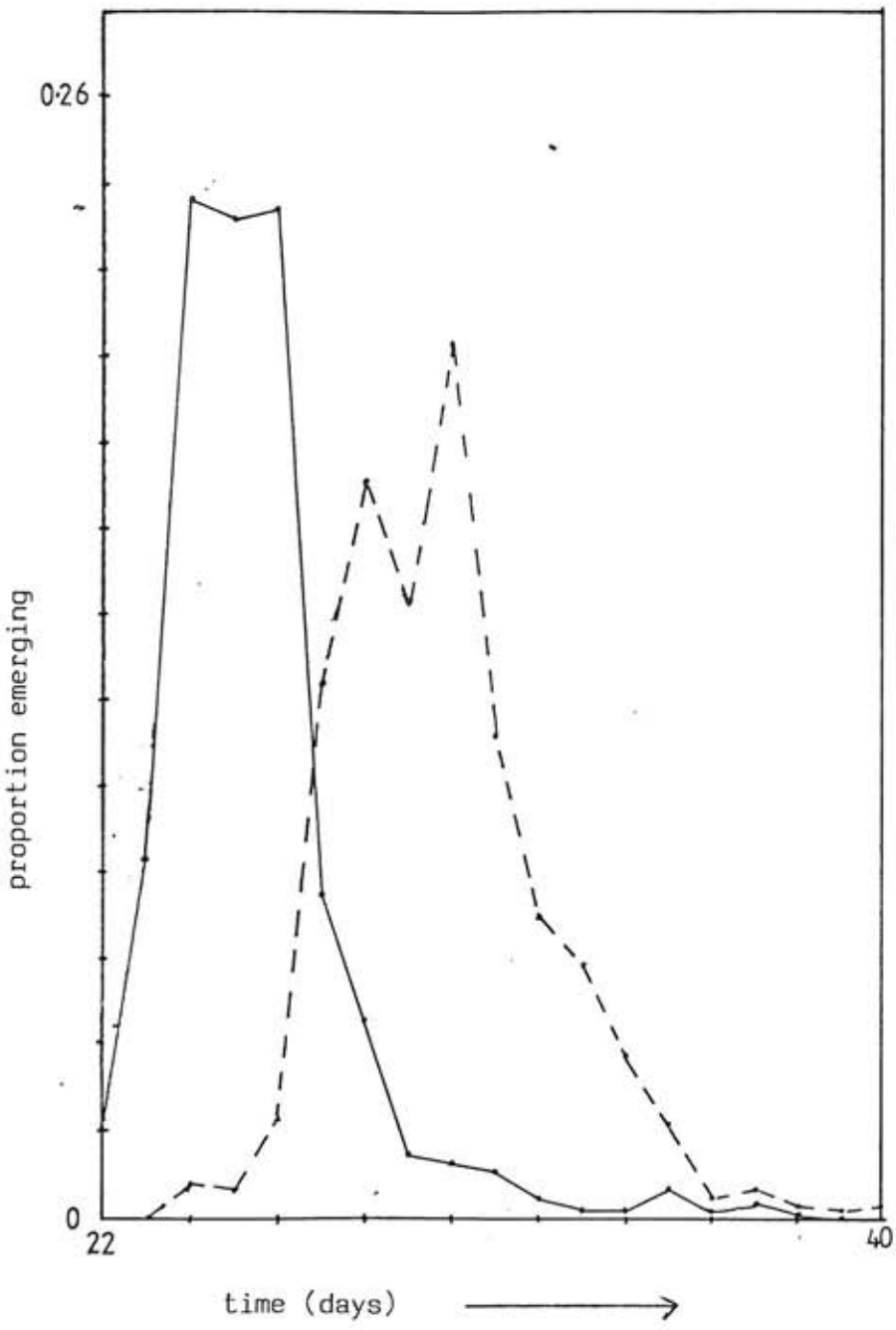

Figure 2.5. (AE experiment)

Proportin of adults to emerge each day from a cohort of eggs laid on day 0.

——— larvae supplied with BGYF food

— — — larvae supplied with BG food.

emergence distribution for BG differs from that for BGYF; the mean egg to adult generation time is ≃ 29 days for BG and ≃ 25 days for BGYF.

(5) Continuous (CTS) Experiments

These experiments studied the population of a closed community of Plodia over a period of two years. Individual populations were enclosed in a container of area 520cm². Each week, 1 section of food (1/12th of the total) was removed and replaced with new medium in rotation; dead adult moths were removed, counted, weighed and sexed. Each experiment began by introducing a number of animals into a cage containing 12 sections of new food. There were three replicates of each of the following experiments:-

(a) BG

Each section of food contained 5g of the BG food mixture.

15 male and 15 female final instar larvae were introduced.

(b) BGYF 1/3

To measure the effects of density, this experiment used a cage 1/3rd of the size of other experiments, with food sections containing 2.33g of BGYF. The experiment began with 5 male and 5 female final instar larvae.

(c) BGYF 1

Each section of food contained 7g of the BGYF food mixture; the experiment began with 15 male and 15 female final instar larvae.

(d) BGYF 2

Each section of food contained 7g of BGYF; the experiment began with 30 adults (15♂, 15♀), 30 final instar larvae (15♂, 15♀), 30 small larvae (15♂, 15♀) and 30 eggs.

Figs. 2.6 shows the number of dead adult moths collected each week for one replicate of each of these four experiments. We note that as adult moths live approximately a week (AS experiment), these data give a rough guide to the size of the adult population 7 days previously.

In all experiments, there is a single large population peak at the beginning of the experiment, which is evidently due to the abundance of food initially present; thereafter the population fluctuates. Fourier transforming the data (Figs 2.7) shows that these population fluctuations are quasi-periodic, with a period of $\simeq$ 38 days for all BGYF experiments and $\simeq$ 43 days for the BG experiments - that is, periods of about 1.5 times the egg to adult generation time as measured by the AE experiment (c.f. Fig 2.5). It can be seen that the mean population density varies between the two food media,

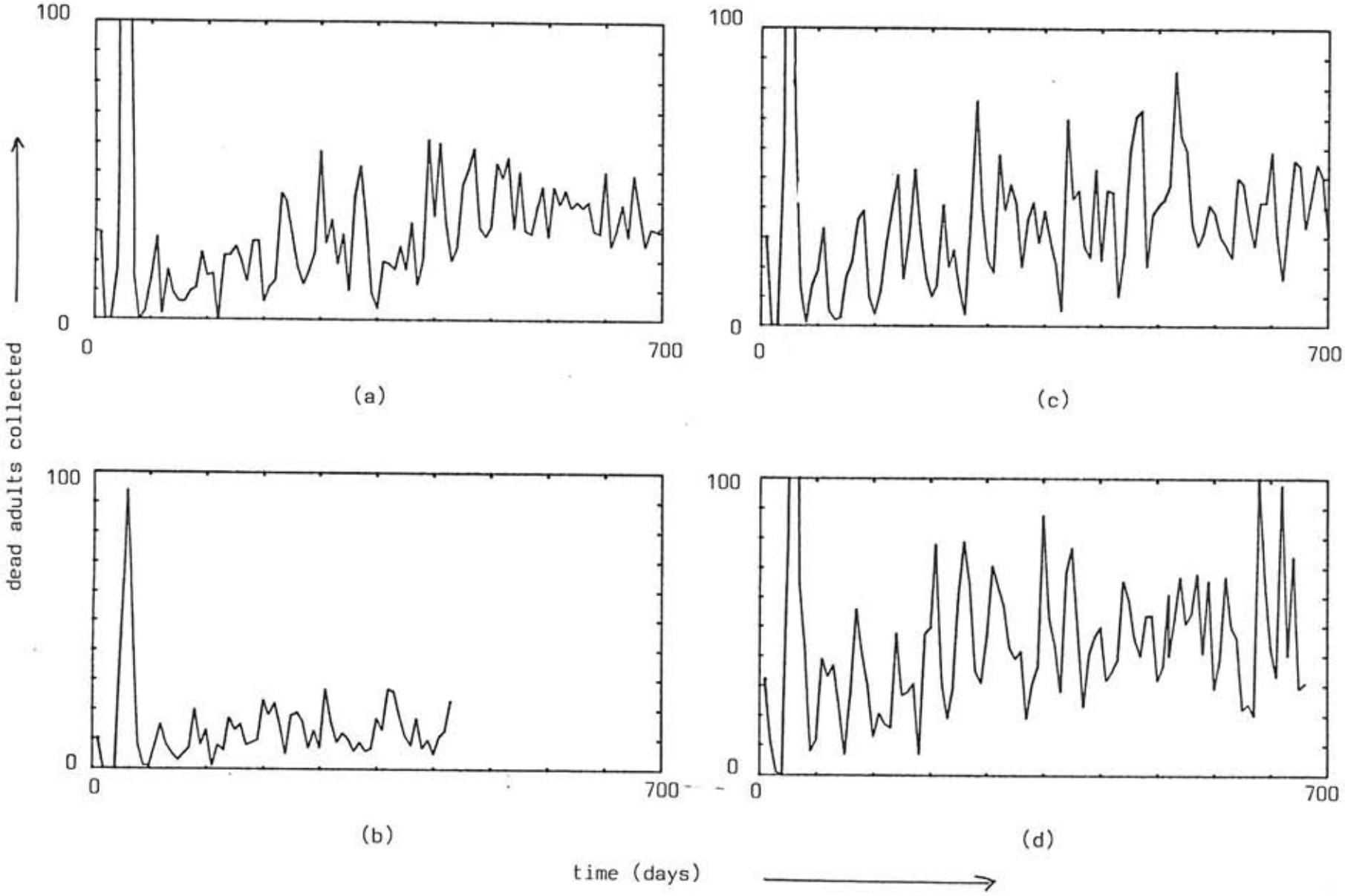
100
0
0
700
(a)
100
0
0
700
(c)
dead adults collected
100
0
0
700
(b)
100
0
0
700
(d)
time (days)

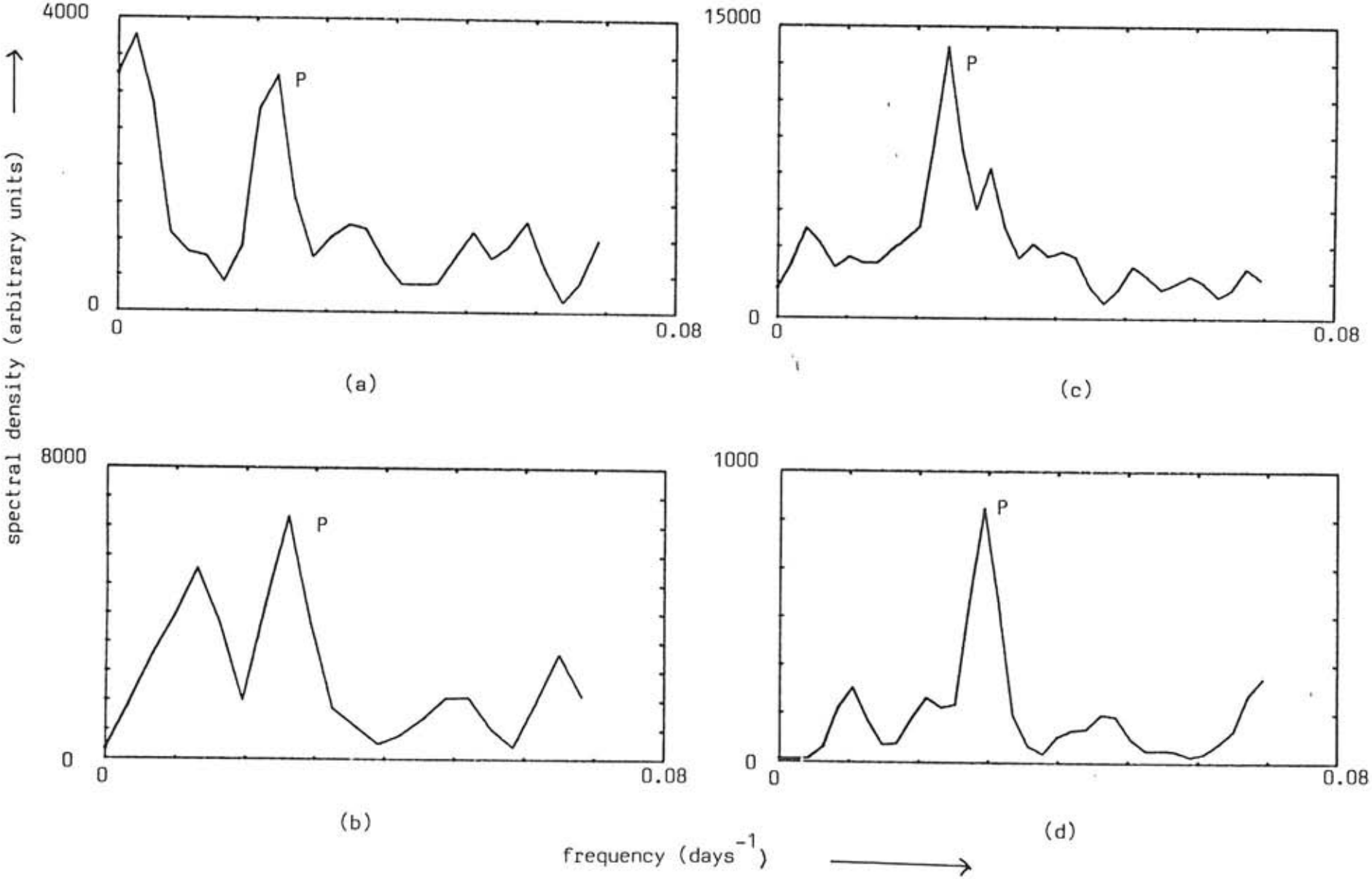
4000
P
0
0
0.08
(a)
15000
P
0
0
0.08
(c)
8000
P
0
0
0.08
(b)
1000
P
0
0
0.08
(d)
spectral density (arbitrary units)
frequency (days^{-1})

with a mean density of ≃ 45 adults per full size arena for BGYF and ≃ 36 adults per full size arena for BG.

Fig 2.8 shows regression lines for mean weight of dead adults against the total number of moths collected. It can be seen that for all experiments, the mean adult weight decreases with an increase in the adult population; mean weight varies with adult density in much the same way for all experiments.

Figs 2.9 and 2.10 show the sex ratio plotted against adult density and mean adult weight; it can be seen that throughout the experiments, about half the adult population is female.

These continuous experiments were run down by removing adult moths as they emerged, thereby preventing mating and oviposition. The remaining food from the BG and BGYF1 experiments was reserved and used for a set of cohort experiments - the Old Bran experiments.

(6) Old Bran (OB) Experiments

Each of the 12 sections of bran was divided into three; each 1/3rd placed in a lunch pack (as used in the BGYF1/3 experiments) to make up three replicates of the original, but one third of the size. This was done for 2 replicates of the BG experiments, providing 6 boxes, and

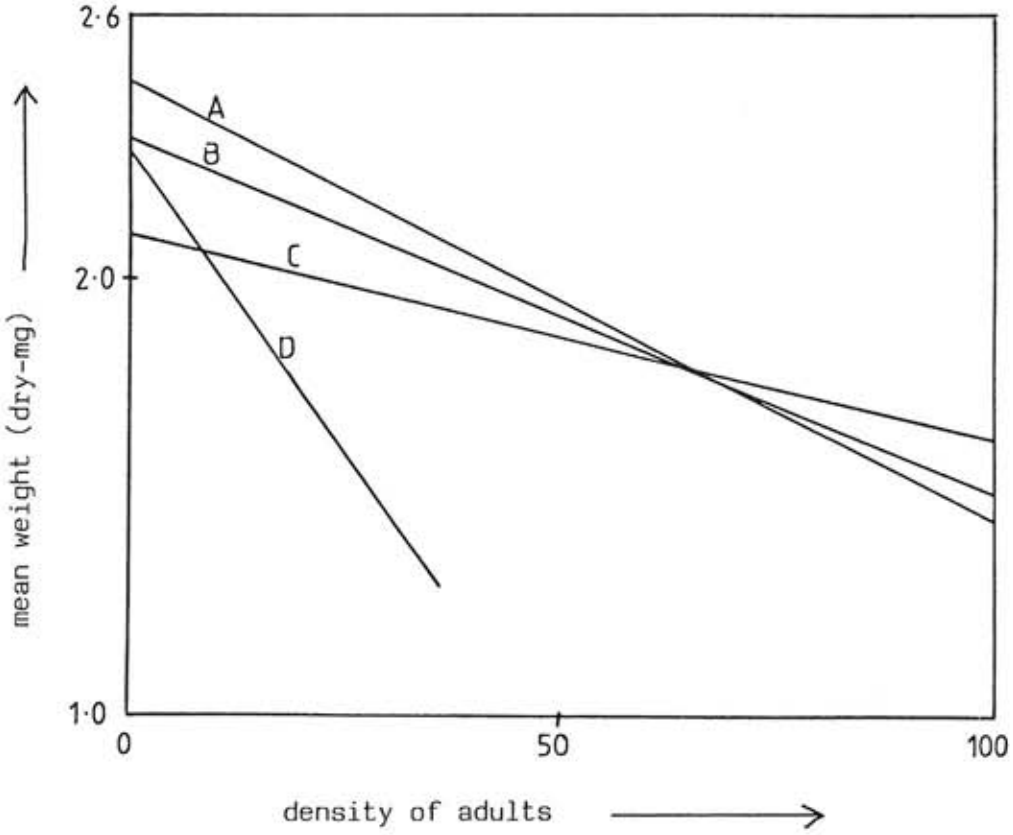
2·6
2·0
1·0
A
B
C
D
mean weight (dry-mg)
0
50
100
density of adults

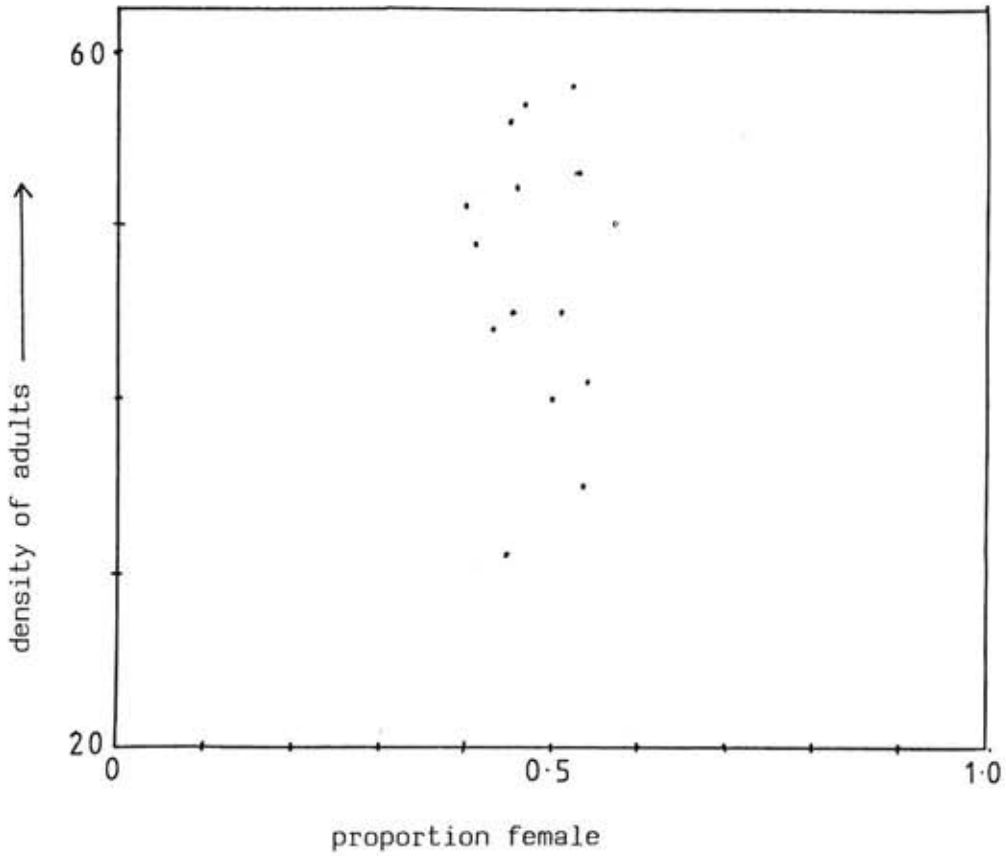

Figure 2.9. Sex ratio of dead adults collected during the CTS experiments versus density of adults.

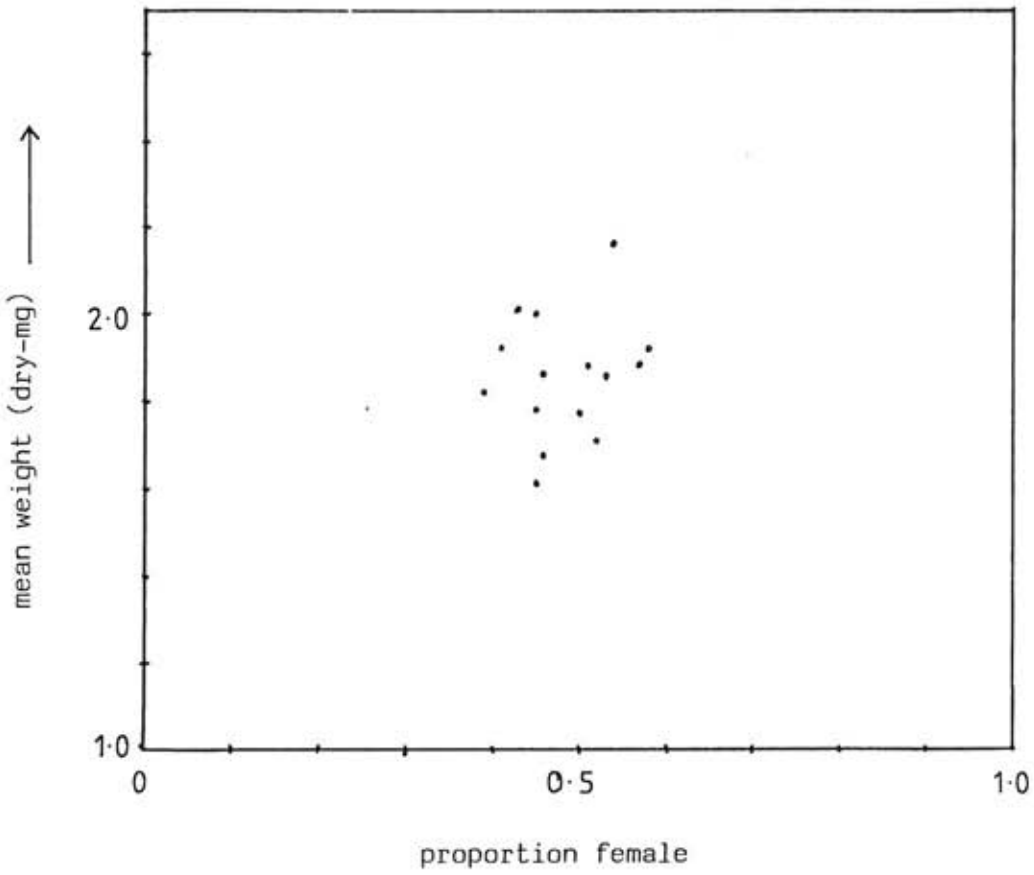

Figure 2.10. Mean weight of dead adults collected during CTS experiments plotted against the proportion female.

for all 3 of the BGYF1 replicates (9 boxes).

For the BG cohort experiments, varying numbers of newly-laid eggs were placed in the boxes and allowed to develop. The number of eggs to hatch was noted. Adult moths were removed and sexed as they emerged. For the BGYF cohort experiments, numbers of first instar larvae were introduced and allowed to develop. Adults were removed, sexed and also weighed each day.

Figs 2.11 show the survival from larva to adult plotted against initial larval density for BG and BGYF experiments; it can be seen that survival decreases as initial larval density increases. Fig 2.12 shows the mean larva to adult development time for each cohort plotted against initial larval density - we note that development time is longer than that observed during the AE experiments. Fig 2.13 shows the mean adult weight plotted against initial larval density for the BGYF experiments - it can be seen that mean weight decreases with an increase in initial density.

Second cohorts introduced to food remaining after the above experiments did not survive, although there appeared to be food available, indicating that larvae may, in some way, be conditioning the food.

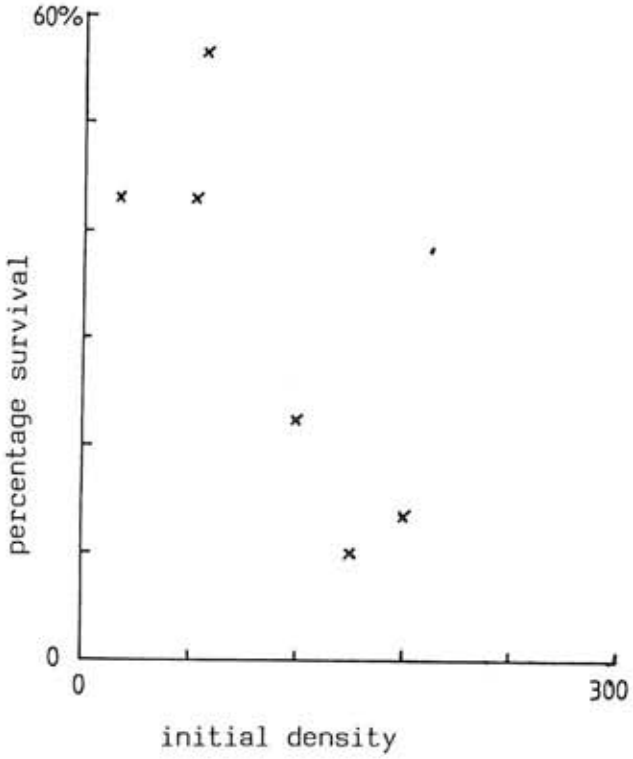
60%
percentage survival
0
0
300
initial density

(a)

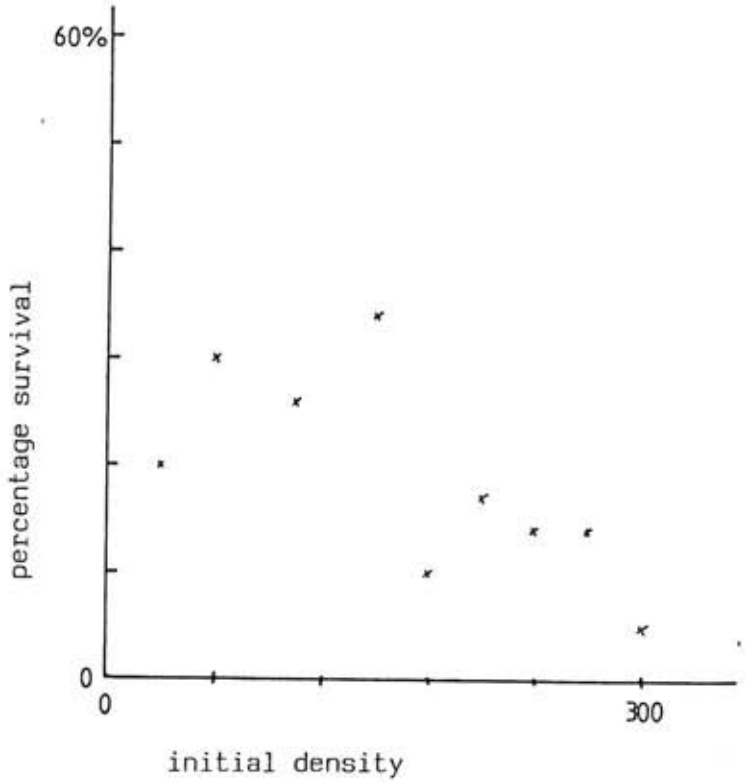
60%
percentage survival
0
0
300
initial density

(b)

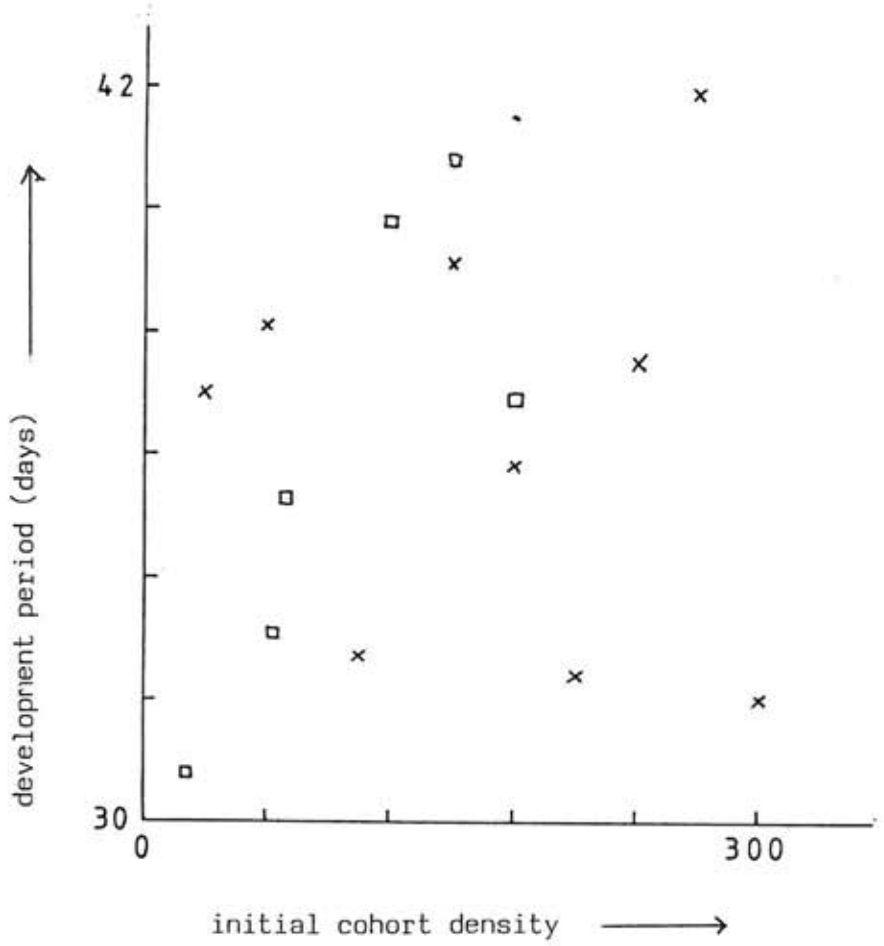

Figure 2.12. Mean (larva to adult) development period of OB cohorts :-

□ BG food supplied

× BGYF food supplied.

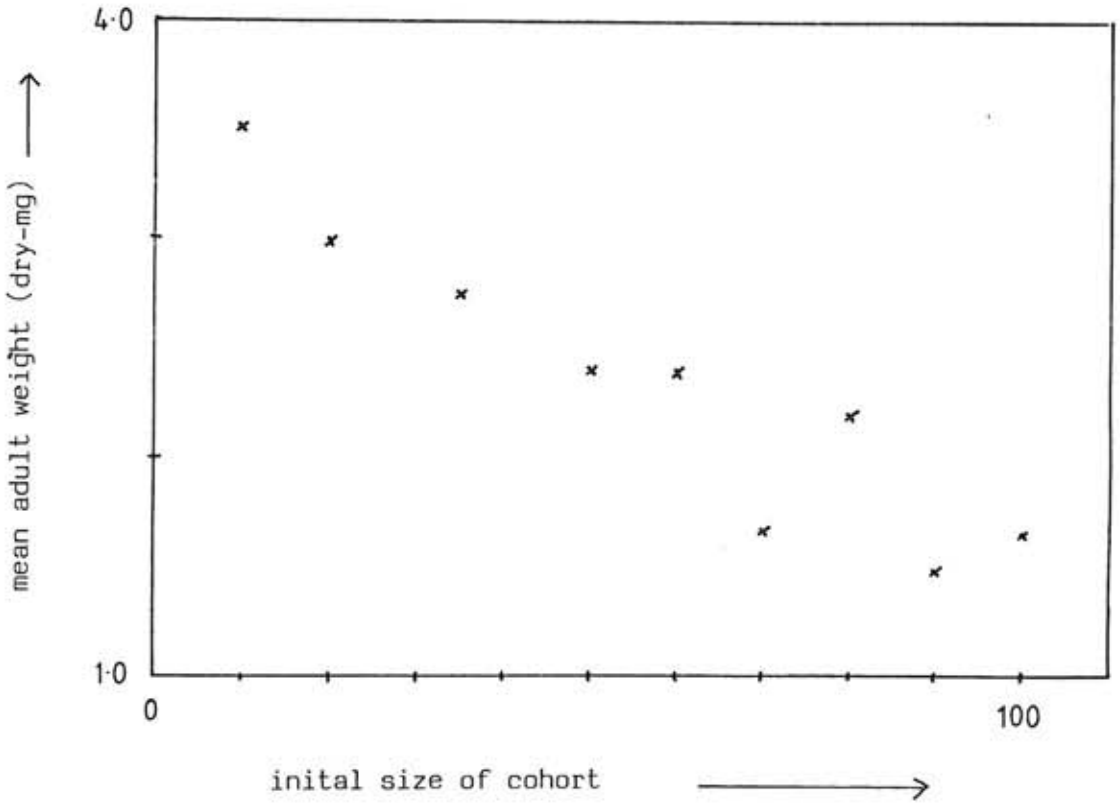

Figure 2.13. Mean adult emergence weight of OB cohorts, BGYF food supplied.

(7) Other Observations

During these experiments, the time taken for eggs to hatch was observed to be between 3 and 4 days. Pupation time was observed to be about 7 days.

2.2 Modelling Approximations

In this section we review the data of the York experiments. As we use a stage-structured model we shall interpret the data with a view to making a number of broad based assumptions about the behaviour of individuals in particular stages of the life-cycle (modelling approximations), which will describe the general features of behaviour while discarding the natural variability found in the data.

All stages of the life-cycle may be adversely affected by unsuitable temperatures (Adler 1960, Cline 1970, Tzanakakis 1959, Zacher 1939). However, we are concerned with experiments carried out in the laboratory at a constant temperature of 28^0C, so that the effects of temperature on mortality and development need not be considered. In particular, although the length of the developmental period of eggs varies with temperature (e.g. Snyman 1949), we are able to assume a constant egg development time which we take to be 3.5 days (see also Snyman 1949).

We also assume a constant pupation time of 7 days, and following Benson (1973) who states that 'mortality of pupae in these moths is fairly small and unimportant', we shall assume that all pupations are successful.

Both Podoler (1974) and Snyman (1949) report variations in sex ratio with changes in larval density. However, no such changes are observed in the CTS experiments, where the sex ratio is approximately 1:1, and therefore we shall assume a constant sex ratio, and will not distinguish between individuals of different sex.

The AS experiment shows all adults survive for a given period; thereafter the population decays exponentially (Figs 2.1). Although the survival curve varies for males and females, in view of our assumption (above) that we do not distinguish between males and females, we shall approximate adult survival using the female survival curve (Fig 2.1(b)). (Evidently, as adult females reproduce, it is necessary to have a good estimate of female longevity; assuming that this applies also to adult males implies, in modelling terms, that our model will yield a slightly inflated population density.) We assume that all adults survive to day 6, and that thereafter an adult cohort will decay exponentially.

Female fecundity was found to vary dramatically between individuals (Fig 2.2). However, other workers have

found the number of eggs a female lays to be correlated with her weight (Podoler, 1974) or size (Snyman, 1949) at emergence. (We note that the AF experiment measured female weight after death.) Thus, we do not, at the moment, make any assumption as to the egg laying capacity of adult females, but note that as most females lay most of their eggs within the first 6 days after emergence, we shall assume that eggs are laid at a constant rate over this period.

The AE experiment shows that within a given cohort there is a wide variety of egg to adult development times (see also Hill 1928 and Zacher 1939). As we are assuming constant egg and pupa development times, this implies that individual variation between larvae results in a distribution of maturation periods out of the larval stage; we shall incorporate this effect into our model (this is dealt with in Appendix A).

Significant differences in behaviour - in emergence times (AE), survival curves (OB), cycle period and adult density (CTS) - were observed between experiments conducted using BG and BGYF food media. Williams (1964) also found food quality to have a significant effect on development time and mortality in Plodia. We shall incorporate these differences by assuming that parameters pertaining to larval development, mortality and factors which may be influenced by food quality, are

medium-specific. Initially, we confine ourselves to considering a model in which the food supplied is BGYF, and we shall fit all parameters accordingly.

To summarize, we make the following modelling approximations based on the York data, supplemented where necessary by information obtained elsewhere :-

(A1) Any parameters relating to food quality are medium specific.

(A2) The time taken for eggs to hatch is constant (3.5 days).

(A3) The pupa development time and survival are constant (7 days and 100% respectively).

(A4) We do not distinguish between males and females.

(A5) All adults survive for 6 days, thereafter the population decays exponentially.

(A6) Adult females lay their eggs at a constant rate over 6 days.

(A7) Maturation out of the larval stage is distributed.

2.3 An Outline Model

We use a stage-structured model which implicity assumes that all individuals within a given stage have identical (time-dependent) vital rates. For each stage it is necessary to determine the stage duration and through-stage survival. We discuss the modelling approximations

of Section 2.2 with a view to constructing a stage-structured model of Plodia.

We shall take account of the four distinct development stages of Plodia - the egg, larva, pupa and adult stages. We do not include separate male and female stages, as we assume (A4) that the sex of an individual does not influence its development. (A5) and (A6) lead us to include two adult stages in our model:-

(i) a Young Adult reproducing stage, with fixed maturation period and no deaths, and

(ii) an Old Adult non-reproducing stage with constant per capita death rate.

Egg, pupa and Young Adult stages all have fixed maturation periods (A2, A3, A5); in addition the pupa stage has fixed survival (A3). We shall deal with distributed maturation out of the larval stage (A7) by defining a mortality-corrected maturation distribution $\Psi(q)$ (Gurney et al 1985), which is the distribution of development indices which would be observed at maturation for a single cohort if all survive.

Fig 2.14 illustrates our Outline Model. We have completely specified the dynamics of the pupa and both adult stages. We note that the pupa stage merely acts as a time-delay between maturation out of the larval stage and recruitment into the Young Adult stage. We also note that the Old Adult stage can have no effect on the

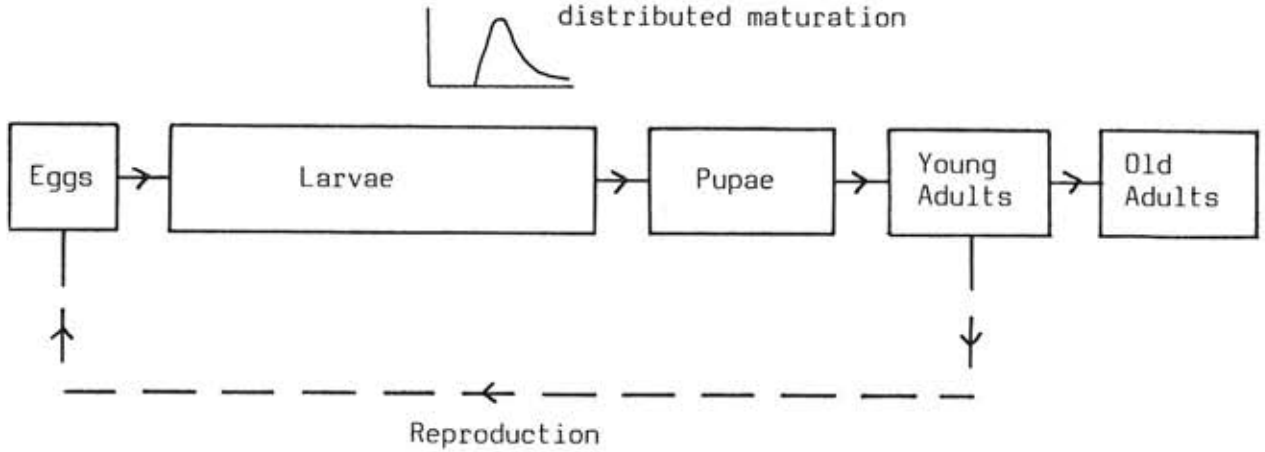

Development period	τ_E	?	τ_P	τ_A	-
Per capita death rate	?	?	0	0	δ_A

Figure 2.14. Schematic of the 'Outline Model' developed in Section 2.3 (see text).

dynamics of the population, but merely provides a more accurate estimate of the size of the adult population.

We have yet to define the functional dependence of the following quantities :-

(i) egg survival - determined by the egg per capita death rate

(ii) larval per capita death rate

(iii) larval maturation period - determined by the choice of development index and development rate

(iv) adult (female) fecundity.

CHAPTER THREE

Chapter Three: Factors Regulating the Population.

It can be seen from Figs 2.6 that the Plodia population is neither growing exponentially nor tending to extinction; the quasi-periodic fluctuations observed imply that population regulation is occuring. The Outline Model of Section 2.3 pinpoints those areas of the life-cycle at which density-dependent effects may come into play - these are the egg per capita death rate, the larval per capita death rate, the larval maturation time and adult fecundity. We note that density dependence in one or both of the larval per capita death rate or/and the maturation time ultimately results in a variable through stage survival; variation in the egg per capita death rate similarly results in a variable through-stage survival.

In this Chapter, we aim to determine the extent to which variation in egg survival, larval survival, adult fecundity govern the population dynamics of Plodia, with reference to the CTS experiments. We assume ab initio that larval survival varies with food density:- Beddington et al (1976) show that through instar survival rises with feeding rate for many arthropod larvae; mortality of Plodia larvae arises predominantly from increasing larval numbers per unit food available (Benson 1973, Podoler 1974, Snyman 1949; this is also seen in the OB experiments, Figs 2.11). The following

argument shows that variation in larval survival as a result of competition for food cannot be the only means of population regulation in Plodia during the CTS experiments.

3.1 Steady State argument for cannibalism and interference

For the purposes of this argument, we suppose that the populations of the CTS experiments are fluctuating around a steady state. We know that for any model we choose to construct, the following equation must hold in a steady state:-

$$E^* S_E^* S^* = 1 \qquad (3.1)$$

where

E = number of eggs produced per adult lifetime

S_E = egg survival

S = survival larva → adult

and * denotes a steady state value.

Suppose that adult fecundity and egg survival do not vary, so that the only means of population regulation is via changes in survival from larva to adulthood. Then each female will lay a given number of eggs, of which a constant proportion will hatch. The observed mean number of eggs produced per female lifetime during the AF experiment is 75. We estimate from the CTS experiments

(Figs 2.9, 2.10) that half the adult population is female, giving $E \simeq 37.5$ eggs per adult lifetime. The EH experiment (Fig 2.4) shows that half the eggs laid during the first 6 days of the female's lifetime hatch, and so we take $S_E \simeq 0.5$.

We are assuming that larval survival depends on food density. As the OB experiments used food remaining from the CTS experiments, we estimate S^* (the steady state larva → adult survival) by considering the survival/density data of the OB experiments, where the initial food density is approximately that present during the CTS experiments. Fitting a straight line to the data (Fig 2.11(b)), we estimate survival to be $\simeq 0.35$ at the intercept (i.e. at zero larval density). That is, we would expect to see 35% of larvae surviving to adulthood if food density was maintained at the level present during the continuous experiments, and so we estimate $S^* \simeq 0.35$.

Using the estimates given above,

$$E\, S_E\, S^* = 6.6 \qquad (3.2)$$

or, the population is capable of multiplying more than 6-fold over the generation! This is evidently not what happens, and we conclude that there must be another source of population regulation which we have not so far

taken into account, and which must invalidate one or more of our estimates. We consider each of our estimates in turn.

As discussed in Section 2.2, female fecundity was found to vary dramatically between individuals. Although no correlation was found between number of eggs laid and female weight, Podoler (1974) and Snyman (1949) found a relationship between eggs laid and female weight or size at emergence. We suppose that such a relationship <u>does</u> exist, but was not observed as the York experiments measure weight after death. If weight-dependent fecundity is to be the only 'extra' means of population regulation, it follows from our estimates of S_E, S^* and equation (3.1) that E^* would have to take a value of 5.7 eggs laid per adult lifetime - a remarkably low number. Moreover, Podoler (1974) predicts values of between 74 and 85 eggs per female lifetime for the range of female weights observed during the CTS experiments, so that our estimate of $E \approx 37.5$ eggs per adult lifetime (that is, 75 eggs per female lifetime) is, if anything, an underestimate. Thus, it is evident that weight-dependent fecundity cannot be the sole 'extra' source of regulation. For the moment, we shall assume that fecundity is constant, and take $E = 37.5$ eggs per adult lifetime, although we shall re-examine this possibility in Chapter 6.

The EH experiment, which provided our estimate of S_E, was conducted in the absence of individuals in other stages of the life-cycle. We consider the possibility of cannibalism of eggs by larvae (see, for example, Benson 1974). This would affect egg mortality during the CTS experiments where both eggs and larvae are present at any one time, but would not occur during the EH experiment, so that $S_E \propto 0.5$ would be an overestimate. If egg cannibalism is to be the only extra source of mortality, it follows from equation (3.1) and the estimates $S^* \propto 0.35$, $E \propto 37.5$ that the steady state egg survival must be $S_E^* = 0.076$ - or, cannibalism will reduce egg survival from 50% to less than 8%!

Lastly, we consider our estimate of S^*. We consider the possibility of interference between larvae - that is, an increase in larval mortality due to an increase in the density of larvae (see, for example, Snyman 1949). If this occurs, we can no longer use 0.35 as an estimate of S^*, as this figure applies to an effective zero density of larvae, which is not the case during the CTS experiments. Thus, interference between larvae would imply that we have overestimated the steady state larva → adult survival; if this is to be the only 'extra' means of population regulation, it follows from equation (3.1) that interference between larvae must reduce survival from 35% to 5.3% in the steady state.

3.2 A Range of Steady States

We have shown that if any one of the mechanisms discussed above - weight-dependent fecundity, cannibalism of eggs by larvae, interference between larvae - is to account for the extra regulatory mechanism implied by equation (3.2), it must have a strong effect on the dynamics of the population. Podoler's results have led us to discount weight-dependent fecundity as a possible source of this extra regulation, and so we shall now include in our model the assumption that the number of eggs laid per adult lifetime is a constant, which we shall take to be $E = 37.5$.

We have shown that if egg cannibalism operates alone, egg survival must drop from 50% in the EH experiment to 7.6% in the CTS experiments; if interference operates alone, larva → adult survival at the steady state food density must drop from 35% in the OB experiment to 5.3% during the CTS experiments. We conclude that it is likely that both interference and cannibalism occur, and shall include both these mechanisms in our model.

In the argument of Section 3.1, we considered the quantity S which represents survival through both larva and pupa stages. We note that as our Outline Model assumes pupa survival is 100% (A3), the quantity S may be taken to be larval survival. Given that we are assuming

constant fecundity, we know that S^*_E and S^* are related (equation (3.1)) by

$$S^* = \frac{1}{ES^*_E} \propto \frac{0.026}{S^*_E} , \qquad (3.3)$$

and we can also say that

$S^*_E \leqslant 0.5$ (equality iff no cannibalism)

$S^* \leqslant 0.35$ (equality iff no interference)

Thus we can fix on a range of permissible steady state survivals, as shown by Fig 3.1. We shall not consider survivals which lie outside this range.

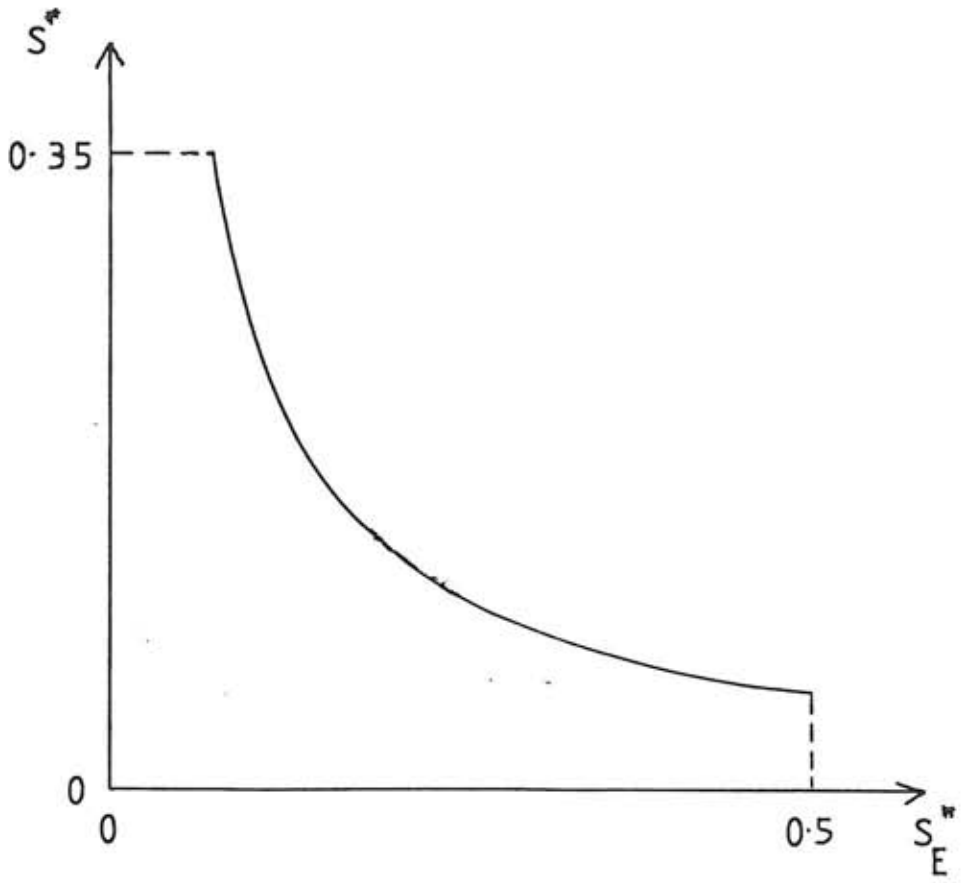

Figure 3.1. Range of 'permissible' steady state survivals (see text) for a constant fecundity model with E = 37.5 eggs per adult lifetime.

CHAPTER FOUR

Chapter 4: Mechanisms of Regulation II

We have shown in Chapter 3 that as well as population regulation via larval competition for food, our model must include both cannibalism of eggs by larvae and interference between larvae. Egg cannibalism implies egg survival will be dependent upon larval density. Our Outline Model assumes (A2) that the egg stage is of constant duration; it follows that the egg per capita death rate must depend on larval density.

Larval competition (which includes both interference and competition for food) affects larval survival. These mechanisms must operate via density-dependence in one or both of the larval maturation period or/and the per capita death rate. The experiments of Podoler (1974) show that larval survival to 20 days decreases as food per larva decreases; also survival decreases with an increase in the initial size of cohort (that is, with an increase in competition) during the OB experiments while no increase in maturation period is detected (Figs 2.11, 2.12). Thus it can be seen that changes in larval survival due to a variable maturation period (in which larvae are exposed for different times to a more or less constant per capita death rate) will not account for these data, and we must assume that the per capita death rate will vary as the extent of larval competition varies. We do not discard the possibility of there also

being a variable maturation time.

In this Chapter, we derive suitable functional forms for both egg and larval per capita death rates. We begin by considering a larval search rate, whose form encompasses both interference and competition for food and which governs, in particular ways, the per capita death rates. The functional form chosen for the egg death rate enables us to limit further the range of steady state survivals given in Chapter 3.

4.1 The Larval Search Rate

We shall consider a search rate which is dependent upon handling times, as first considered by Holling (1959) and discussed in detail with reference to arthropod predator-prey systems by Hassell (1978). We assume that both feeding and larva-larva encounters are time-consuming (we suppose that egg handling time is negligible) and therefore act to reduce the rate at which an individual may search.

We define variables

$\rho_L(t)$ = density of larvae at time t

$\rho_M(t)$ = density of food at time t

$A(t)$ = individual (larval) search rate at time t

and parameters

a = maximum area of search per unit time

τ_L = handling time per larva-larva encounter

τ_M = handling time per unit food encountered

so that the search rate A(t) may be written as

$$A(t) = \frac{a}{1+aX_M\tau_M\rho_M(t)+aX_L\tau_L\rho_L(t)} \qquad (4.1)$$

where X_M and X_L denote the searching efficiencies for food and (other) larvae respectively.

Although the parameters a, τ_M, τ_L are functions of several components, analyzed in detail by Holling (1965, 1966), and may themselves be density-dependent (e.g. Hassell et al 1977), we shall assume that they may be regarded as constant.

It follows from equation (4.1) that we have included interference effects by reducing the available searching time in direct proportion to the frequency of larva-larva encounters (see also Hassell 1978, Chapter 5).

We suppose that larvae search systematically so that the number of larva-food encounters rises linearly with food density, and that each food item encountered is eaten, so

that the individual food uptake rate $I_M(t)$ is given by

$$I_M(t) = A(t)\rho_M(t) \qquad (4.2)$$

Thus, $I_M(t)$ may be written as

$$I_M(t) = \frac{I_{max}\rho_M(t)}{\alpha+\beta\rho_L(t)+\rho_M(t)} \qquad (4.3)$$

where

$$I_{max} = \frac{1}{X_M\tau_M}$$

is the maximum possible feeding rate and the parameter groups α and β are given by

$$\alpha = \frac{1}{aX_M\tau_M} \qquad \beta = \frac{X_L\tau_L}{X_M\tau_M}$$

We note that equation (4.3) may be considered as a variant of the familiar 'disc equation' of Holling (1959) which describes the relationship between the number of prey consumed per predator and applies here with food items considered as 'prey' and larvae the 'predators'; the equation is modified to include interference effects via the term $\beta\rho_L(t)$. It can be seen that at constant larval density, the assumption that a, τ_M, τ_L are constant yields a Type II functional response to food (prey) density, typical of many arthropods (Hassell et al 1977).

4.2 The Egg per capita Death Rate

We denote the egg per capita death rate and maturation time by $\delta_E(t)$ and τ_E respectively. We suppose that larvae search systematically so that the number of larva-egg encounters rises linearly with larval density, and that each larva-egg encounter results in an egg 'death'. Then δ_E may be written as

$$\delta_E(t) = \Delta_E + A(t)\rho_L(t) \qquad (4.4)$$

where the parameter Δ_E is the baseline egg death rate, which accounts for the 50% of eggs which fail to hatch in the absence of any cannibalism (EH experiment). That is, Δ_E will be given by

$$0.5 = \exp(-\Delta_E \tau_E). \qquad (4.5)$$

Thus it can be seen that egg survival is dependent upon larval density; the proportion of eggs laid at time $t-\tau_E$ which hatch at time t is given by

$$S_E(t) = \exp\left[-\tau_E \int_{t-\tau_E}^{t} \delta_E(t')dt'\right] \qquad (4.6)$$

4.3 The Larval per capita Death Rate

The instantaneous larval death rate and its relationship to food density is difficult to determine experimentally: during the course of any experiment measuring larval

survival, larvae are both consuming food and dying. We follow the modelling strategy of Gurney and Nisbet (1985) who, based on the findings of Beddington et al (1976), argued that the per capita death rate could be related to the instantaneous feeding rate. We shall consider two forms which such a relationship may assume.

Evidently the per capita death rate must increase as the feeding rate decreases. The simplest functional relationship which has this property is the inverse relationship, namely

$$\delta_A(t) = \frac{\eta}{I_M(t)} \qquad (4.7)$$

That is, δ_A decreases as I_M increases, and will take a non-zero value c when the feeding rate reaches its maximum value (c.f. Fig 4.1(a)). This value c is the baseline death rate, representing the proportion of larvae who die even when food is superabundant. However, with this form of death rate, $\delta_A \to \infty$ as I_M falls to zero, so that if no food is available, <u>all</u> larvae die immediately. That is, this death rate does not take into account in any way the possibility that 'food reserves' may sustain an individual for a short time at low food densities. For this reason, we shall also consider a second form of death rate which does, in a very crude way, take food reserves into account, namely the relationship

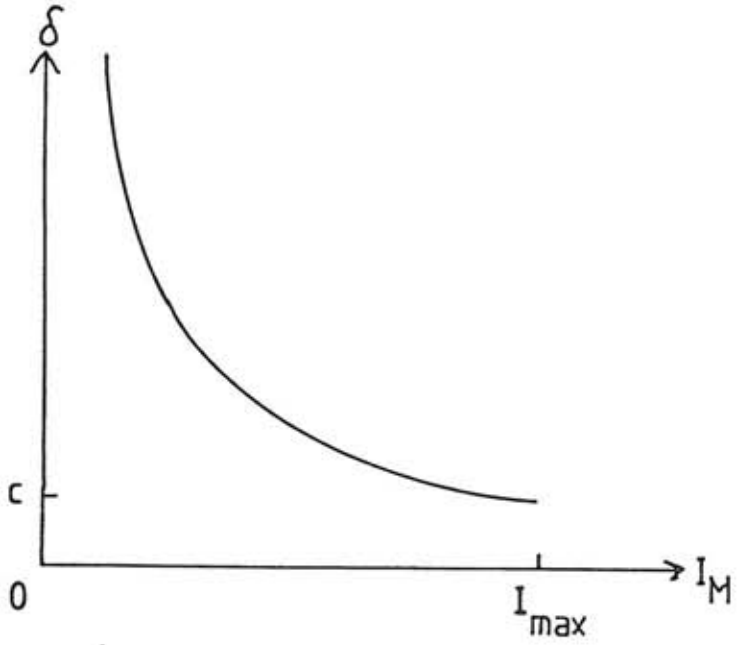

(a)

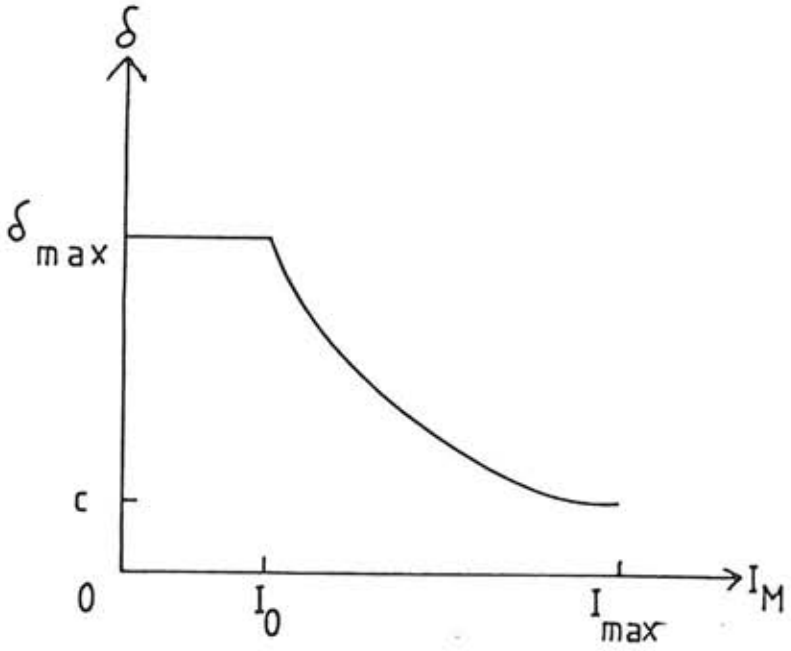

(b)

$$\delta_B(t) = \begin{cases} \delta_{max} & I_M(t) \leq I_0 \\ \dfrac{\eta}{I_M(t)-K} & I_M(t) \geq I_0 \end{cases} \qquad (4.8)$$

(c.f. Fig 4.1(b)).

For feeding rates above a threshold feeding rate I_0, this death rate varies in much the same way with feeding rate. For feeding rates below this threshold the per capita death rate is constant - the population will decay exponentially (with mean lifetime of $1/\delta_{max}$) for as long as feeding rates stay below the threshold, so that the larvae do not all die instantly. Thus, this form of death rate may be considered to represent the case of food reserves sustaining the population for a limited period when food is in short supply. However, we note that equation (4.8) implies that we do not differentiate between small newly-recruited larvae with no feeding history and large well-fed larvae which are almost ready to pupate.

4.4 Larval Development

To incorporate the observed distribution of larval maturation periods (AE experiment), we must take into account that larvae may mature at a wide variety of indices (see Appendix A). We must include a mortality-corrected maturation distribution $\Psi(q)$ in our model.

Nevertheless, we would expect to see a more or less fixed distribution of indices at maturation, although mortality will, to some extent, affect the shape of the distribution.

The question of whether or not the (model) larval stage has a variable maturation time, and if so, the variation of the maturation time, depends on our choice of development index and functional form of the corresponding development rate (Gurney et al 1985). The two most obvious candidates for development index are chronological age, where time-in-stage governs maturation, or weight gained, where an individual's feeding history governs maturation. In the former case there will be very little variation in mean maturation periods and regulation mechanisms will affect larval survival only through variation in the per capita death rate. In the latter case mean maturation periods will also vary so that regulation mechanisms will affect larval survival both through the per capita death rate and through the length of time spent in the stage.

Evidently, neither of the above - time in stage or weight gained in stage - is solely responsible for controlling the development of Plodia larvae : we observe that mean larval maturation periods vary from ∝ 15 days during the AE experiment to ∝ 25 days during the OB experiments, whereas both CTS and OB experiments show mean weight to

be negatively correlated with density.

However, none of the data available indicate what factors control development, so enabling us to choose an appropriate development index. Consequently, we shall investigate the suitability of each of time in stage and weight gained as development indices by considering each in turn.

In the case of a time in stage development index, the development rate is evidently unity throughout all experiments, and the maturation distribution may be estimated from the data of the AE experiment after correction for mortality . In the case of a weight gain development index, the development rate will be the instantaneous growth rate. Beddington et al (1976) conclude that in many arthropod species, the growth rate is directly proportional to the excess feeding rate above some threshold feeding rate; they also show, after Mukerji and Guppy (1970), that such a relationship applies to the fifth instar Lepidoptera Pseudaletia unipuncta (Haw.). For simplicity, we shall assume that the threshold feeding rate is negligible, and suppose the instantaneous per capita growth rate, g(t), is given by

$$g(t) = \epsilon I_M(t) \qquad (4.9)$$

where ϵ is the efficiency with which larvae convert food eaten into weight gained.

4.5 A Working Range of Steady States

We developed a range of permissible steady state egg and larval survivals in Section 3.2. We now find that, by virtue of defining the egg per capita death rate, we are able to limit further the range of possible steady state survivals.

It follows from equations (4.2), (4.4)-(4.6) that the steady state egg survival may be written

$$S_E^* = \frac{1}{2} \exp\left[- \frac{I_M^* \rho_L^*}{\rho_M^*} \tau_E \right] \qquad (4.10)$$

Now in a steady state, there can be no build up or decay of food, which implies that the total food uptake rate must balance the food supply rate which we denote by Φ. That is,

$$\Phi = I_M^* \rho_L^* \qquad (4.11)$$

It follows from equation (4.10) that we may express S^*_E directly in terms of the steady state food density and the (known) parameters Φ and τ_E, viz

$$S_E^* = \frac{1}{2} \exp\left[- \frac{\Phi \tau_E}{\rho_M^*} \right]. \qquad (4.12)$$

During the continuous experiments, larvae were observed to be living only on the 2 or 3 newest sections of food.

Thus, we estimate that ρ_M^* must lie between say 0.5 and 5 sections of food. It follows from equation (4.12) that by taking τ_E = 3.5 days and Φ = 1 section of food per week, we may estimate S^*_E for this range of steady state food densities; the corresponding steady state larval survival S^*_L may then be found from equation (3.3).

We find that

ρ_M^* = 0.5 sections $\Rightarrow S_E^*$ = 0.184 $\Rightarrow S_L^*$ = 0.145

ρ_M^* = 1 section $\Rightarrow S_E^*$ = 0.303 $\Rightarrow S_L^*$ = 0.088

ρ_M^* = 3 sections $\Rightarrow S_E^*$ = 0.423 $\Rightarrow S_L^*$ = 0.063

ρ_M^* = 5 sections $\Rightarrow S_E^*$ = 0.452 $\Rightarrow S_L^*$ = 0.059

Thus, it would appear that interference has a significant effect in controlling the population size. In view of these figures, we limit further our range of permissible steady states, and shall only consider a working range of steady states in which S^*_E lies between, say, 18% and 45% (c.f. Fig 4.2). We note that the above argument does NOT depend on the functional form chosen for the larval search rate A(t), but merely on the validity of equations (4.2) and (4.4)-(4.6).

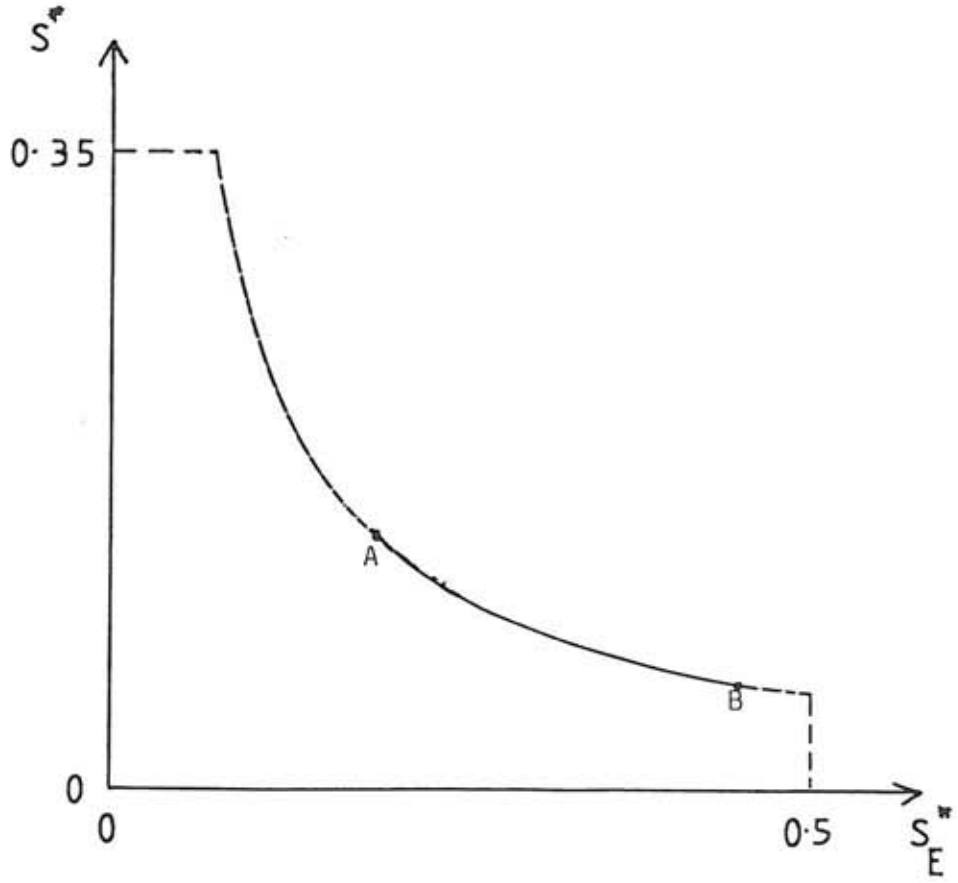

Figure 4.2. The portion AB of the range of permissible steady states forms the working range of of steady states.

CHAPTER FIVE

Chapter 5: Four Models

It follows from Chapter 4 (Sections 4.3 and 4.4) that we have four models to consider. We shall consider two models in which the larval per capita death rate takes the form given by equation (4.7), in one of which we take time in stage to be a suitable measure of larval development, in the second we take weight gained to be a measure of development and suppose that the development (growth) rate is given by equation (4.9). Our second pair of models also considers each of these development indices, but supposes that the larval per capita death rate is given by equation (4.8). We consider the models:-

	development index	death rate
Model I	time in stage	$\delta_A(t)$
Model II	weight gained	$\delta_A(t)$
Model III	time in stage	$\delta_B(t)$
Model IV	weight gained	$\delta_B(t)$

We have, in the Outline Model of Chapter 2 and the Chapter 4 assumptions of how the population regulation mechanisms act on the population, all the required components for constructing a mathematical model of the population dynamics. In this Chapter, we give the equations governing the dynamics of each stage. We

present numerical solutions of these equations for each of our four models for points which lie on our working range of steady state survivals.

5.1 The Model Equations

The population N(t) of each stage is governed by the balance equation

$$\frac{dN}{dt} = R(t) - M(t) - \delta(t)N(t)$$

where R(t), M(t), and $\delta(t)$ are, respectively, the recruitment rate into the stage, maturation rate out of the stage, and the per capita death rate. We relate the maturation rate out of the stage to the recruitment rate some time previously using formulae given by Gurney et al (1986). We assume that all transitions between stages are successful, so that an individual on maturing out of one stage is immediately recruited into the next stage. For the reader's convenience, Tables 5.1 and 5.2 provide a list of the notation used in the model equations.

(1) Egg stage

Young Adult females lay a constant number of eggs each day, and a constant proportion of the adult population is female, so that the rate at which eggs are laid is directly proportional to the size of the Young Adult population. Eggs hatch after a fixed development time,

Notation	Variable
$\rho_E(t)$	density of eggs at time t
$\rho_L(t)$	density of larvae at time t
$\rho_P(t)$	density of pupae at time t
$\rho_{YA}(t)$	density of young adults at time t
$\rho_{OA}(t)$	density of old adults at time t
$\rho_M(t)$	density of food at time t
$R_E(t)$	recruitment rate into egg stage at time t
$R_L(t)$	recruitment rate into larval stage at time t
$R_p(t)$	recruitment rate into pupa stage at time t
$R_{YA}(t)$	recruitment rate into young adult stage at time t
$R_{OA}(t)$	recruitment rate into old adult stage at time t
$M_E(t)$	maturation rate out of egg stage at time t
$M_L(t)$	maturation rate out of larval stage at time t
$M_p(t)$	maturation rate out of pupa stage at time t
$M_{YA}(t)$	maturation rate out of young adult stage at time t
$I_M(t)$	larval per capita food uptake rate at time t
$\delta_L(t)$	larval per capita death rate at time t
$g(t)$	larval growth rate at time t
$D(t)$	larval development rate at time t
$\delta_E(t)$	egg per capita death rate at time t

Table 5.1 Notation used for variables in the Model Equations.

Notation	Parameter
e	number of eggs laid per adult per day
τ_E	egg development period
τ_p	pupa development period
τ_A	young adult development period
Δ_E	'baseline' egg per capita death rate (in absence of cannibalism)
δ_A	old adult per capita death rate
I_{max}	maximum larval feeding rate
Φ	food supply rate
δ_{max}, η, κ, I_0	parameters of the larval per capita death rate (c.f. equations (4.7) or (4.8))
α, β	parameters of the larval food uptake rate.

Table 5.2 Notation used for parameters of the model.

and may fail to hatch or be cannibalised by larvae. Thus

$$\frac{d\rho_E}{dt} = R_E(t) - M_E(t) - \delta_E(t)\,\rho_E(t)$$

$$R_E(t) = e\,\rho_{YA}(t)$$

$$M_E(t) = R_E(t-\tau_E)\exp(-\tau_E \int_{t-\tau_E}^{t} \delta_E(t')dt')$$

$$\delta_E(t) = \Delta_E + A(t)\,\rho_L(t) = \Delta_E + \frac{I_M(t)\,\rho_L(t)}{\rho_M(t)}$$

(2) Larva Stage

Larvae may mature over a range of development indices, as determined by a mortality-corrected maturation distribution $\Psi(q)$. The shape of this distribution is estimated in Appendix A. The mean maturation time is constant for Models I, III; the mean maturation weight is constant for Models II, IV. Competition for food and interference between larvae imply feeding and per capita death rates are density-dependent. For this stage, we may write

$$\frac{d\rho_L}{dt} = R_L(t) - M_L(t) - \delta_L(t)\rho_L(t)$$

$$R_L(t) = M_E(t)$$

$$M_L(t) = D(t) \int_0^t \Psi(\int_x^t D(u)du)\exp(-\int_x^t \delta(u)du)R_L(x)dx$$

$$D(t) = \begin{cases} 1 & \text{for Models I, III} \\ g(t) & \text{for Models II, IV} \end{cases}$$

$$\delta(t) = \begin{cases} \delta_A(t) & \text{for Models I, II} \\ \delta_B(t) & \text{for Models III, IV} \end{cases}$$

where $\delta_A(t) = \frac{\eta}{I_M(t)}$; $\delta_B(t) = \begin{cases} \delta_{max} & I_M(t) \leq I_o \\ \frac{\eta}{I_M(t)-K} & I_M(t) \geq I_o \end{cases}$

$$I_M(t) = \frac{I_{max}\rho_M(t)}{\alpha+\beta\rho_L(t)+\rho_M(t)}$$

(6) Pupa Stage

The maturation time is constant, all pupations are successful. Thus

$$\frac{d\rho_p}{dt} = R_p(t) - M_p(t)$$

where $R_p(t) = M_L(t)$

$$M_p(t) = R_p(t-\tau_p)$$

(7) Young Adult Stage

There are no deaths in the young adult stage. There is a constant maturation period, so that

$$\frac{d\rho_{YA}}{dt} = R_{YA}(t) - M_{YA}(t)$$

where $R_{YA}(t) = M_p(t)$

$$M_{YA}(t) = R_{YA}(t-\tau_A)$$

(8) Old Adult Stage

No maturation out of the stage and a constant per capita death rate give

$$\frac{d\rho_{OA}}{dt} = R_{OA}(t) - \delta_A \rho_{OA}(t)$$

$$R_{OA}(t) = M_{YA}(t)$$

(9) Food Dynamics

We assume food is supplied at a constant rate and is not removed so that

$$\frac{d\rho_M}{dt} = \Phi - I_M(t)\rho_L(t)$$

5.2 Numerical solutions.

All parameters, with the exception of the α and β parameters of the larval feeding rate, are estimated or inferred from the data. This parameter estimation is set out in Appendix B. Values of α and β are chosen to correspond to a given point on the 'working range' of steady states (c.f. Fig 4.2).

The above equations governing the model behaviour are converted into sets of ordinary delay-differential equations (see Gurney et al, 1986) which we solve numerically using the package SOLVER (Maas, Nisbet and Gurney, 1982) on a SAGE II microcomputer. Calculations are initialled by modelling an innoculation of 60 eggs into the culture at time t = 0; we choose an initial food density which corresponds to the 12 sections of new food present at the beginning of the CTS experiments.

Figs. 5.1 - 5.4 show adult density plotted against time for each of our four models at the given points on the working range of steady states. The experimental data is of the number of dead adults collected each week; however, initial inclusion of a 'corpse' class into which Old Adults mature and which is emptied weekly showed very little difference between the corpse count and the adult population 7 days previously. As these models gave weekly counts, which tended to obscure the underlying dynamics, we have chosen to present the density of adults (both Young Adults and Old Adults).

The four models show that the functional dependence of the per capita death rate δ on the feeding rate I_M is important in determining the model behaviour. With the first form of death rate we consider, both models (Figs 5.1, 5.2) exhibit damped oscillations leading to a stable steady state. This behaviour does not resemble

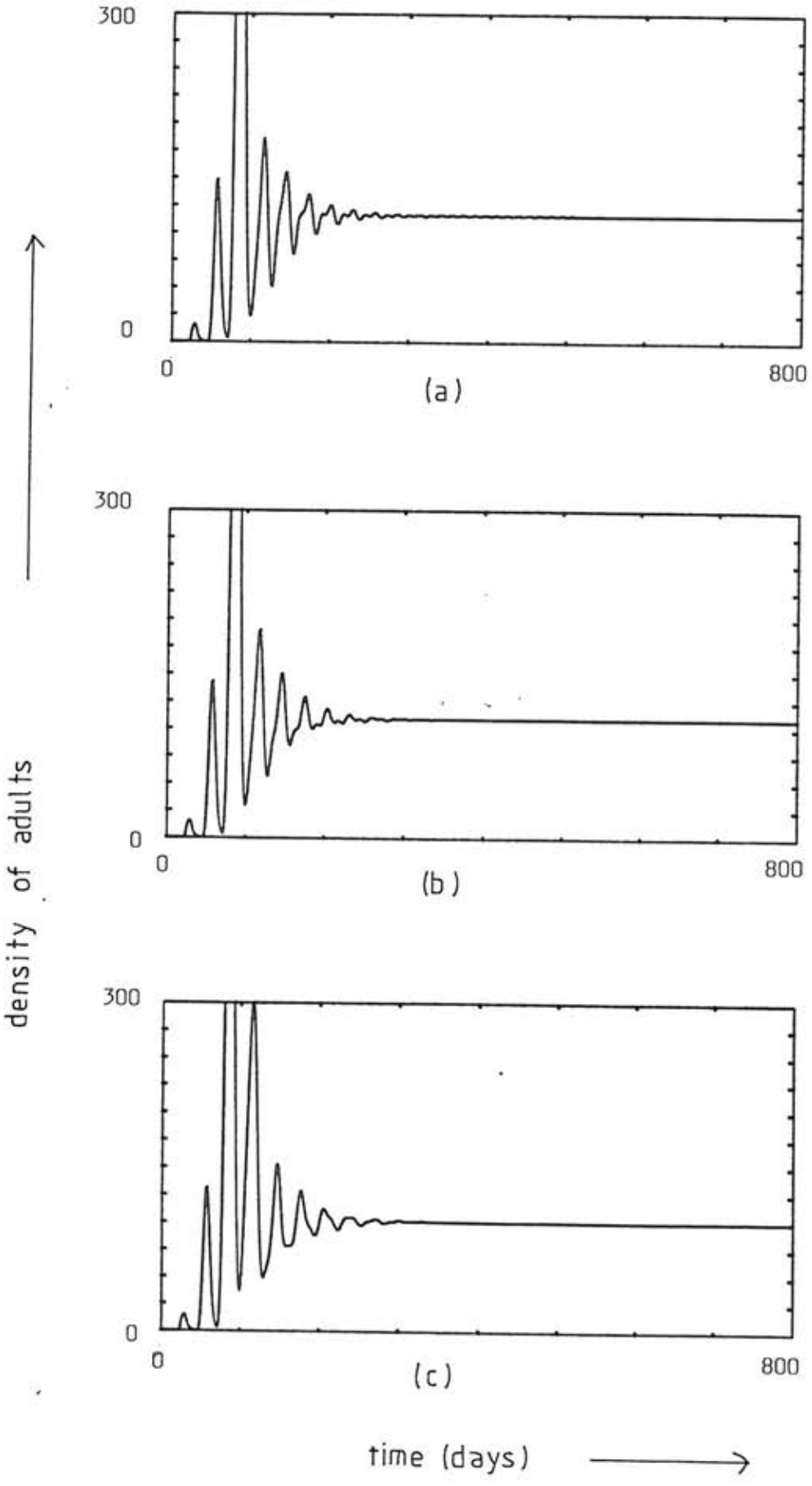
300
0
0
800
(a)
300
0
0
800
(b)
300
0
0
800
(c)
density of adults
time (days)

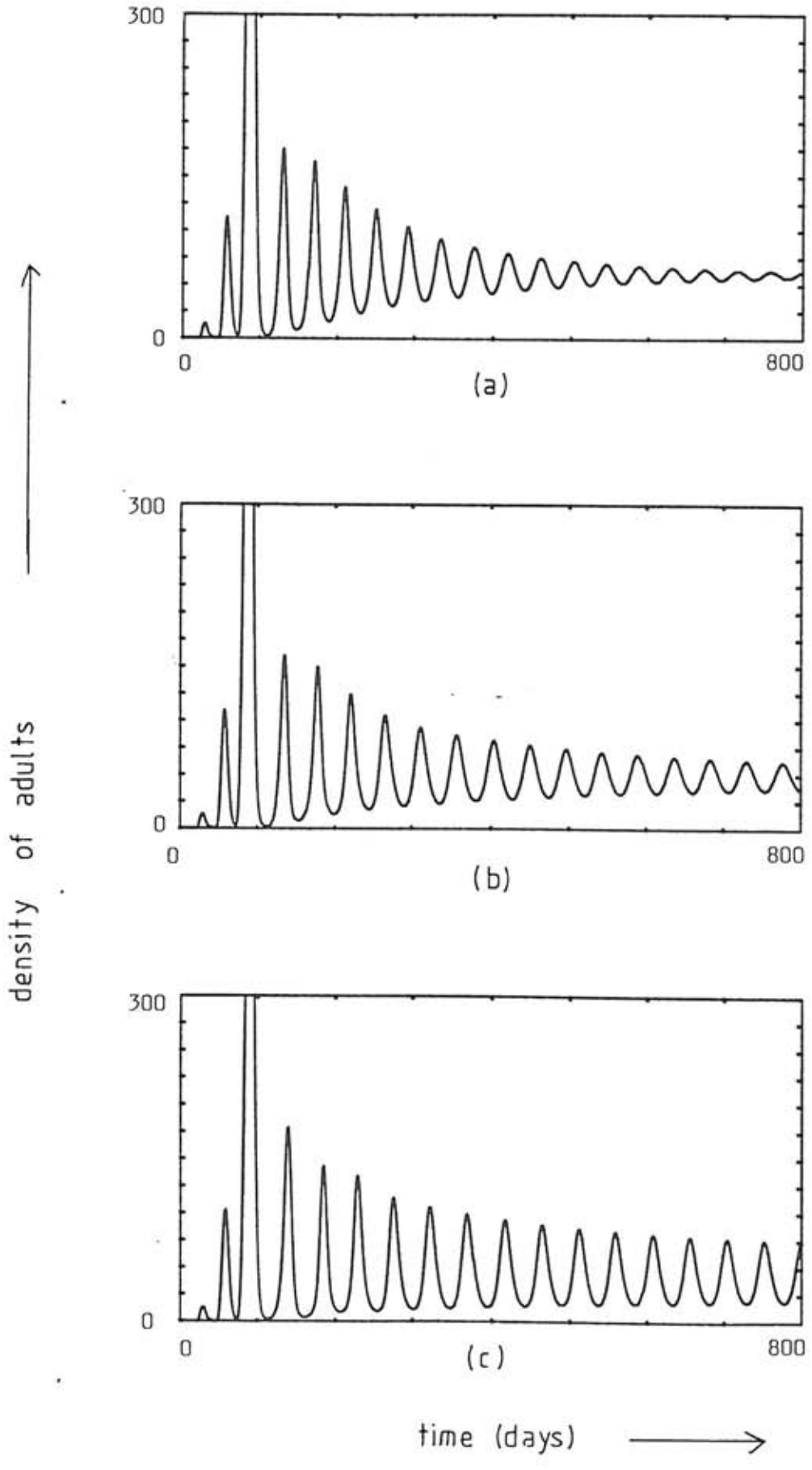
300
0
0
800
(a)
300
0
0
800
(b)
300
0
0
800
(c)
density of adults
time (days)

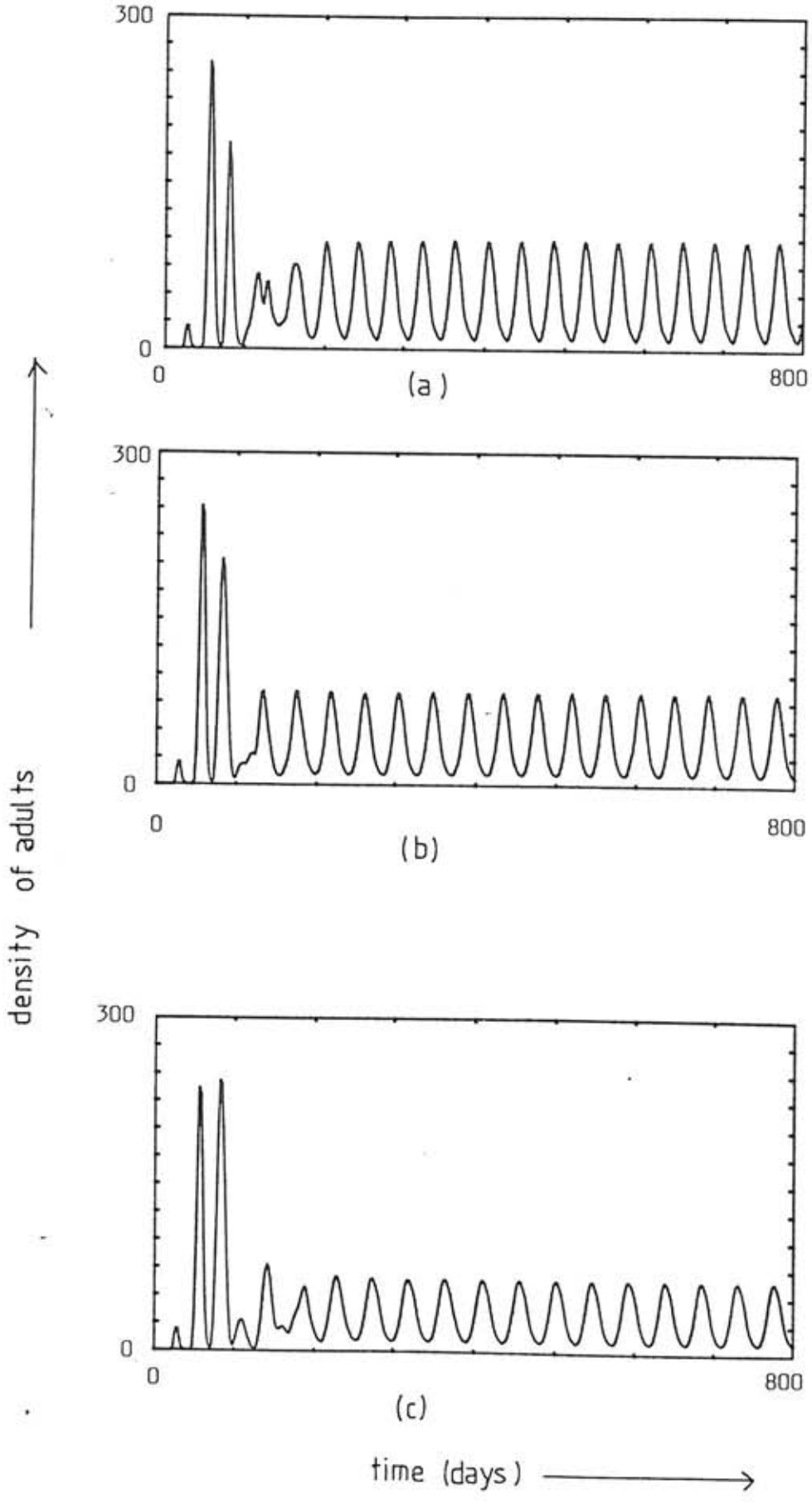
300
0
0
800
(a)
300
0
0
800
(b)
300
0
0
800
(c)
density of adults
time (days)

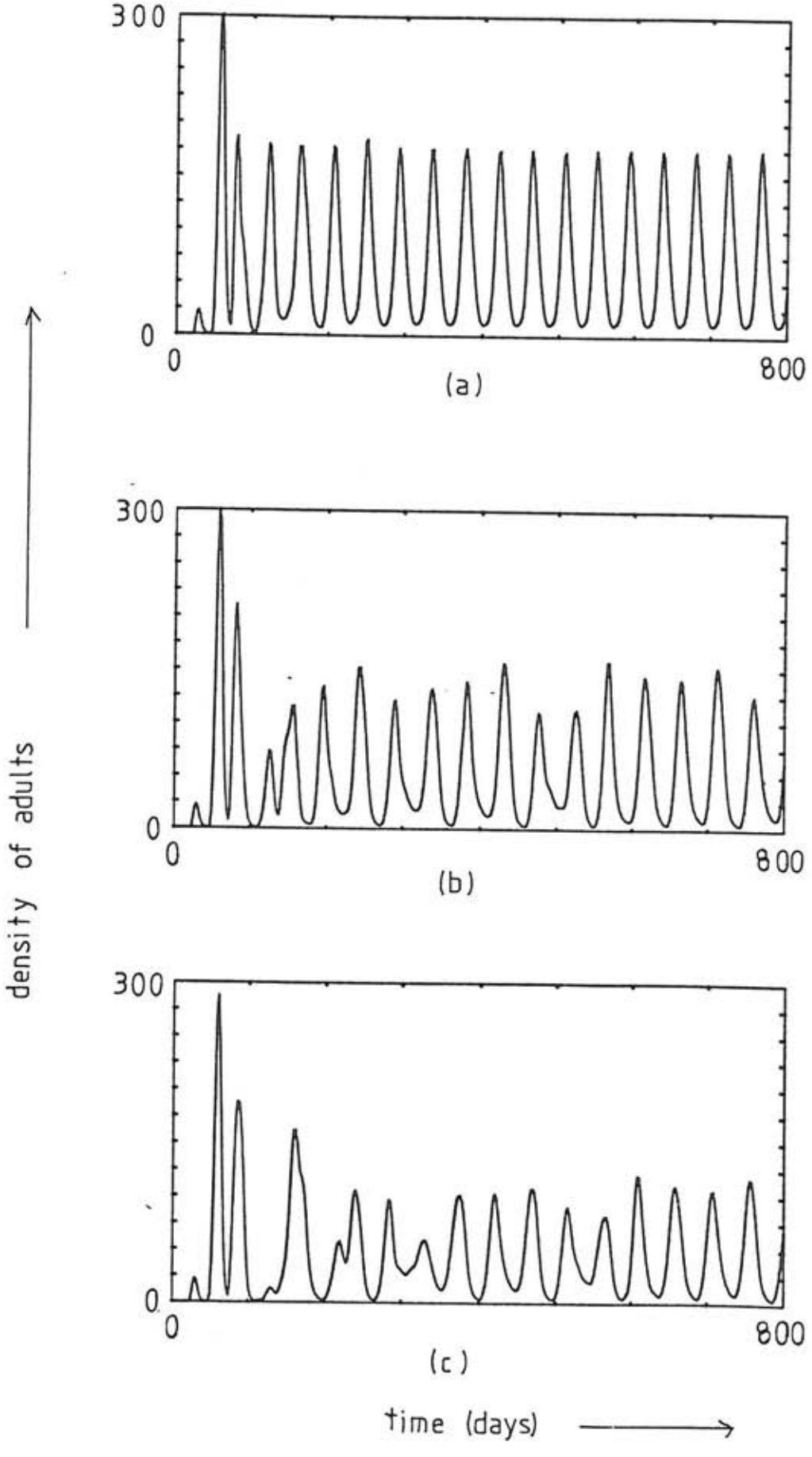
300
0
0
800
(a)
300
0
0
800
(b)
300
0
0
800
(c)
density of adults
time (days)

the fluctuations of the CTS experiment populations; for Model I it is not possible to obtain a steady state population of less than 95 adults at any point on the working range. With the second form of death rate considered, both models (Figs 5.3, 5.4) show the rapid establishment of limit cycles, behaviour not unlike that of the CTS experiments. The cycle periods of these oscillations are between 40 and 46 days for Model III and between 43 and 51 days for Model IV (c.f. Figs 5.3, 5.4), that is, they are larger than those of the Plodia populations. Both models have multiple initial population 'peaks'. These simulations show that consideration of food reserves (which we have incorporated into our model by considering the second form of death rate, albeit in a crude way) may have an important role to play in successful modelling of the Plodia populations; unfortunately we know of no data which could provide a more accurate estimate of how the per capita death rate may depend on feeding rate and/or feeding history.

It can be seen that the choice of development index can affect the behaviour of the model. Figs 5.3 and 5.4 show smaller cycle periods for 'time' as development index than 'weight' as development index; it can also be seen that the amplitude of these cycles may depend upon the index of larval development.

We have shown the behaviour of our models at the given points on the working range of steady states (c.f. Fig 4.3). It may be seen that as we move along this range, the amplitude of the cycles of both Model III and Model IV decrease, and approach that shown by Plodia as larval survival is decreased. This confirms our belief (Chapter 4) that larval interference has a significant effect on the regulation of the Plodia populations.

CHAPTER SIX

Chapter 6: Variable Fecundity

It is probable, although no such correlation was found in the AF experiment, that the fecundity of an adult female is related to her weight at emergence, as found by both Podoler (1974) and Snyman (1949), and that the explanation of the absence of such a relationship in the AF data lies in the fact that the weights recorded here are weights after death. Indeed, adult moths do not feed, so we would expect weight to be lost during the adults lifetime, in the case of adult females it is not unreasonable to suppose this reduction in weight may be related in some way to fecundity.

In this Chapter, we investigate the effect of introducing weight-dependent fecundity into our model. As Models I and II simulations do not in any way resemble the fluctuations of the CTS experiments, and Model IV has weight gained as a development index so that weight-dependent fecundity can have little or no effect on these fluctuations, we confine our attention to Model III. We use the relationship between fecundity and emergence weight given by Podoler (1974), whose larvae were fed on a similar food medium.

We begin by, as in our previous work, finding a new 'working range' of steady state egg and larva survivals - the previous working range only applies to the case where

fecundity is constant - and examine the behaviour of our model over this range. We conclude with a direct comparison between models with variable and constant fecundity.

6.1 Working range of Steady States

The relationship between steady state egg and larva→adult survivals given by equation (3.3), which provided our initial range of possible steady state survivals, applies to a constant fecundity model and does not apply to a model in which fecundity is variable. Our new range must be found by considering equation (3.1), or

$$E^* S_E^* S_L^* = 1 \qquad (6.1)$$

where, as no deaths occur during the pupa stage of the life-cycle, we replace larva→adult survival with larval survival. As argued in Section 3.2 we shall, as a result of the data of the EH and OB experiments, only consider values

$S_E^* \leq 0.5$ (equality iff no cannibalism)

$S_L^* \leq 0.35$ (equality iff no interference).

It can be shown that for a model with time in stage as development index and mortality corrected maturation distribution of the form given in Appendix A, the steady state larval survival is given by

$$S_L^* = \frac{\exp(-\delta^* \tau_{min})}{(r_0 \delta^* + 1)^6} \qquad (6.2)$$

where δ^* is the steady state larval per capita death rate, and the parameters r_0, τ_{min} are defined and estimated in Appendices A and B. Thus we may, for each value of S^*_L (< 0.35) find from equation (6.2) the steady state per capita death rate δ^*.

This in turn gives, via equation (4.8) (using parameter values given in Appendix B) the value of the steady state feeding rate I_M^*.

It can be shown that for this model the mean (steady state) larval maturation time τ^* is given by

$$\bar{\tau}^* = \tau_{min} + \frac{6 r_0}{\delta^* r_0 + 1} \qquad (6.3)$$

so that we may now find the (mean) steady state larval weight at maturation

$$w^* = \epsilon I_M^* \bar{\tau}^*$$

(c.f. equation (4.9)).

To find the number of eggs, E(w) which an individual larva maturing at weight w will lay as an adult, we use the relationship given by Podoler (1974), or

$$\log_{10}(E(w)) = 1.389 + 0.074w \qquad (6.4)$$

[N.B. The original equation has been modified to allow for exactly half the adult population being female, the weight lost during pupation (20% loss) and conversion from wet weight to dry weight.]

Thus, for each value of $S_L^* < 0.35$ we may, following the above procedure, find the (mean) steady state number of eggs produced per adult lifetime E^*, from which we find the corresponding steady state egg survival S_E^* (equation (6.1)).

We now note that equation (4.12) of Section 4.5, which relates steady state egg survival to steady state food density, is also valid in the context of a variable fecundity model, and hence following our argument of Section 4.5 take as our working range of steady states that part of the curve relating S_L^* and S_E^* on which S_E^* lies between 18% and 45%. Fig 6.1 shows our working range of steady state survivals, the dashed line corresponds to our previous working range for the constant fecundity model. We emphasize that this relationship is valid only for values of the relevant parameters as given in Appendix B. We note that along this working range, steady state fecundity E^* varies between 38.9 and 39.6 eggs per adult lifetime - figures not too different from those of the constant fecundity model.

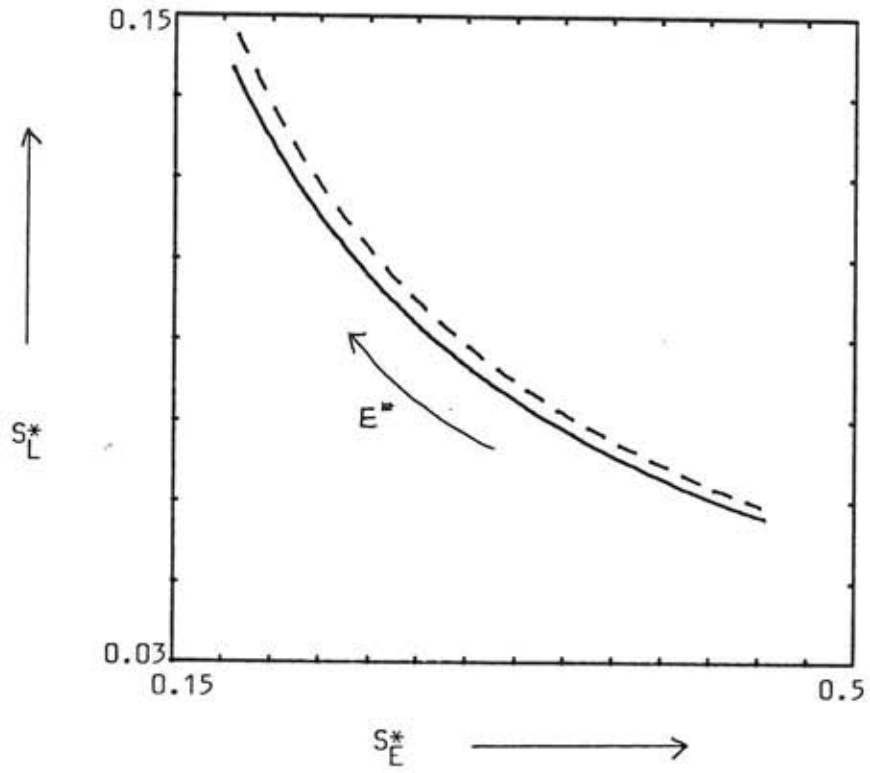

Figure 6.1. Working range of steady state survivals (———) for the variable fecundity model. The dashed line (----) shows the original (constant fecundity model) working range. E* increases along the range in the direction indicated.

6.2 Including Variable Fecundity

We include equations describing variable fecundity in our model in the following way. We write the maturation rate out of the larva stage as

$$M_L(t) = \int_o^t P(x,t)\ R_L(x)dx \qquad (6.5)$$

where P(x,t) denotes the proportion of individuals recruited at time x who mature out of the stage at time t, and note that the maturation weight of these individuals is given by

$$w(x,t) = \int_x^t g(t')dt' \qquad (6.6)$$

where g(t) is the individual growth rate as given by equation (4.9). The total number of eggs, E(w(x,t)), which such an individual will lay during its adult lifetime is given by equation (6.4); it will lay these eggs at a rate

$$f(w(x,t)) = \frac{E(w(x,t))}{\tau_A} \qquad (6.7)$$

eggs per day. Thus we take the total instantaneous egg production rate to be

$$R_E(t) = \int_{t-\tau_A-\tau_P}^{t-\tau_P} \int_o^u P(x,u)R_L(x)f(w(x,u))dxdu \qquad (6.8)$$

(c.f. Gurney and Nisbet (1985); equation (2.3) after correcting for distributed maturation, time spent

pupating, and the finite adult lifetime.)

6.3 Numerical Solutions

As with the models of Chapter 5, we find numerical solutions for our model with parameter values as estimated in the relevant section of Appendix B. As before, we assign values to the parameters α,β which will correspond to a chosen point of the working range of steady state survivals. Figs 6.2 show the behaviour of the model for three such points with a sharp innoculation of 60 eggs and an initial food density equivalent to 12 sections of unused food. We see that introducing weight dependent fecundity into Model III does not alter the basic behaviour of the model. The only noticable difference in the model behaviour is that while the constant fecundity model exhibits 2 large population peaks at the beginning of the simulation (Fig 5.3), the variable fecundity model has a single large initial population peak as observed in the CTS experiments; after the initial transient we observe the establishment of limit cycles whose amplitudes and periods closely resemble those of the constant fecundity model.

6.4 Variable versus constant fecundity

Variable fecundity is a 'delayed' effect of larval

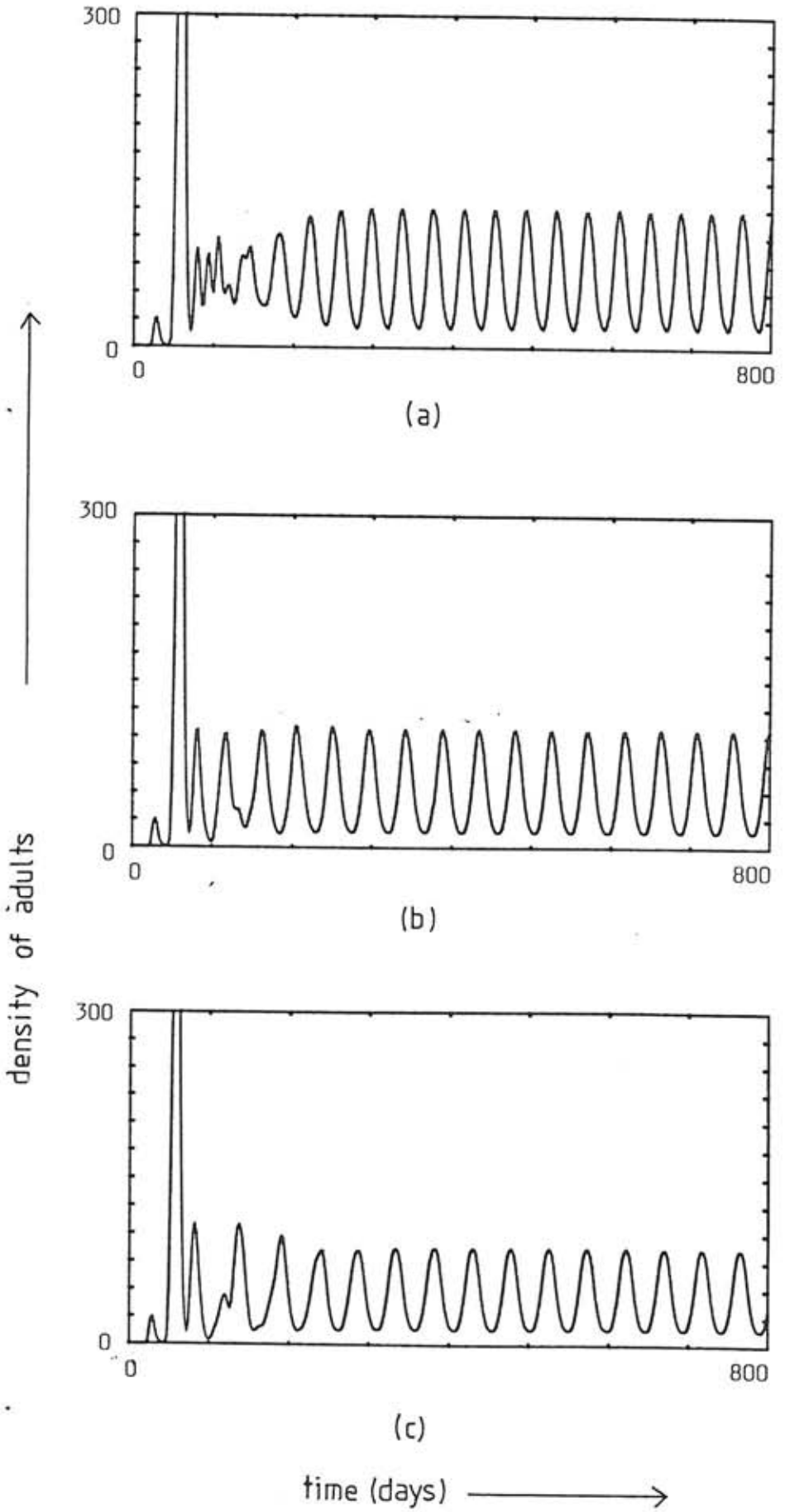
300
0
0
800
(a)
300
0
0
800
(b)
300
0
0
800
(c)
density of adults
time (days)

density on future recruitment so that were this the only means of population regulation we would expect oscillation periods in excess of twice the delay - the egg to adult generation time (Gurney and Nisbet, 1985). Our variable fecundity model contains both delayed regulation and immediate regulation implied by the density-dependent larval per capita death rate; we might expect the period of these oscillations to exceed those of the constant fecundity model. However, the similarity in cycle periods of both constant and variable fecundity models over the whole working range (Figs 5.3 and 6.2) suggest that cycle periods associated with immediate regulation dominate.

As shown by Fig 6.1, the simulations of Figs 5.3 and 6.2 cannot be directly compared as values of the steady state survivals and consequently the α, β parameters are not identical. Thus, we conclude this Chapter with a direct comparison between constant and variable fecundity. We choose one of our variable fecundity models (that with $S_L^* = 12.8\%$, $S_E^* = 19.8\%$) and consider the equivalent constant fecundity model which has identical steady state survivals and a constant fecundity parameter E whose value is that of the steady state E^* of the variable fecundity model.

Figs 6.3 shows the behaviour of these models for an innoculation of 60 eggs. We observe that the constant

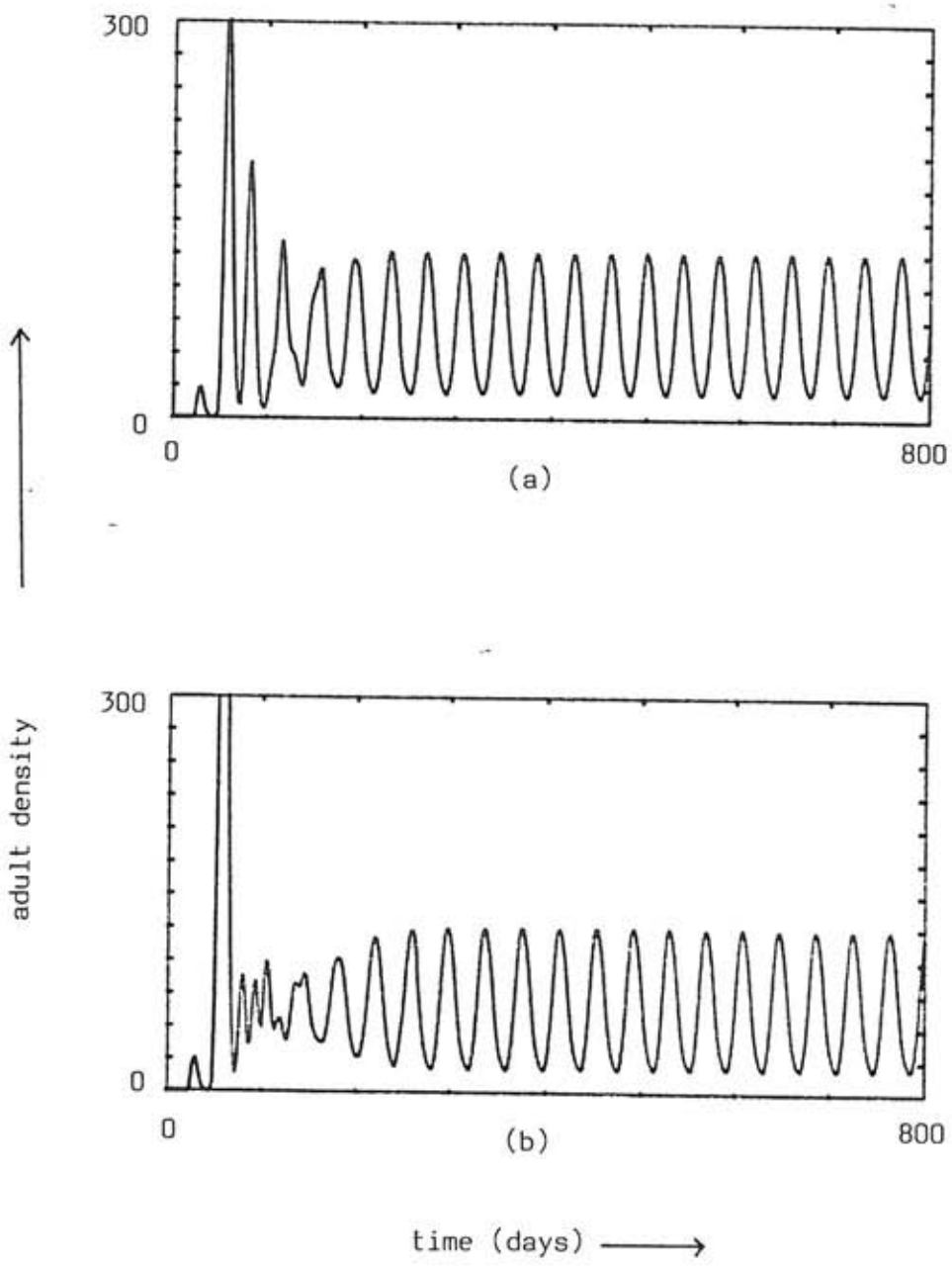

Figure 6.3. Numerical solutions for values of α and β chosen to correspond to the point $S_L^* = 12.8\%$, $S_E^* = 19.75\%$ on the working range of steady states

(a) fecundity constant, cycle period 38.8 days,

(b) incorporating weight-dependent fecundity, cycle period 39.0 days.

fecundity model has a cycle period of 38.8 days, the variable fecundity model a cycle period of 39.0 days; that is, the introduction of delayed regulation does increase cycle period - but very slightly! Fig 6.3 confirms that weight-dependent fecundity results in an initial population 'burst' of one generation as observed in the CTS experiments, whereas the constant fecundity model contains two large initial population peaks.

In view of the data presented by Podoler (1974) and Snyman (1949), the observation that the AF experiment measures female weight after death, and the simulations presented in this Chapter, we conclude that it is almost certain that the fecundity of an adult female depends on her weight at emergence. This implies that weight-dependent fecundity is another potential source of regulation of the Plodia populations.

However, as discussed in Chapter 3, the inclusion of variable fecundity in our model cannot significantly affect the range of possible steady state survivals ; this is also shown by Fig 6.1. Based on Fig 6.1 and the simulations of constant and variable fecundity (Figs 5.3, 6.2 and also Fig 6.3), we conclude that regulation by variations in fecundity has no significant effect on the long-term dynamics of the population, and its contribution towards regulation of the CTS experiment populations is negligible.

CHAPTER SEVEN

Chapter 7: Interlude.

7.1 Summary.

The study of *Plodia* was motivated by a need to investigate the effects of density in the pre-adult stages on the dynamics of a population in culture. We have shown (Chapter 3) that a number of such factors operate in regulating the CTS experiment populations, these being larval competition for food and larval interference, both of which act to vary larval survival, and cannibalism of eggs by larvae (which evidently varies egg survival).

As discussed in Chapter 6 the fecundity of adult females almost certainly depends upon weight at emergence, thereby providing an additional source of population regulation. However, we have shown that this mechanism has almost *no* effect on the long-term dynamics of the population; it is larval competition (for food and by interference) and egg cannibalism which are almost wholly responsible for regulation of the CTS experiment populations.

We have been able (Chapters 3 and 4) to roughly estimate the extent to which each of the above mechanisms contributes towards regulation. We have shown that competition for food reduces larval survival from a

maximum of ≃ 90% to ≃ 35% at the food density of the CTS experiments, with survival reduced further to ≃ 10% as a result of interference. Further experiments along the lines of those of Bakker (1961) on larvae of the fruit fly Drosophia melanogaster would provide further information on the relative sizes of these two types of larval competition.

Models III and IV show, respectively, cycle periods of between 1.5 to 1.8 and 1.6 to 1.96 times the (steady state) delay, the delay in this case being the egg to adult development time. These cycle periods correspond to period to mean (steady state) generation time ratios of 1.2-1.35 and 1.26-1.4, and therefore suggest that the population fluctuations of the CTS experiment may result from the perturbation of a stable limit cycle whose period is 'one and a bit' times the generation time.

7.2 Failures of the model

Neither of the development indices we have considered is a suitable measure of larval development. Larvae may pupate both over a wide range of mean weights (e.g. Snyman, 1949, also CTS and OB experiments) and after a wide range of mean maturation periods (e.g. Podoler 1974, also AE and OB experiments); it is likely that larval competition for food affects both maturation time and weight. Our models assume that maturation is triggered

by either chronological age (Model III) or by weight (Model IV); consequently neither model can possibly reproduce all the data - time in stage as development index will not produce the increase in development time observed between AE and OB experiments, weight as development index will not give the weight/density curves of the CTS and OB experiments. It may be necessary to consider as a measure of development some quantity dependent upon both of these.

The mean egg to adult development period increases from $\simeq$ 25 days during the AE experiment to $>$ 32 days during the OB experiments; we expect the development period of the CTS experiment to lie between these two figures. Thus, as the observed cycle period is $\simeq$ 38 days, we find the Plodia populations have a period to delay ratio of between 1.2 and 1.5, or a period to generation time ratio lying between 0.95 and 1.15. That is, the Plodia population fluctuations appear to have a period very close to the generation time; our models are yielding period to delay ratios which are too large.

7.3 The OB data

We have included in our model two ways in which larvae may compete - via changes in food density (competition for food) and by direct interference. Closer inspection of the OB data suggests that larvae may also be competing

in a third way.

It can be see from Table 7.1 that the mean cohort emergence time is systematically related to the replicate of the CTS experiment from which its food originated. That is, cohorts feeding on food remaining from a given replicate show much the same maturation period regardless of the initial size of the cohort whereas the maturation period varies between replicates. This suggests that the development time depends on the 'history' of the food provided.

Plodia larvae spin large quantities of silk and deposit faeces (Benson, 1974) and may also emit pheromones. Examination of the medium remaining after the OB experiments showed that it consisted of ∝ 40% faeces and ∝ 60% bran (with faeces making up 60% of the oldest section), and that approximately 25% of the area was covered with silk. We would expect the presence of such quantities - which we shall refer to collectively as 'junk' - to reduce the rate at which an individual may search, thereby increasing the maturation time. Such an effect would explain the data of the OB experiments :- the three replicates of the CTS experiments are not identical, so that the medium remaining would contain differing amounts of 'junk'. During the OB experiments, larvae are both feeding and producing 'junk'; this also provides an explanation of why second OB cohorts fail to

Replicate of CTS experiment from which food is obtained	Initial larval density (larvae per unit area)	Mean larva to adult maturation time (days)
1	60	38.1
	150	39.2
	270	41.9
2	30	37.0
	180	35.8
	240	37.5
3	105	32.7
	210	32.4
	300	32.0

Table 7.1

survive.

7.4 Discussion

We believe that we have adequately represented the dynamics of all stages of the life-cycle with the obvious exception of the larval stage. Within this stage there are two 'flaws' in the structure of our model :- neither of the development indices we have considered is a true measure of the development of *Plodia* larvae; our model includes two ways in which larvae may compete, yet the OB data show that larvae may also be competing by depositing 'junk'.

In the models of Chapters 4 and 6, the population oscillations all have period to delay ratios in excess of that of the CTS experiment population. Although many factors may influence the size of this ratio - such as the extent of egg cannibalism or the functional form of the larval per capita death rate - we shall consider whether the excessively large (model) period to delay ratios may be a *direct* result of the failiure of our models to properly reflect the types of competition and/or the development of *Plodia* larvae.

The mechanism(s) whereby 'junk' may act to increase the maturation time - i.e. decrease the development rate -

are by no means obvious. In the case of faeces, we might expect their presence to reduce the larval search rate via a handling time (as discussed in Chapter 4) thereby decreasing the development rate. We note that Plodia larvae convert food eaten into weight gained with an efficiency of ≈ 10% (see Appendix B), so we would expect a considerable proportion of food eaten to be deposited as faeces. We would also expect the presence of silk and possibly pheromones to impede larval search, although this may not necessarily occur through a handling time. It may be that these quantities act to make certain areas and food items inaccessible to searching larvae, thus slowing development.

However, this type of competition is fundamentally quite different from either competition for food or interference competition. When larvae compete by depositing junk, they are producing quantities which act to decrease the rate at which other larvae may develop.

In Section II we propose to consider a strategic model of larval competition whose purpose is to determine the extent to which the above factors - choice of development index or manner of competition - may influence the dynamics of the model.

7.5 Introduction to Section II.

Our Section I study of the population dynamics of *Plodia* highlights two problems. We are unable to find a suitable measure of larval development, and we find that larval competition occurs in a combination of three ways, but are unable to determine the extent to which each type of competition contributes towards regulation of the population.

Such questions are in general difficult or costly and time consuming to answer experimentally. Evidently determining what factor or factors are responsible for triggering pupation requires some knowledge of what to measure! Similarly, measuring the extent of different types of competition would require *a priori* knowledge of how competition may occur. Standard competition experiments measure survival and stage duration for a given size of cohort provided with a known quantity of food; such experiments would also necessarily measure any competition which occurred via junk density.

These problems are common to all laboratory insect populations in which it is not immediately obvious as to what triggers pupation and/or where there is the possibility that there may be more than one type of competition. Thus, there is evidently a need for a theoretical study to determine how these factors may

affect the dynamics of the population. Furthermore, such a study should not be confined to one particular insect species.

Consequently, we approach the problem of considering how the type of competition or choice of development index may influence the population dynamics in a general way. We shall consider a strategic model of larval competition, capable of answering these questions, in which the type of competition and larval development index are not defined.

7.5.1 A strategic model of larval competition.

We are concerned with how the dynamics of the larval stage of the life-cycle can influence the stability and cycle period of our model. Thus, we shall consider a simple two-stage model comprising of an adult and a larval stage.

As we are not concerned with the effect of the dynamics of the adult stage on model behaviour, we simplify the dynamics of this stage by assuming a constant per capita death rate and constant adult fecundity; we assume that recruitment to the larval stage will be at all times directly proportional to the size of the adult population.

Our model is to be capable of determining the extent to which the choice of a larval development index can influence the behaviour of of the model, and must therefore allow for a variable maturation time.

We do not wish to examine how variations in the functional form of the larval per capita death rate influence the behaviour of our model, so we shall choose one particular functional form. As population regulation will occur via the variable maturation time it is not necessary to include a time-dependent per capita death rate and so we shall, for simplicity, take the larval per capita death rate to be constant.

The model we are to be considering is a two-stage model in which the sole means of population regulation is via the variable larval maturation time. We shall assume that an individual larva matures into an adult upon gaining a fixed increment Q of development. We further assume that competition between larvae ultimately results in a time-dependent larval development rate.

We define variables

$\rho_L(t)$ = density of larvae at time t

$\rho_A(t)$ = density of adults at time t

R(t) = recruitment rate into the larva stage at time t

$M(t)$ = maturation rate out of the larva stage at time t

$D(t)$ = larval development rate at time t

$\tau(t)$ = time spent in stage by a larva maturing at time t.

Without loss of generality, we take our unit of time to be the mean adult lifetime (i.e. the inverse of the adult per capita death rate). Then we may write

$$\frac{d\rho_L}{dt} = L\rho_A(t) - M(t) - \delta\rho_L(t)$$

$$\frac{d\rho_A}{dt} = M(t) - \rho_A(t) \qquad (7.1)$$

$$Q = \int_{t-\tau(t)}^{t} D(t')dt'$$

$$R(t) = L\rho_A(t)$$

$$M(t) = R(t-\tau(t))\, e^{-\delta\tau(t)} \frac{D(t)}{D(t-\tau(t))}$$

where

L = mean number of offspring produced per adult lifetime

δ = larval per capita death rate

The model is not yet complete as we have not specified any relationship between the development rate D(t) and the density of larvae $\rho_L(t)$. Such a relationship may be found by considering a particular type of competition and a given index of larval development. The models we shall be considering throughout this section will be given by equations (7.1) together with an appropriate relationship between D(t) and $\rho_L(t)$.

7.5.2 . Period to delay ratios.

Gurney & Nisbet (1985) have shown that the size of the period to delay ratio may be used to distinguish between two broad classes of competition. As discussed in Section 7.4 we wish to determine whether the size of this ratio may be systematically related to the manner of competition, in which case it would provide a useful means of discriminating between types of competition.

We shall be considering models which are given by equations (7.1); the model has a single delay - the larval maturation time. It follows that the characteristic equation will be of the form

$$F(\lambda) + G(\lambda)e^{-\lambda\tau} = 0 \qquad (7.2)$$

where F and G are analytic functions of λ. The stability

of systems with characteristic equations of this form in which F and G are low order polynomials have been studied in detail by Cooke & Grossman (1982); more recently Cooke & van den Driessche (1986) deal with analytic F and G. Cycle periods are generally found numerically, although Mahaffy (1982) shows that when F and G are polynomials of a particular form, the period to delay ratio at the stability boundary will be greater than 2.

To determine what factors control the size of the period to delay ratio requires a method for estimating this ratio - we do not wish to be confined to numerical studies. As many biological models exhibiting periodic solutions have characteristic equations of the form (7.2) (e.g. Busenberg & Cooke 1982, Cushing 1977, MacDonald 1978) we present in Chapter 8 a technique for evaluating the period to delay ratio near stability boundaries for systems whose characteristic equation is of this form.

7.5.3 . Larval competition.

Determining how different types of larval competition may influence the stability and cycle period of our model requires that we compare and contrast the behaviour of models in which only one type of competition occurs. Thus, for the three types of competition found in *Plodia* we would have to consider three models. In each model, competition would operate in just one way - by direct

interference, by competition for food or by the deposition of junk.

For the class of models given by equations (7.1), competition between larvae implies that the development rate must depend in some way on the density of larvae. Bearing in mind that we wish to consider in as general a way as is possible the effect of the manner of competition on the dynamics of our model, we consider, in Chapter 9, two separate models of larval competition. In the first model we assume that larvae compete 'directly', that is, that the sole means of competition is by interference so that the development rate D(t) is a function of the larval density $\rho_L(t)$. We assume that changes in the development rate, and therefore changes in the maturation time, can occur solely through changes in $\rho_L(t)$. In the second model we assume that the development rate is a function of a single time-dependent quantity X(t), and that larvae compete by varying this quantity. We do not specify the quantity X(t) - it may, for example, represent food density or junk density. In this model, competition is 'indirect'; it is mediated through the quantity X.

Both these classes of models consider general relationships. The functional dependence of D(t) on either $\rho_L(t)$ or X(t) is not specified - we merely assume such a relationship exists. We apply the technique

developed in Chapter 8 to determine the period to generation time ratio for each class of model. We show that this ratio is smallest when competition is direct. We also show that when competition is direct, the period to generation time ratio may be estimated knowing only the value of the (steady state) delay.

In Chapter 10 we return to the problems encountered in our Section I study of Plodia. We have shown that larvae compete in three ways - by direct interference, by competing for food and by depositing 'junk'. We shall in Chapter 10 consider how these three quite different types of competition may affect the dynamics of the population. We shall consider a strategic model of the form given by equations (7.1), in which we shall derive a functional form for the development rate, in which both the age and weight play a part in determining the state of development of an individual larva, which incorporates the three types of competition. We then consider separately three special cases of the model - in each, just one of the three types of competition operates. Evidently, in each of these models the development rate will be a function of a single time-dependent variable (larval, food or junk density), so that we shall be considering one model of direct interference and two of indirect competition, as discussed in Chapter 9.

SECTION II

STRATEGIC MODELS OF LARVAL COMPETITION

CHAPTER 8

Chapter 8 : Period to delay Ratios near Stability Boundaries.

In this Chapter, we present a technique for evaluating the size of the period to delay ratio at the stability boundary or boundaries, for systems having a characteristic equation of the form

$$F(\lambda) + G(\lambda)\, e^{-\lambda\tau} = 0. \qquad (8.1)$$

We choose τ or one of the parameters of F and G to be a "free" parameter. For any values of the remaining parameters, the free parameter is given a value which will ensure that the point in parameter space lies on the stability boundary.

In Section 8.1 we consider characteristic equations (8.1) in which F and G are independent of the delay τ. In this case, τ itself is a natural choice for the free parameter, and the period to delay ratio T/τ may be easily found for any given values of the parameters of F and G. We also establish the conditions for which T/τ will take values in the ranges $(1,2)$, $(2,4)$ and $(4,\infty)$.

When characteristic equations of the form (8.1) arise from the linearization about a steady state of a non-linear system, the functions F and G may depend on the

delay - or, when such systems have a variable delay, the steady state delay. In this case, the particular form of the equation will determine the most convenient choice of the free parameter, τ is not necessarily the most suitable, and such equations should be considered individually. In Section 8.2, we consider one particular model of the type given by equations (7.1) - the Gurney & Nisbet (1985) Maturation Time model, whose characteristic equation is of this form, and show how with a suitable choice of the free parameter, many of the methods of Section 8.1 may be adapted and we find the period to delay ratio for given parameter values.

8.1 Linear Systems with One Delay

We consider linear systems which have a characteristic equation of the form

$$F(\lambda) + G(\lambda)e^{-\lambda\tau} = 0 \qquad (8.2)$$

where F and G are regular functions of λ and do not depend on the delay τ. Even for simple equations of this form, the stability properties can be complicated, with the possibility of several changes between stability and instability as the delay τ is increased (Cooke & Grossman 1982, Cooke & van den Driessche 1986). We assume F and G are such that

$$\overline{F(-i\omega)} = F(i\omega); \qquad \overline{G(-i\omega)} = G(i\omega);$$

for real ω, so that purely imaginary solutions occur as complex conjugate pairs.

We seek to evaluate the ratio of the period of oscillations to the delay, T/τ, at bifurcation points where solutions become unstable, that is, at the stability boundary or boundaries. The stability boundary defines a relationship between the coefficients c_i of F and G and the delay τ, implying that at any point on the boundary, it is possible to evaluate T/τ in terms of the c_i alone; at each point τ is given a value which ensures that the characteristic equation has a purely imaginary solution.

We begin by writing equation (8.1) in the form

$$P(\lambda) + iQ(\lambda) - [A(\lambda) + iB(\lambda)]\, e^{-\lambda\tau} = 0 \qquad (8.3)$$

where A, B, P and Q are real-valued functions of λ and the c_i. As solutions of equation (8.3) will occur as complex conjugate pairs, we seek only solutions $\lambda = i\omega$ where $\omega>0$. For equations (8.3) having a zero solution, see Appendix C. Substituting $\lambda=i\omega$ into equation (8.3) yields a pair of simultaneous equations.

$$\begin{aligned} A_\omega \cos\omega\tau + B_\omega \sin\omega\tau &= P_\omega \\ B_\omega \cos\omega\tau - A_\omega \sin\omega\tau &= Q_\omega \end{aligned} \qquad (8.4)$$

where $A_\omega = A(i\omega)$, $B_\omega = B(i\omega)$, $P_\omega = P(i\omega)$ and $Q_\omega = Q(i\omega)$

are functions of ω and the c_i. Equations (8.4) have solutions

$$\cos\omega\tau = \frac{X^2-1}{X^2+1} \qquad \sin\omega\tau = \frac{2X}{X^2+1} \tag{8.5}$$

where $X \left[\equiv \cot\frac{\omega\tau}{2}\right]$ is given by

$$X = \frac{B_\omega P_\omega - A_\omega Q_\omega}{A_\omega^2 + B_\omega^2 - A_\omega P_\omega - B_\omega Q_\omega} \; . \tag{8.6}$$

From equations (8.4) it can be seen that if $\omega \in \mathbb{R}$ solutions exist, then

$$A_\omega^2 + B_\omega^2 = P_\omega^2 + Q_\omega^2. \tag{8.7}$$

If no values of the coefficients give $\omega \in \mathbb{R}$ solutions to equation (8.7), then no changes in stability can occur. If such solutions do exist, then equation (8.7) defines a relationship between ω and the c_i, and can therefore be used to eliminate ω from the expression A_ω, B_ω, P_ω, Q_ω, so that X can now be found knowing only the values of c_i.

It can be seen from equations (8.5) that as X increases from $-\infty$ to ∞, $\cos\omega\tau$ will decrease from 1 to -1 and then increase to 1 (c.f. Fig 8.1); and that moreover

$$\frac{d}{dX}(\omega\tau) = \frac{-2}{X^2+1} < 0 \qquad \text{for all X.} \tag{8.8}$$

That is, as X increases from $-\infty$ to ∞, $\omega\tau$ must decrease monotonically from $2m\pi$ to $2(m-1)\pi$ for some $m \in \mathbb{N}$, and is

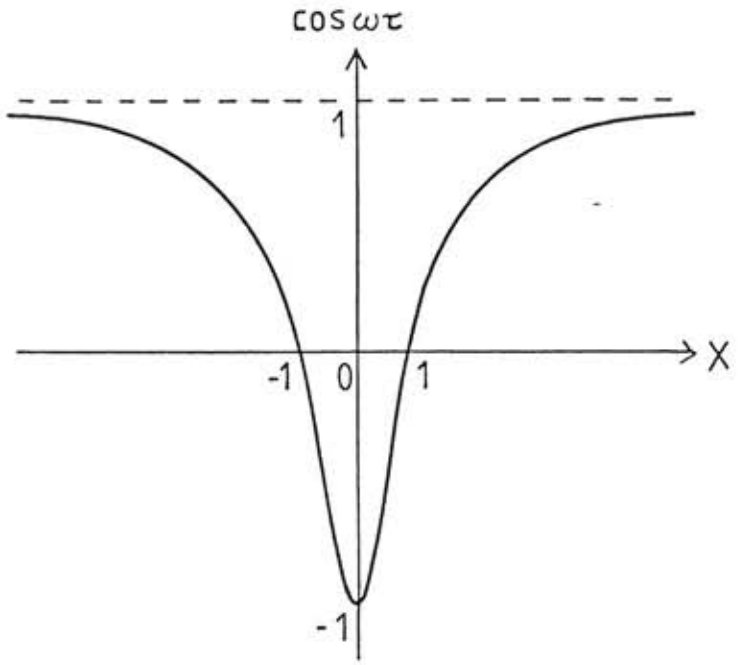

Figure 8.1. Variation of cosωτ with X.

therefore given by

$$\omega\tau = \begin{cases} 2m\pi - \alpha & X<0 \\ 2(m-1)\pi + \alpha & X\geq 0 \end{cases} \qquad (8.9)$$

where $\alpha = \cos^{-1}\left[\frac{X^2 - 1}{X^2 + 1}\right] \in [0,\pi]$ and m = 1, 2, 3...

Fig 8.2 shows the first three of these curves (i.e. m=1,2,3).

Roots cross the imaginary axis when equations (8.6),(8.7) and (8.9) are all satisfied; as X and ω may be found in terms of the c_i using (8.6) and (8.7), it follows that equation (8.9) defines a relationship between τ and the c_i. For any given values of the c_i, there exist a number of values of τ (given by m=1,2,3...) which will ensure that the characteristic equation (8.2) will have purely imaginary solutions. It is this multiplicity of values of τ for given c_i which can in some cases give rise to stability switching. Cooke and Grossman (1982) show that if (8.2) is stable for τ = 0 and if

$$Z = \text{sign}\left[\frac{d\,(Re\lambda)}{d\tau}\right]_{\lambda = i\omega}$$

is positive for m = 1, 3, ... 2k + 1 and negative for m = 2, 4, ..., 2k (for some k) then changes in stability will occur as the delay parameter is increased. However, if the system is stable for τ = 0 and Z is positive for <u>all</u> values of m, then the system will become unstable when τ reaches a value given by equation (8.9) for m = 1,

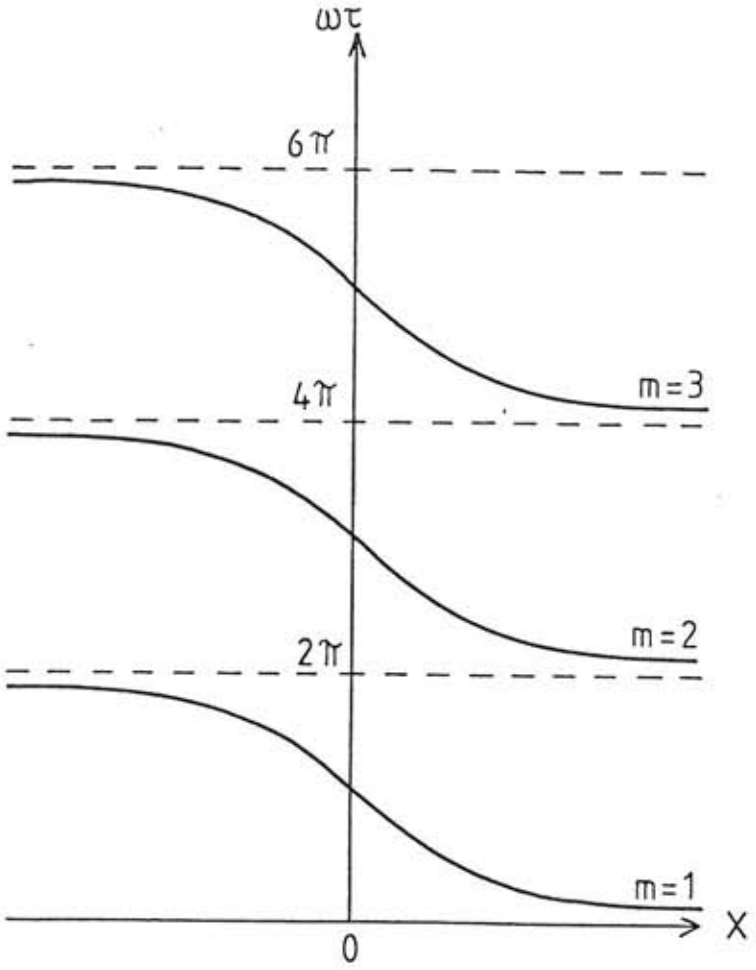

Figure 8.2. Variation of $\omega\tau$ with X for $\omega > 0$ and $m = 1,2,3$.

and remain unstable as τ is increased further. The solutions m = 2, 3,... then correspond to new roots λ crossing the imaginary axis from left to right.

The period to delay ratio, T/τ, is related to $\omega\tau$, for $\omega>0$, by

$$T/\tau = \frac{2\pi}{\omega\tau}$$

and is thus given by

$$T/\tau = \begin{cases} \dfrac{1}{m - \frac{\alpha}{2\pi}} & X < 0 \\ \dfrac{1}{m - 1 + \frac{\alpha}{2\pi}} & X \geq 0 \end{cases} \qquad (8.10)$$

where $\alpha = \cos^{-1}\left[\dfrac{X^2 - 1}{X^2 + 1}\right] \in [0,\pi]$ and m = 1, 2, 3....

We have only considered the positive root $\lambda = i\omega$ where $\omega>0$. For the conjugate root $\lambda = -i\omega$, X will change sign, and $\omega\tau$ will lie in the interval $(-2m\pi,-2(m-1)\pi)$ for some $m\in\mathbb{N}$; we have confirmed that the period to delay ratio T/τ is exactly the same for both roots, and is given by equation (8.10) where X is evaluated at the positive root.

The above procedure makes use of the fact that τ only appears in the exponential term of the characteristic equation, so that X is independent of τ at the stability boundary, making τ a natural choice for the free

parameter. However, it should be emphasized that all the above equations hold at a stability boundary even when F and G depend on the delay τ. In particular, equation (8.10) defining the relationship between T/τ and X holds at a boundary. It can be seen that for any particular value of m, that is, for a given stability boundary, T/τ will lie in the interval

$$\left[\frac{1}{m} , \frac{1}{m-1} \right]$$

so that periods exceeding the delay are only possible for

m = 1 (c.f. Fig. 8.3). Furthermore, it can be seen that X must be negative for $T/\tau \epsilon$ (1, 2), $X \epsilon$ (0, 1) for $T/\tau \epsilon$ (2, 4), and T/τ will be greater than 4 for X > 1, so that calculating the range of X provides bounds on the period to delay ratio. Fig. 8.3 also shows that when stability switching (in the sense of Cooke and Grossman) occurs, the period will exceed the delay only at the first stable-unstable change, and that the period to delay ratio becomes progressively smaller with each further stable-unstable change.

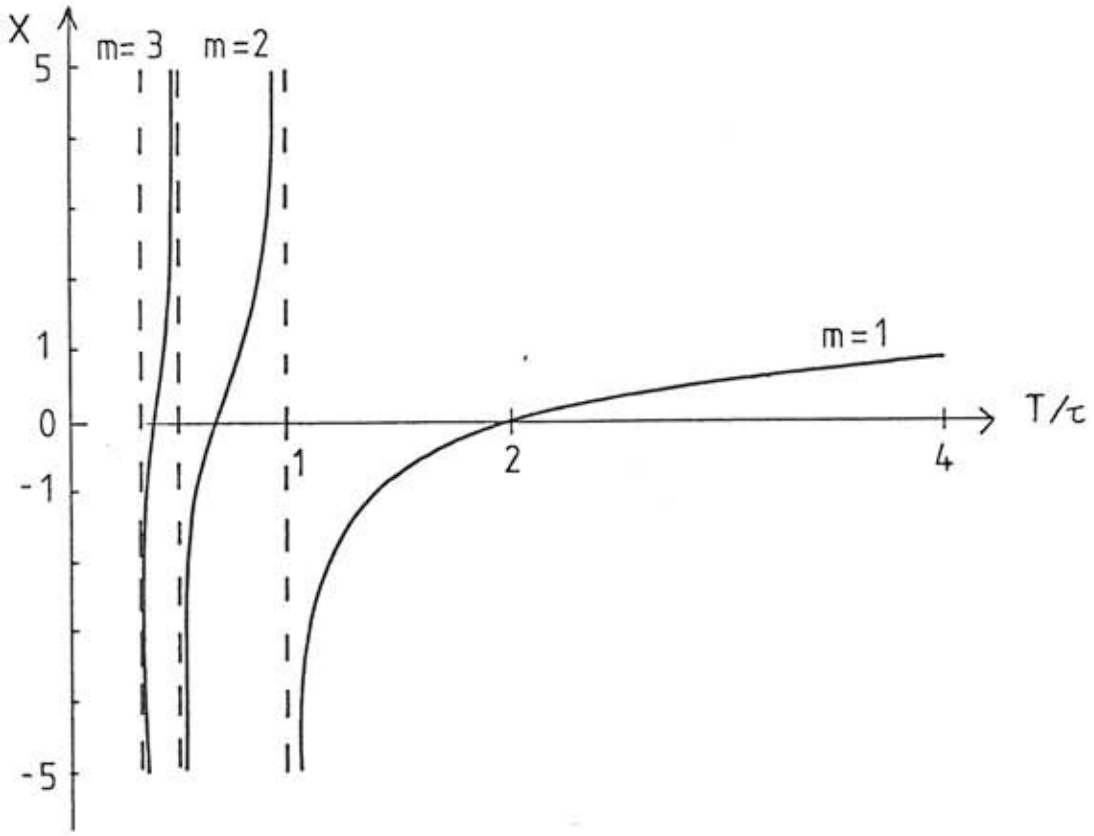

Figure 8.3. Variation of the period to delay ratio, T/τ with X for m = 1,2,3. For each $m \in \mathbb{N}$, T/τ lies in the interval $(1/m, 1/(m-1))$.

8.2. A Model of Larval Competition

We now illustrate how to deal with the general case of characteristic equations of the form (8.1) in which F and G depend on τ by considering a particular example - the Gurney & Nisbet (1985) Maturation Time model. After suitable scaling, this model is of the form given by equations (7.1). Larvae mature into adults upon reaching a given weight, and the growth, or development, rate D(t) is given by

$$D(t) = \frac{1}{1 + \rho_L(t)} \qquad (8.11)$$

As the maximum possible development rate is 1, it follows that the parameter Q of equations (7.1) represents the minimum possible larval maturation period, τ_{min}. The model has a single non-trivial steady state, which is positive provided values of the parameters are such that it is possible for each adult to produce at least one surviving offspring. This condition is satisfied provided $L > 1$ and $\tau > \tau_{min}$: in the following we assume these conditions hold.

It can be shown (see Appendix C) that linearization about this steady state yields the characteristic equation

$$\lambda^2 + \lambda(1-\Gamma) + \Gamma(L-1) - [\lambda(1-\Gamma) + \Gamma(L-1)]\, e^{-\lambda\tau} = 0 \qquad (8.12)$$

where

$$\Gamma = \frac{\ln(L)}{(L-1)} \frac{1}{\tau} \left[1 - \frac{\tau_{min}}{\tau} \right] \qquad (8.13)$$

and τ is the steady state larval maturation time. This equation is of the form of equation (8.1), but F and G now depend on the delay τ. Equation (8.12) has the solution $\lambda=0$ for all values of the parameters: we show in Appendix C that this is not a valid eigenvalue for the model, and hence seek only non-zero imaginary eigenvalues $\lambda=i\omega$. Equations (8.4) and (8.5) become

$$\Gamma(L-1)\cos\omega\tau + \omega(1-\Gamma)\sin\omega\tau = \Gamma(L-1) - \omega^2$$

$$\omega(1-\Gamma)\cos\omega\tau - \Gamma(L-1)\sin\omega\tau = \omega(1-\Gamma) \qquad (8.14)$$

and

$$\omega^2 = 2\Gamma(L-1) \qquad (8.15)$$

Solving (14) for $\cos\omega\tau$ and $\sin\omega\tau$ enables us to calculate X (c.f.equation (8.5)) as

$$X = \frac{\sin\omega\tau}{1-\cos\omega\tau} = \frac{\omega(\Gamma-1)}{\Gamma(L-1)} \qquad (8.16)$$

We use equations (8.15), (8.16) and (8.9) to find those curves in parameter space where the characteristic equation has purely imaginary solutions. Fig.8.4 shows the first three of these curves (i.e. m=1, 2, 3) for one particular value of L. To determine if each of these curves represents a change in stability, we use a slight variation of the Cooke and Grossman technique: we observe that for a given value of L, contours of constant Γ (the

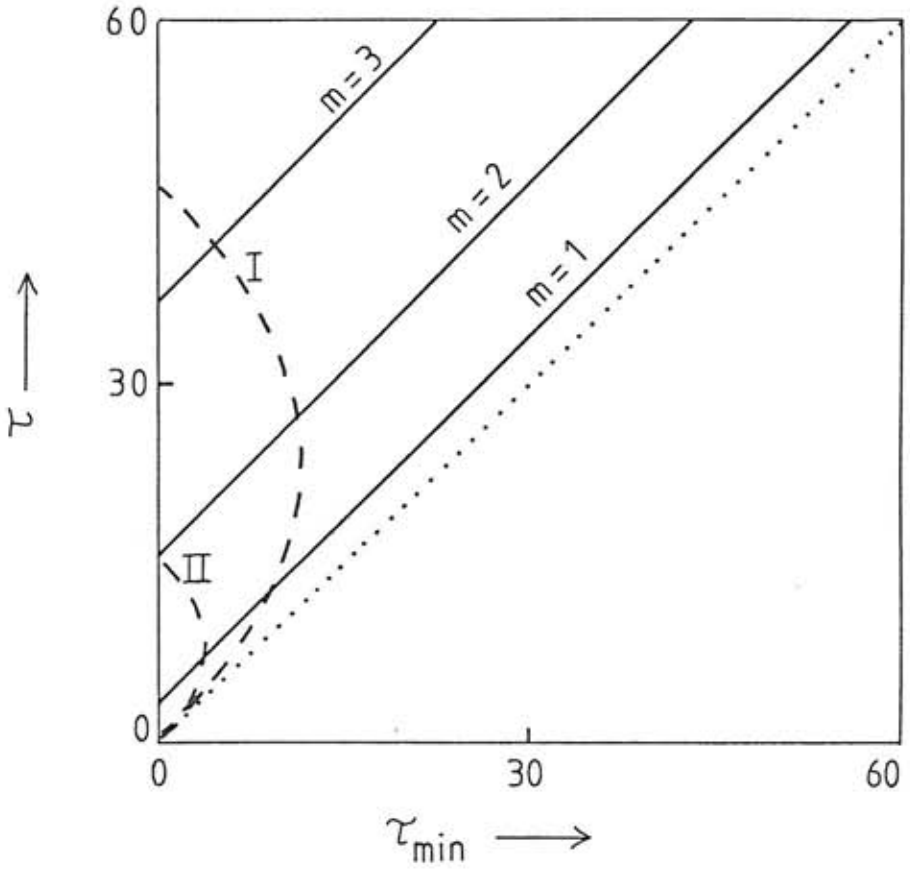

— Figure 8.4. Curves where Re(λ) = 0 for L = 100 and m = 1,2,3. The dashed lines (---) are curves of constant Γ :- I is Γ = 0.001, II is Γ = 0.003.

dashed lines in Fig. 8.4) cover the whole region of parameter space, and so we find the rate of change of $Re(\lambda)$ with τ along an arbitrary Γ = constant curve when $\lambda=i\omega$. It can be shown that

$$\left[\frac{dRe(\lambda)}{d\tau} \right]_{\substack{\lambda=i\omega \\ \Gamma=const}} > 0$$

for all values of m, L and Γ, implying (see Fig 8.4) that it is the curve m=1 which is the local stability boundary - other values of m corresond to new roots crossing the imaginary axis from left to right, and not to a further change in stability. It follows (equation (8.10) and Fig 8.3) that periods will, as expected, exceed the delay.

Fig. 8.5 shows the local stability boundary for L=5, L=10, L=50 and L=200. For each given value of L and points (τ_{min},τ) lying below the boundary, the steady state is locally stable, above the boundary it is locally unstable. It can be seen from Fig. 8.5 that the delay must be above a certain minimum value τ_L (which depends on L and is the value of τ at which the boundary meets the τ-axis) for instability to be possible.

When calculating the period to delay ratio at the stability boundary, we may use one of two methods. By eliminating ω from equations (8.15) and (8.16) it can be seen that X depends on all three parameters L, τ and

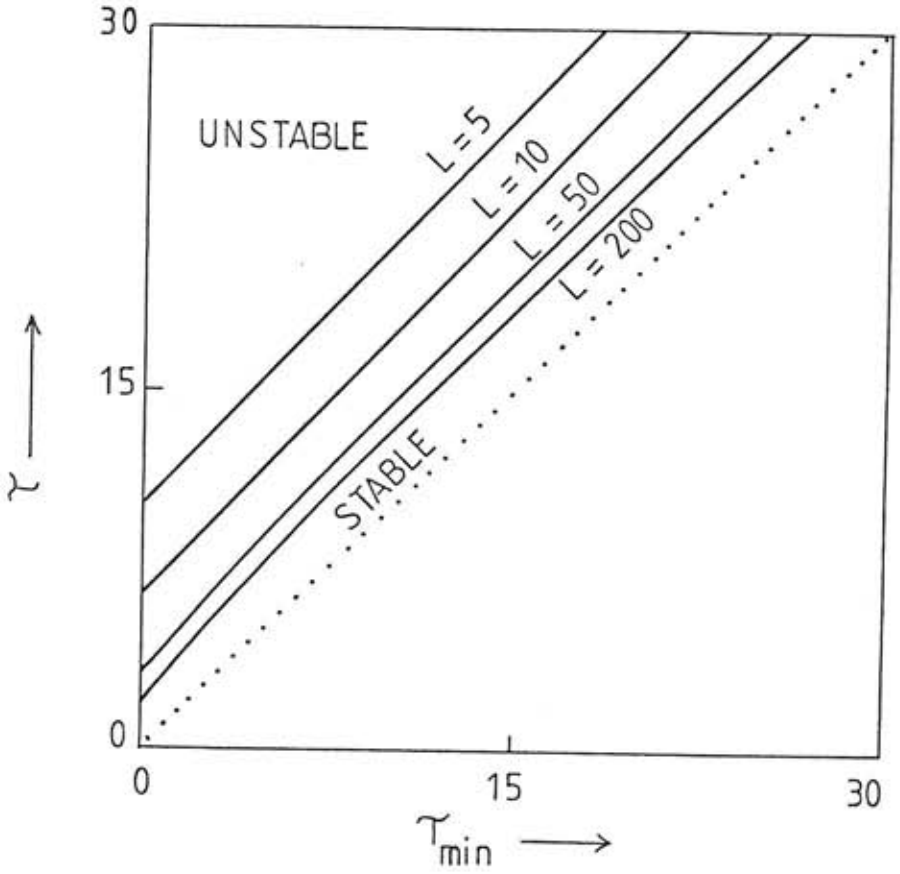

Figure 8.5. Local stability boundaries for L = 5,10,50,100. For each L, the steady state is locally stable for points (τ_{min},τ) lying below the boundary.

τ_{min}. Hence, for any given values of L, τ and τ_{min} which lie on a stability boundary we may find X and therefore T/τ. Alternatively, following the approach of Section 8.1, we may choose one of L, τ or τ_{min} to be a free parameter. As τ_{min} only appears in the parameter group Γ, we choose this as our free parameter. For each value of L and any value of τ above the threshold value τ_L, a value of τ_{min} (and therefore Γ) can be found which will ensure that the point in parameter space lies on the local stability boundary (c.f. Fig 8.5); for values $\tau < \tau_L$ no such value of τ_{min} can be found and the steady state is always locally stable.

With τ_{min}, or Γ, as our free parameter, we eliminate Γ from equations (8.15) and (8.16) to give

$$X = \frac{\omega}{L - 1} - \frac{2}{\omega}$$

or, writing $f = \omega\tau$

$$2\tau^2 + Xf\tau - \frac{f^2}{L - 1} = 0 \qquad (8.17)$$

where

$$X = \frac{\sin f}{1 - \cos f} \qquad (8.18)$$

Thus, it is possible to use equations (8.17) and (8.18) to calculate the period to delay ratio

$$\frac{T}{\tau} = \frac{2\pi}{f}$$

for any given values of L and τ. In Fig 8.6 we plot

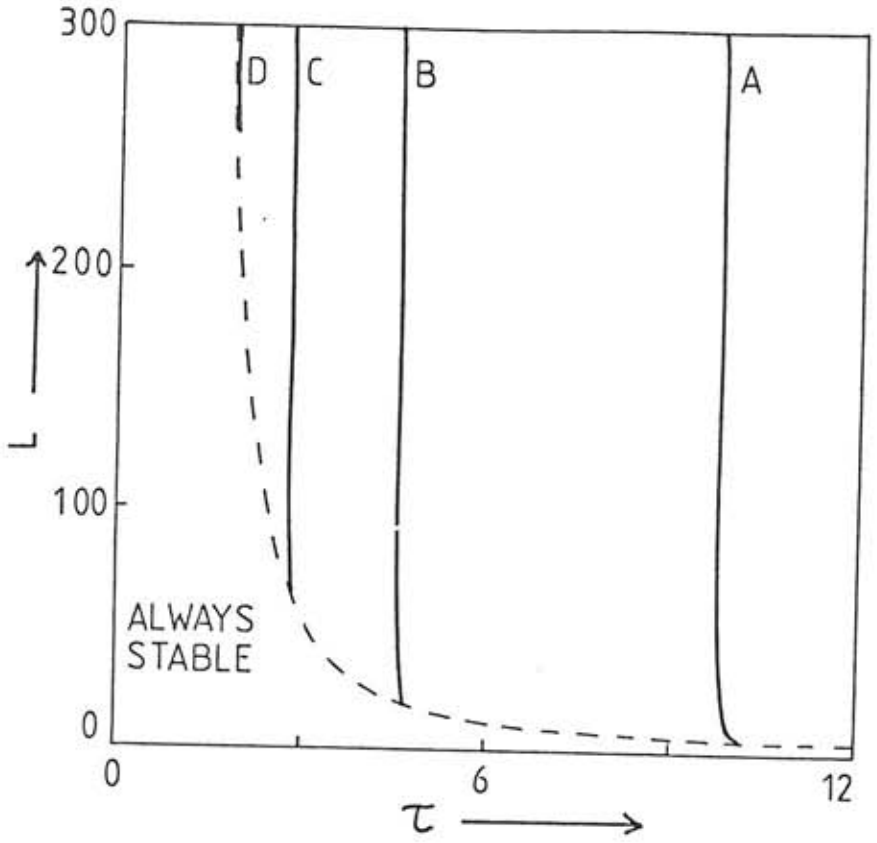

Figure 8.6. Contours of constant period to delay ratio.
A is the curve $T/\tau = 1.1$, B is the curve $T/\tau = 1.2$,
C is the curve $T/\tau = 1.3$ and D is the curve $T/\tau = 1.4$.
For values of L and τ lying below the boundary
curve (---), the steady state is always locally
stable.

contours of constant T/τ in the L-τ plane. Below the boundary curve (dashed line) the values of L and τ are such that τ is below the threshold value τ_L, i.e. the steady state is always stable in this region. It can be seen from Fig 8.6 that period to delay ratios significantly exceeding 1 can, as reported by Gurney & Nisbet (1985), only occur at 'extreme' values of the parameters (for example, $T/\tau < 1.41$ when $L \leq 300$).

CHAPTER 9

Chapter 9 : A general, variable maturation time model

In Chapter 8 we considered one particular model of the form given by equations (7.1) - the Gurney & Nisbet (1985) 'MT' model. In this model, larvae mature into adults on reaching a given weight - that is, weight gained since recruitment is taken to be the larval development index, and the growth, or development, rate is a given function of larval density (equation (8.11)).

In this Chapter, we consider two general models of larval competition resulting in a variable time in stage. Unlike the 'MT' model, we do not specify a particular development index, nor do we assume any given relationship between the development rate and larval density - we merely suppose that the development rate depends on larval density in one of two general ways.

We consider separately 'direct' or 'interference' competition and 'indirect' competition. For our direct competition model, we assume the development rate depends explicitly on the larval density at all times. For 'indirect' competition, we assume the development rate depends on a single, unspecified, quantity which in turn varies as larval density varies. We consider general forms of both these models in which the precise relationship between development rate and larval density is undefined - we are, in effect, considering a whole

class of models of the form given by equations (7.1).

Analysis of the resulting characteristic equations, using the free parameter method developed in Chapter 8, enables us to estimate the period to generation time ratio for such models.

9.1 Comments about the model

We shall consider a model of the form given by equations (7.1). The model is incomplete, as we have not specified any relationship between the development rate D(t) and the larval density $\rho_L(t)$ - that is, we have not defined the mechanism of competition. In sections 9.2 and 9.3 we consider two general ways in which D(t) may depend on $\rho_L(t)$. We simplify our model by choosing our unit of development so that the maximum possible development rate is unity. It follows that the parameter Q of equations (7.1) will represent the minimum possible larval maturation period, τ_{min}.

Before proceeding, we note that it follows from equations (7.1) that in a steady state,

$$Le^{-\delta\tau} = 1 \qquad (9.1)$$

where τ denotes the steady state delay. That is, the parameters L, δ and τ are three dependent quantities

which must satisfy the above equation. As our aim is to estimate the size of the period to generation time ratio, which will evidently depend on the steady state delay, we shall choose L and τ to be two independent parameters, and assume δ is given by

$$\delta = \frac{\ell n(L)}{\tau}$$

to ensure that equation (9.1) is satisfied. Furthermore, we shall assume that the population is capable of sustaining itself, so that at least one offspring produced by an adult will, at maximum development rate, survive to adulthood, which implies

$$Le^{-\delta\tau_{min}} > 1$$

and so it can be seen that the parameters L and τ must satisfy

$$L > 1 \quad \text{and} \quad \tau > \tau_{min}. \qquad (9.2)$$

9.2 Interference competition

We now consider 'direct' or 'interference' competition, where we assume the development rate D(t) is solely a function of the larval density $\rho_L(t)$. We consider a

general relationship and write

$$D(t) = H(\rho_L(t)) \tag{9.3}$$

where $H(\rho_L)$ is a continuous, single valued function defined for all $\rho_L \epsilon [0,\infty)$, taking values in the interval $[0,1]$. Evidently, as we are considering a model of larval competition, H must be a decreasing function of ρ_L.

It follows from equations (7.1),(9.1) and (9.3) that in a steady state,

$$D^* = \frac{\tau_{min}}{\tau} \qquad \rho_A{}^* = \frac{\ell n(L)}{(L-1)\tau}\,\rho_L{}^* \qquad \rho_L{}^* = H^{-1}(D^*) \tag{9.4}$$

(where * denotes a steady state value), so that D^* depends only the ratio τ/τ_{min}, but both steady state populations depend also on the values of any parameters of the function H. We consider a small deviation

$$\rho_L(t) = \rho_L{}^* + \ell(t)$$
$$\rho_A(t) = \rho_A{}^* + a(t)$$
$$\tau(t) = \tau^* + q(t)$$

about this steady state. By substituting the above into equations (7.1), (9.3) and neglecting terms higher than

first order, it can be shown that

$$\frac{d\ell}{dt} = La(t)-a(t-\tau)+\delta\rho_A^* a(t)-b\rho_A^*(\ell(t)-\ell(t-\tau))-\delta\ell(t)$$

$$\frac{da}{dt} = a(t-\tau)-\delta\rho_A^* q(t)+b\rho_A^*(\ell(t)-\ell(t-\tau))-a(t) \qquad (9.5)$$

$$q(t) = -b\int_{t-\tau}^{t}\ell(t')dt'$$

where

$$b = \frac{H'(\rho_L^*)}{D^*}$$

Seeking solutions $\ell(t) = \ell_0 e^{\lambda t}$, $a(t) = a_0 e^{\lambda t}$, $q(t) = q_0 e^{\lambda t}$ to equations (9.5) yields the characteristic equation

$$\frac{\rho_A^*}{\rho_L^*}\eta(\lambda+1-L)\frac{(1-e^{-\lambda\tau})}{\lambda} = \lambda+1-e^{-\lambda\tau},$$

or, using (9.4)

$$\frac{\ell n(L)}{(L-1)\tau}\eta\,(\lambda+1-L)\frac{(1-e^{-\lambda\tau})}{\lambda} = \lambda+1-e^{-\lambda\tau} \qquad (9.6)$$

where

$$\eta = -b\rho_L^* = -\rho_L^* \frac{H'(\rho_L^*)}{H(\rho_L^*)} \qquad (9.7)$$

or

$$\eta = -\frac{\rho_L^*}{D^*}\frac{dD^*}{d\rho_L^*}$$

The parameter group η will, in general, depend on τ/τ_{min}, and any parameters of the function H. We note that as H is a decreasing function of ρ_L, η must be strictly positive.

9.3 Indirect competition

We now consider those models in which competition is indirect. We suppose that the development rate D(t) depends on a single, unspecified, variable X(t), that is

$$D(t) = g(X(t)) \qquad (9.8)$$

and that X(t) varies as $\rho_L(t)$ varies in such a manner that we may write

$$\frac{dX}{dt} = f(X(t), \rho_L(t)) \ . \qquad (9.9)$$

X may, for example, represent food density, in which case

we would expect

$$g'(X) > 0 \quad \text{and} \quad \frac{\partial f}{\partial \rho_L} < 0,$$

or X may represent some quantity detrimental to development, in which case

$$g'(X) < 0 \quad \text{and} \quad \frac{\partial f}{\partial \rho_L} > 0.$$

We replace the pair of equations (9.8) and (9.9) with the single X-independent equation

$$\frac{dD}{dt} = F(D(t), \rho_L(t)) \tag{9.10}$$

where $F(D,\rho_L)$ is easily found for any given functions $f(X,\rho_L)$ and $g(X)$. As larvae are competing, it follows that $F(D,\rho_L)$ must be such that

$$\frac{\partial F}{\partial \rho_L} < 0 \tag{9.11}$$

It can be seen from equations (7.1) and (9.10) that in a steady state

$$D^* = \frac{\tau_{min}}{\tau} \qquad \rho_A{}^* = \frac{\ell n(L)}{(L-1)\tau}\,\rho_L{}^* \tag{9.12}$$

$$F(D^*,\ \rho_L{}^*) = 0$$

so that the steady state populations depend on τ_{min}/τ and any parameters of the function F.

We consider a small deviation

$$\rho_L(t) = \rho_L{}^* + \ell(t)$$
$$\rho_A(t) = \rho_A{}^* + a(t)$$
$$\tau(t) = \tau + q(t)$$
$$D(t) = D^* + \Delta(t)$$

about the steady state. Substituting into equations (7.1) and (9.10) and approximating by first order terms yields the equations

$$\frac{d\ell}{dt} = La(t)-a(t-\tau)+\delta\rho_A{}^* q(t) - \frac{\rho_A{}^*}{D^*}\,(\Delta(t)-\Delta(t-\tau))-\delta\ell(t)$$

$$\frac{da}{dt} = a(t-\tau)-\delta\rho_A{}^* q(t) + \frac{\rho_A{}^*}{D^*}\,(\Delta(t)-\Delta(t-\tau))-a(t)$$

$$q(t) = -\int_{t-\tau}^{t} \frac{\Delta(t')}{D^*}\,dt'$$

$$\frac{d\Delta}{dt} = c\ell(t) + d\Delta(t)$$

where

$$c = \left.\frac{\partial F}{\partial \rho_L}\right|_* \quad \text{and} \quad d = \left.\frac{\partial F}{\partial D}\right|_* \tag{9.13}$$

It can be show that the above equations yield the characteristic equation

$$\frac{\ell n(L)}{(L-1)\tau}\,\eta'(\lambda+1-L)\,\frac{(1-e^{-\lambda\tau})}{\lambda} = (1+p\lambda)(\lambda+1-e^{-\lambda\tau}) \tag{9.14}$$

where

$$\eta' = \frac{\rho_L}{D^*}\,\frac{c}{d} \quad \text{and} \quad p = -\frac{1}{d} \tag{9.15}$$

Now at a steady state

$$F(D^*, \rho_L{}^*) = 0$$

so that

$$\left.\frac{\partial F}{\partial D}\right|_* \frac{dD^*}{d\rho_L{}^*} + \left.\frac{\partial F}{\partial \rho_L}\right|_* = 0$$

or

$$d \frac{dD^*}{d\rho_L^*} + c = 0, \qquad (9.16)$$

so that η' may be written as

$$\eta' = - \frac{\rho_L^*}{D^*} \frac{dD^*}{d\rho_L^*} , \qquad (9.17)$$

that is, η' is the same quantity which appears in the characteristic equation (9.6). Again, competition between larvae implies an increase in the steady state larva population and must correspond to a decrease in the steady state development rate, so that $\eta' > 0$. It follows from equation (9.11) that $c < 0$, so that it can be seen from equation (9.16) that the parameter group d is strictly negative, that is, p must be greater than zero.

When considering a particular indirect competition model, with given functions $g(X)$ and $f(X,\rho_L)$, η' may be found in the following way. It follows from equations (9.8) and (9.9) that in a steady state

$$D^* = g(X^*) \quad \text{and} \quad f(X^*,\rho_L^*) = 0,$$

and we write the latter equation as

$$\rho_L^* = h(X^*),$$

then it may be shown that η' is given by

$$\eta' = - \frac{g'(X^*)}{g(X^*)} \frac{h(X^*)}{h'(X^*)} . \qquad (9.18)$$

and p is given by

$$p = \frac{-1}{\frac{\partial f}{\partial X}\Big|_*} \qquad (9.19)$$

9.4 A characteristic equation

Both direct and indirect competition models yield a characteristic equation

$$\frac{\ell n(L)}{(L-1)\tau} \eta \ (\lambda+1-L) \ \frac{(1-e^{-\lambda\tau})}{\lambda} = (1+p\lambda)(\lambda+1-e^{-\lambda\tau}) \qquad (9.20)$$

where for both forms of competition

$$\eta = - \frac{\rho_L^*}{D^*} \frac{dD^*}{d\rho_L^*} > 0.$$

When competition is direct, $p = 0$, whereas for indirect competition, $p > 0$. Both η and p are groups of model parameters.

We shall consider only those models in which the relationship between D^* and ρ_L^* is such that η can only take values in the interval $(0,1)$. The restriction $\eta < 1$ implies that

$$D^* + \rho_L^* \frac{dD^*}{d\rho_L^*} = \frac{d}{d\rho_L^*}(D^*\rho_L^*) > 0$$

For fixed values of the parameters L and τ_{min}, this boils down to a statement that (see equations (9.4) or (9.12))

$$\frac{d\rho_A^*}{d\rho_L^*} > 0 \qquad (9.21)$$

where the derivative is a measure of the relative changes in the sizes of the steady state populations due to a variation in the parameter τ. All models we shall be considering satisfy this restriction.

The characteristic equation (9.20) is of the form of equation (8.1) in which the functions $F(\lambda)$ and $G(\lambda)$ also depend on the delay τ. We seek non-zero imaginary eigenvalues $\lambda = i\omega$. For this characteristic equation, A_ω, B_ω, P_ω and Q_ω (c.f. equation (8.4)) are given by:-

$$A_\omega = \chi(L-1)-p\omega^2 \qquad B_\omega = (1-\chi)\omega$$

$$P_\omega = \chi(L-1)-p\omega^2-\omega^2 \qquad Q_\omega = (1-\chi)\omega-p\omega^3$$

where

$$\chi = \frac{\ell n(L)}{(L-1)\tau}\,\eta .$$

Equation (8.7) now becomes

$$p^2\omega^4 + (1+2p\chi)\omega^2-2\chi(L-1) = 0 \qquad (9.22)$$

and it can be shown from equation (8.6) and the above that X may be written as

$$X = \frac{p\omega^2-2(1-\chi)}{\omega} . \qquad (9.23)$$

We use equations (8.9), (9.22) and (9.23) to find local stability boundaries for $p \geqslant 0$ and $0 < \eta \leqslant 1$; these are shown in Fig. 9.1. It can be seen that increasing the delay parameter τ, which is the ratio of the steady state maturation time to the mean adult lifetime, will ultimately destabilize the steady state. We note that stability is decreased as fecundity (i.e. the

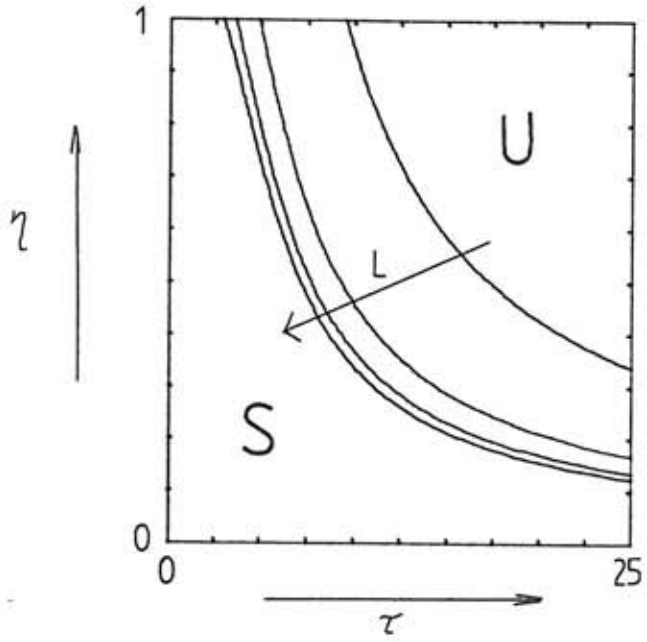

(a) p=1

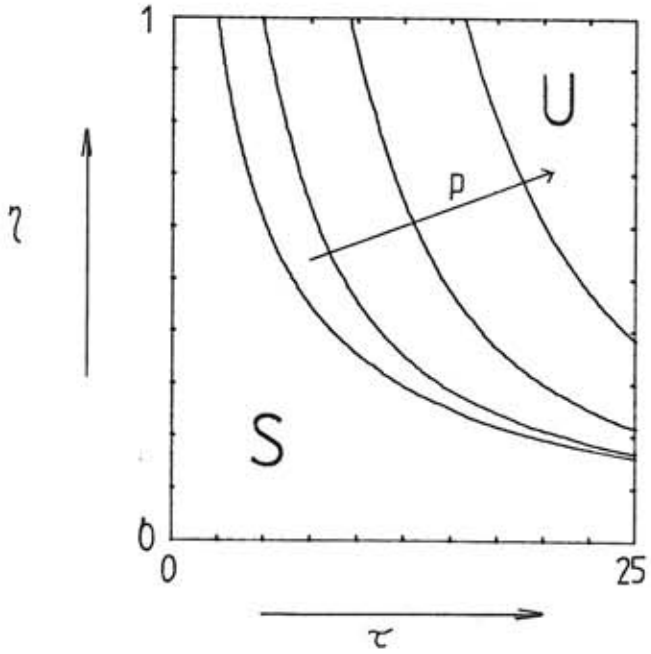

(b) L=100

parameter L) is increased - a stability decrease in the sense that the range of parameter values for which the steady state is locally stable is decreased. The remaining model parameters, that is, the minimum delay τ_{min} and any parameters of the functions H (equation (9.3)) or F (equation (9.10)) may influence local stability through the parameter groups η or/and p. Fig. 9.1(b) shows local stability boundaries for one value of L and for p = 0,1,2.5,5. As the parameter p can only take non-negative values, the steady state must always be locally stable for points (τ,η) lying below the curve p=0. It follows that the delay τ must be greater than a certain value τ_0, which is the point at which p=0 and η=1 and which will depend on the value of L, before instability is possible.

As the parameter groups p and η are restricted to taking values $p \geqslant 0$ and $0 < \eta \leqslant 1$, we now consider in turn the limiting cases $p > 0$ and $\eta = 1$.

(i) <u>p = 0</u>

When p = 0, the characteristic equation (9.20) reduces to exactly that considered in Chapter 8, where χ now replaces the parameter Γ of equation (8.12). By treating η or χ as a free parameter, the period to delay ratio T/τ may be found for any given values of L and τ using equations (8.17) and (8.18). We note that the

restriction $0 < \eta < 1$ implies that our free parameter χ takes the same range of values as Γ, so that Fig. 8.6 shows the contours of constant period to delay ratio for our present case, with the boundary curve corresponding to the contour $\eta = 1$. For points (τ,L) lying below the boundary curve, the values of L and τ are such that no $\eta\epsilon(0,1)$ can be found so that (L,τ,η) lies on a stability boundary, and it follows that for those models satisfying equation (9.21), the steady state is always locally stable in this region (c.f. Fig. 9.1).

As the mean (normalized) adult lifetime is unity, the period to generation time ratio is given by

$$\frac{T}{1+\tau} = \frac{T/\tau}{1+1/\tau} \qquad (9.24)$$

and may now be found for any pair of values of L and τ. Fig. 9.2(a) shows $T/1+\tau$ plotted as a function of τ for $L = 100,300,500$. These curves are, as expected, almost indistinguishable - Fig. 8.6 shows that the period to delay ratio is almost independent of L - although the end points A,B,C, which correspond to $\eta = 1$, <u>are</u> dependent upon the value of L. It follows from equation (8.17) that a good approximation can be found using

$$\tau = \frac{-Xf}{2}. \qquad (9.25)$$

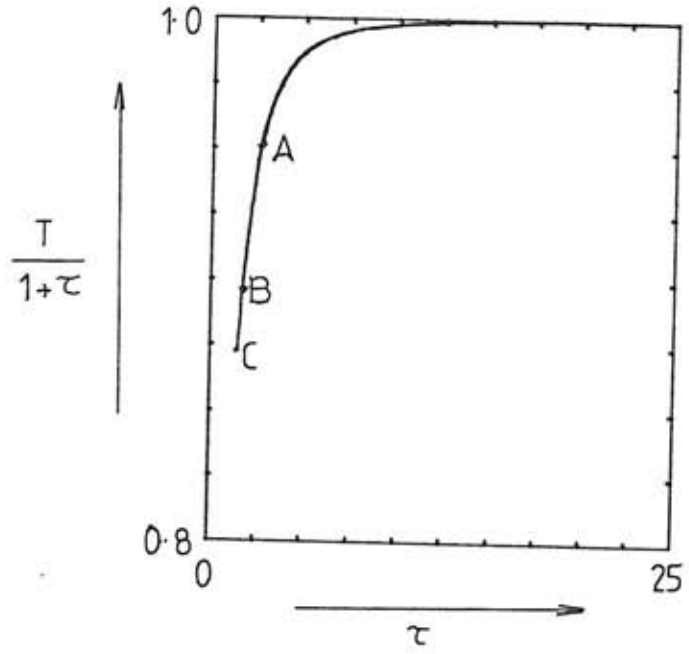

(a)

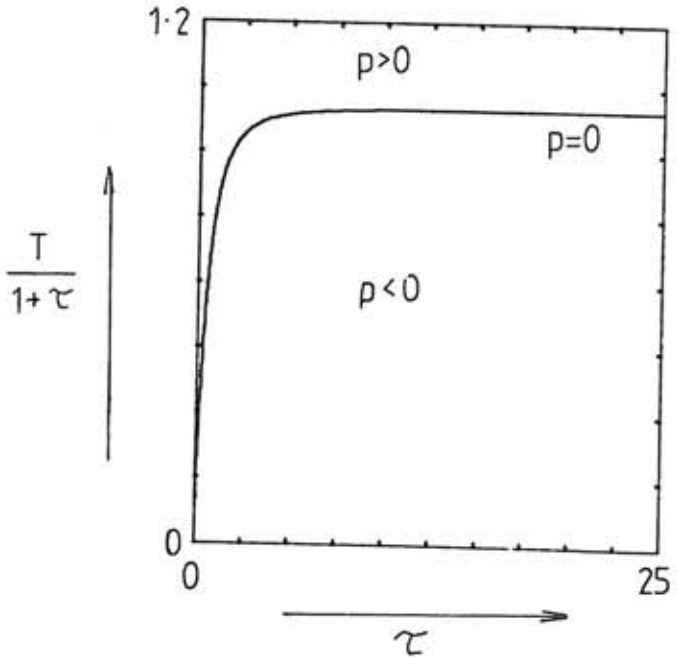

(b)

Fig. 9.2(b) shows $T/1+\tau$ as a function of τ using this approximation. As this is the curve p = 0, it divides the plane into those regions where $p < 0$ and $p > 0$, and thus it can be seen that this curve gives a lower bound on the period to generation time ratio.

Equations (9.24) and (9.25) may be used to estimate a lower bound for this ratio for any given value of the delay τ. We now consider our second limiting case.

(ii) $\underline{\eta = 1}$

For a given value of η, $\eta = 1$, we choose p as our free parameter. Eliminating p from equations (9.22) and (9.23) and writing $f = \omega\tau$ yields the equation

$$4\tau^2 + 2(2Xf-K-KL)\tau + [(X^2+1)f^2-2KXf] = 0$$

where

$$X = \frac{\sin f}{1-\cos f}$$

and

$$K = \frac{\ell n(L)}{(L-1)}$$

For any given values of L and τ, the above equations may be used to find the period to delay ratio, T/τ, and the period to generation time ratio, $T/1+\tau$, may then be found from equation (9.24). Fig. 9.3 shows $T/1+\tau$ plotted as a function of τ for L = 100,200,300. Again, as this is the

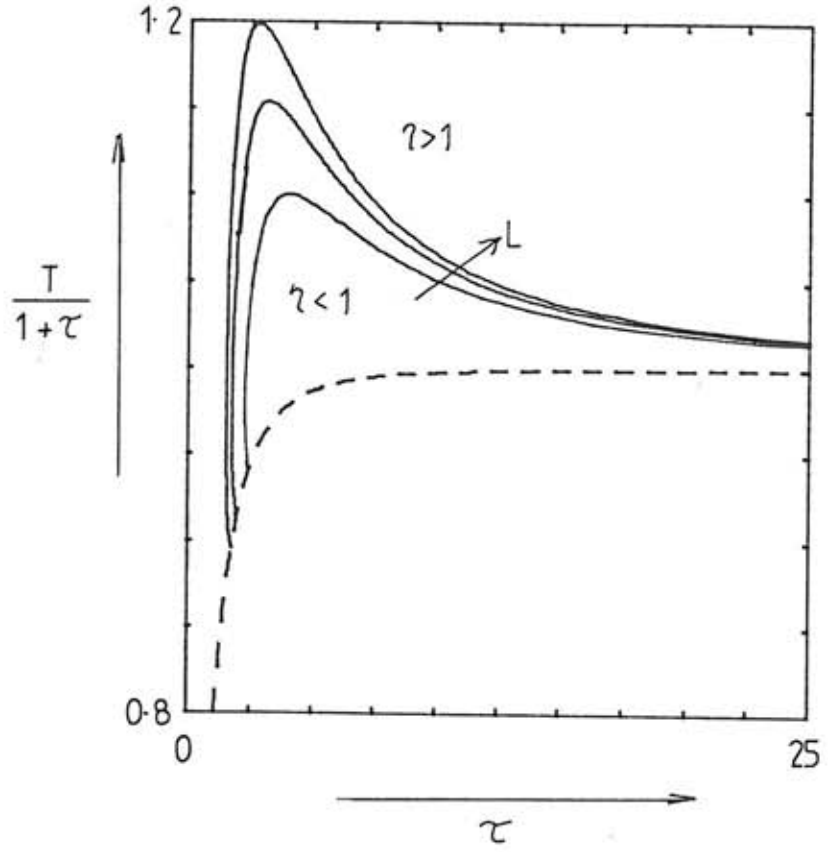

Figure 9.3. Period to generation time ratio for $\gamma = 1$ and L = 100,200,300 (L increasing as shown), using p as a free parameter. The dashed line (----) is the curve p = 0.

curve $\eta=1$, it separates the plane into those regions where $\eta<0$ and $\eta>0$.

It follows from Fig 9.3 that our limiting cases p = 0 and η = 1 provide, respectively, a lower and an upper bound for the period to generation time ratio for the class of models satisfying equation (9.21). Moreover (c.f. Fig. 9.1), these models can only be unstable in the region bounded by these curves.

Hence, direct competition models, where p = 0 will for all values of L and τ have lower period to generation time ratios than indirect competition (p > 0) models.

CHAPTER TEN

Chapter 10 : Three models of larval competition

Our Section I study of Plodia interpunctella (Hubner) showed that an increase in competition between larvae lead to an increase in the time taken for larvae to mature. We found that competition occurred both through direct interference and through competition for food, with the presence of a quantity which we call 'junk' also contributing towards an increased development time.

Questions raised by this work lead us in this Chapter, to consider a simple larval competition model of the type given by equations (7.1). We shall consider a development rate D(t) which incorporates the three types of competition found in Plodia. We then investigate the importance of the particular manner in which larvae compete and how this may affect local stability and cycle period by considering three special cases of our model. In each, one of the above competition mechanisms - direct interference, competition for food, deposition of junk by larvae - operates alone in the absence of the others.

10.1 The basic model

As discussed in Section 7.3, what we refer to as competition via junk is not a simple process. Junk refers to a number of quantities which larvae may deposit, and the mechanisms whereby these quantities

affect the development of larvae are by no means obvious. However, we note that the three types of competition are fundamentally quite different:-

direct interference occurs when the presence of other larvae acts to directly reduce the development rate (as discussed in Chapter 4),
competition for food is the process whereby larvae deplete a quantity which promotes development,
competition via junk refers to the process whereby larvae produce a quantity which reduces development.

Thus, as we wish to consider the effect of each of these mechanisms of competition on the dynamics of a model of the type given by equations (7.1), we shall approximate competition via junk density by representing junk by a single time-dependent variable, whose effect is to reduce the development rate via a 'junk handling time'.

We begin by, as in Chapter 4, considering a variable A(t) which is to be the individual larval search rate. We define handling times

τ_M = time taken to consume 1 unit of food

τ_L = time wasted per larva-larva encounter

τ_J = time wasted per unit junk encountered

and variables

$\rho_M(t)$ = density of food at time t

$\rho_J(t)$ = density of junk at time t

We assume there is a maximum search rate, a, which is reduced by the time spent feeding, by time wasted during larva-larva encounters and by time wasted due to the presence of junk, so that A(t) is given by

$$A(t) = \frac{a}{1+a\tau_M\rho_M(t)+a\tau_L\rho_L(t)+a\tau_J\rho_J(t)} \qquad (10.1)$$

The individual food uptake rate, $I_M(t)$, will be the product of the search rate and the food density,

$$I_M(t) = A(t)\rho_M(t)$$

or

$$I_M(t) = \frac{I_{max}\rho_M(t)}{\alpha+\rho_M(t)+\alpha_2\rho_L(t)+\alpha_3\rho_3(t)} \qquad (10.2)$$

where

$$I_{max} = \frac{1}{\tau_M}$$

is the maximum possible feeding rate, and

$$\alpha = \frac{1}{a\tau_M} \quad , \quad \alpha_2 = \frac{\tau_L}{\tau_M} \quad , \quad \alpha_3 = \frac{\tau_J}{\tau_M} \quad , \qquad (10.3)$$

We now suppose that an individual larva will gain a development increment

q_1 per unit area covered

q_2 per unit food consumed

q_3 per larva-larva encounter

q_4 per unit junk consumed

so that the individual development rate D(t) is given by

$$D(t) = a \frac{(q_1+q_2\rho_M(t)+q_3\rho_L(t)+q_4\rho_J(t))}{1+a\tau_M\rho_M(t)+a\tau_L\rho_L(t)+a\tau_J\rho_J(t)} \qquad (10.4)$$

That is, with this form of development rate, we have included our three types of competition - direct interference, and indirect competition via changes in food and junk densities. We note that when $q_1 = q_3 = q_4 = 0$, it can be seen from equations (10.2) and (10.4) that D(t) is directly proportional to the feeding rate $I_M(t)$. Thus, if a constant proportion of the food eaten by a larva is converted into weight gained, this case represents a development index which is weight gained in the stage. It can also be shown that a development index which is a linear combination of weight gained and time since recruitment may be dealt with by taking

$$q_1 = \frac{q_2}{\tau_L} = \frac{q_3}{\tau_J} \neq 0.$$

so that development rates while searching, during

larva-larva and larva-junk encounters are identical.

Realistically, we would expect no development to occur during larva-larva and larva-junk encounters, and so we take q_3 and q_4 to be zero, and write D(t) in the form

$$D(t) = D_{max} \frac{q_N+\rho_M(t)}{\alpha+\rho_M(t)+\alpha_2\rho_L(t)+\alpha_3\rho_J(t)} \qquad (10.5)$$

where

$$D_{max} = \frac{q_2}{\tau_M}$$

is the maximum possible development rate (during feeding), and $q_N = q_1/q_2$.

We assume that food is supplied at a constant rate, Φ, so that the equation governing the food dynamics is

$$\frac{d\rho_M}{dt} = \Phi - I_M(t)\rho_L(t) \qquad (10.6)$$

Our junk variable, $\rho_J(t)$, represents quantities such as pheromones, silk, or faeces which larvae may deposit. In the case of pheromones or silk, we would expect the rate of deposition to be proportional to the density of larvae present. We suppose that a larva will deposit, as faeces, a constant fraction of food eaten (that which

is not converted into weight), and that this process takes place instantaneously, so that in this case the rate of junk deposition is proportional to the product of the individual food uptake rate and the density of larvae. We further assume that junk is removed at a constant rate, and write

$$\frac{d\rho_J}{dt} = [B+\epsilon I_M(t)]\rho_L(t)-h\rho_J(t) \qquad (10.7)$$

Our model, given by equations (7.1), (10.2), (10.5), (10.6) and (10.7), assumes that larvae compete in a combination of three ways:-

(i) by direct interference,

(ii) indirectly via changes in food density (competition for food),

(iii) indirectly by depositing junk.

We now look at three special cases of the model, in which each of the above competition mechanisms operate alone, in the absence of the remaining two. As in each of these three models the development rate will be a function of a single time-dependent quantity, each model is of the type considered in Chapter 9.

10.2 Interference Competition

We consider a model in which larvae compete only by direct interference. We assume junk is either absent

($\rho_J(t) \equiv 0$) or has no effect on the development rate ($\tau_J = 0$). To ensure there is no indirect competition through changes in food density, we consider a model in which food is maintained at a constant level, that is, we take $\rho_M(t) \equiv F$. Then from equations (7.1) and (10.5) we may write

$$\frac{d\rho_L}{dt} = L\rho_A(t) - M(t) - \delta\rho_L(t)$$

$$\frac{d\rho_A}{dt} = M(t) - \rho_A(t)$$

$$D_F\tau_F = \int_{t-\tau(t)}^{t} D(t')dt' \qquad (10.8)$$

$$D(t) = \frac{D_F}{1+\beta\rho_L(t)}$$

$$M(t) = L\rho_A(t-\tau(t))e^{-\delta\tau(t)} \frac{D(t)}{D(t-\tau(t))},$$

where

$$D_F = D_{max}\frac{q_N+F}{\alpha+F}, \quad \tau_F = \frac{Q}{D_F}$$

are, respectively, the maximum possible development rate and the minimum possible maturation time <u>at food</u>

density F, and the parameter

$$\beta = \frac{\alpha_2}{\alpha + F}$$

is a measure of the intensity of competition.

It follows from equations (10.8) that the model has a single steady state, which is given by

$$\tau = \frac{\ell n(L)}{\delta}, \qquad \rho_L^* = \frac{1}{\beta}\left[\frac{\tau}{\tau_F} - 1\right],$$

$$D^* = D_F \frac{\tau_F}{\tau}, \qquad \rho_A^* = \frac{\delta}{L-1}\rho_L^*, \tag{10.9}$$

where * denotes a steady state and τ is the steady state maturation time. This steady state is positive provided

$$L > 1 \quad \text{and} \quad \tau = \frac{\ell n(L)}{\delta} > \tau_F,$$

that is (for positive parameters), iff

$$Le^{-\delta\tau_F} > 1,$$

which is a statement that in the absence of competition, each adult must be capable of producing at least one offspring which will survive to adulthood when food is

maintained at the constant density F. Thus, if either $L < 1$ or $\tau < \tau_F$, the population must become extinct.

The model, given by equations (10.8), is an interference model of the type considered in Chapter 9. For this model, the function $H(\rho_L)$ of equation (9.3) is given by

$$H(\rho_L) = \frac{D_F}{1+\beta\rho_L}$$

It follows from equation (9.7) that the parameter η of the characteristic equation is given by

$$\eta = (-\rho_L^*) \left[- \frac{\beta}{1+\beta\rho_L^*} \right] ,$$

or, using equations (10.11)

$$\eta = 1 - \frac{\tau_F}{\tau}$$

Thus, it can be seen that $\eta \epsilon (0.1)$, or (9.21) holds. The characteristic equation (c.f. (9.6)) is given by

$$\frac{\ell n(L)}{(L-1)\tau} \left(1 - \frac{\tau_F}{\tau}\right) (\lambda+1-L) \frac{(1-e^{-\lambda\tau})}{\lambda} = \lambda+1-e^{-\lambda\tau} \qquad (10.10)$$

and is the same as the characteristic equation which

arose (equations (8,12), (8.13)) in our study of the Gurney & Nisbet 'MT' model, with τ_F replacing τ_{min}. Thus, local stability boundaries are shown in Fig. 8.4, and are reproduced here for convenience. The model is a direct interference model of the type discussed in Chapter 9; Fig. 9.2 shows the period to generation time ratio near stability boundaries.

It follows from equation (10.10) that it is the values of the parameters L, τ and τ_F which determine the local stability of the steady state and the cycle period near the stability boundary. As the parameter β does not appear in equation (10.10), it follows that the intensity of competition does not influence either stability or cycle period, but merely determines the size of the steady state populations (equations (10.9)).

10.3 Competition for food

For our second model, we suppose that larvae compete indirectly via changes in food density. We assume that there is no direct interference, so that larval density has no effect on the development rate ($\tau_L = 0$), and again assume junk is either absent ($\rho_J(t) \equiv 0$) or has no effect on development ($\tau_J = 0$). From equations (7.1), (10.2), (10.5) and (10.6), it follows that

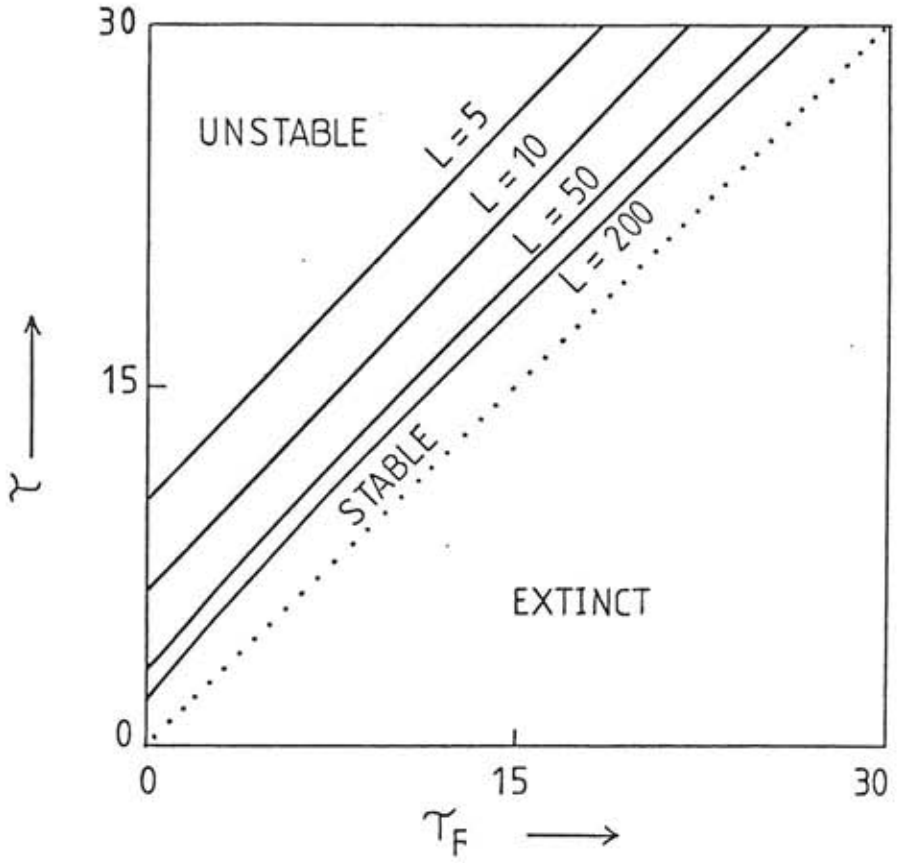

Figure 10.1. Local stability boundaries for the interference competition model.

$$\frac{d\rho_L}{dt} = L\rho_A(t) - M(t) - \delta\rho_L(t)$$

$$\frac{d\rho_A}{dt} = M(t) - \rho_A(t)$$

$$D_{max}\tau_{min} = \int_{t-\tau(t)}^{t} D(t')dt' \qquad (10.11)$$

$$\frac{d\rho_M}{dt} = \Phi - I_M(t)\rho_L(t)$$

$$D(t) = D_{max}\frac{q_N+\rho_M(t)}{\alpha+\rho_M(t)}$$

$$I_M(t) = I_{max}\frac{\rho_M(t)}{\alpha+\rho_M(t)}$$

$$M(t) = L\rho_A(t-\tau(t))e^{-\delta\tau(t)}\frac{D(t)}{D(t-\tau(t))}$$

where $\tau_{min} = Q/D_{max}$ is the minimum possible maturation time. It can be seen that the development rate D(t) has a non-zero minimum value

$$D_{min} = D_{max}\frac{q_N}{\alpha}$$

which implies there is a maximum maturation time, τ_{max}, given by

$$\tau_{max} = \frac{Q}{D_{min}} = \frac{\alpha}{q_N} \tau_{min} ,$$

which is the time taken to mature in the absence of food. By writing D(t) in the form

$$D(t) = D_{max} \left[\frac{q_N}{\alpha} + (1 - \frac{q_N}{\alpha}) \frac{\rho_M(t)}{\alpha+\rho_M(t)} \right]$$

$$= D_{max} \left[\frac{q_N}{\alpha} + \frac{(1 - \frac{q_N}{\alpha})}{I_{max}} I_M(t) \right]$$

(see equations (10.11)) where

$$\frac{q_N}{\alpha} = \frac{\tau_{min}}{\tau_{max}} \epsilon(0,1),$$

it can be seen that the larval development index is a linear combination of weight gained in stage and time since recruitment. That is, when no food is available, larvae mature after a given time, τ_{max}, but feeding promotes development and reduces the maturation time.

We note that for values $\tau > \tau_{max}$,

$$\delta = \frac{\ell n(L)}{\tau} < \frac{\ell n(L)}{\tau_{max}}$$

which implies that

$$Le^{-\delta\tau_{max}} > 1$$

so that the population must grow exponentially. Similarly, it can be shown that the population must become extinct if $L < 1$ or $\tau < \tau_{min}$, so we shall only consider parameter values $L > 1$ and $\tau\epsilon(\tau_{min}, \tau_{max})$.

The model has a single positive steady state given by

$$\tau = \frac{\ell n(L)}{\delta}, \qquad \rho_M^* = \frac{\alpha - q_N \tau/\tau_{min}}{\tau/\tau_{min} - 1},$$

$$D^* = D_{max}\frac{\tau_{min}}{\tau}, \quad \rho_L^* = \frac{\Phi}{I_{max}}\frac{\tau/\tau_{min} - \tau/\tau_{max}}{1 - \tau/\tau_{max}}, \qquad (10.12)$$

$$\rho_A^* = \frac{\delta}{L-1}\rho_L^*$$

This model is an indirect competition model of the type considered in Chapter 9, and so the characteristic equation will be given by equation (9.14). The functions g and f of equations (9.8) and (9.9) are given by

$$g(\rho_M) = D_{max} \frac{q_N+\rho_M}{\alpha+\rho_M}$$

$$f(\rho_M,\rho_L) = \Phi - I_{max} \frac{\rho_M\rho_L}{\alpha+\rho_M}$$

and it can be seen from the latter equation that the function $h(\rho_M^*)$ of equation (9.18) is given by

$$\rho_L^* = h(\rho_M^*) = \frac{\Phi}{I_{max}} \left[1 + \frac{\alpha}{\rho_M^*}\right]$$

It follows from equations (9.18) and (9.19) that η and p are given by

$$\eta = \left[-\frac{\alpha-q_N}{(\alpha+\rho_M^*)(q_N+\rho_M^*)}\right]\left[-\frac{\rho_M^*}{\alpha}(1 + \frac{\alpha}{\rho_M^*})\right]$$

$$p = \frac{(\alpha+\rho_M^*)^2}{I_{max}\alpha\rho_L^*}$$

or using equations (10.12),

$$\eta = 1 - \frac{q_N}{\alpha}\frac{\tau}{\tau_{min}} = 1 - \frac{\tau}{\tau_{max}},$$

$$p = \frac{\alpha}{\Phi} \frac{(1 - \tau_{min}/\tau_{max})(1 - \tau/\tau_{max})\tau/\tau_{min}}{(1 - \tau/\tau_{min})^2} \qquad (10.13)$$

$$\frac{\ell n(L)}{(L-1)\tau} \eta \ (\lambda+1-L) \frac{(1-e^{-\lambda\tau})}{\lambda} = (1 + p\lambda)(\lambda+1-e^{-\lambda\tau}) \ , \qquad (10.14)$$

where p and η are given above. We note that the parameter group p is strictly positive, and $\eta \epsilon (0,1)$ so that this model satisfies the inequality (9.21).

Thus, local stability of the steady state and cycle period near stability boundaries depend on values of the parameters L, τ, τ_{min}, τ_{max} and Φ/α. We note that α may be considered as a scale factor for food density (c.f. equations (10.11)), that is, as

$$\frac{\Phi}{\alpha} = a\Phi\tau_M,$$

it is the amount of food supplied per unit handling time which is of importance. We also note that the parameter I_{max}, which may be regarded as a measure of the intensity of competition, does not appear in the characteristic equation (10.14), and so cannot influence local stability or cycle period.

We now consider the case $q_N = 0$ or a development index which is weight gained in stage (equivalently, $\tau_{max} \to \infty$). It can be seen that with $q_N = 0$, the development rate D(t) is then the most sensitive to changes in food

density. In this case, it follows from equations (10.13) that η and p are given by

$$\eta = 1,$$

$$p = \frac{\alpha}{\Phi} \frac{\tau/\tau_{min}}{(\tau/\tau_{min}-1)^2}$$

Fig. 10.2 shows the local stability boundaries for this case - we treat $\Phi' = \Phi/\alpha$ as a single parameter. It can be seen that increasing the food supply rate, Φ', decreases the stability of the steady state.

As $\eta = 1$, this model is an example of the limiting case we considered in Chapter 9, and so the period to generation time ratio, $T/1+\tau$, estimated using Φ' (effectively, p) as a free parameter, is shown as a function of τ in Fig. 9.3.

For our full model, η is given by equation (10.13), and it can be seen that η must lie between 0 and 1. Fig. 10.3 shows the period to generation time ratio as a function of τ for L = 100 and τ/τ_{max} = 0,0.1,0.3,0.5. It can be seen that reducing the sensitivity of D(t) to changes in food density - that is, increasing q_N - results in a smaller value of η and therefore a lower period to generation time ratio.

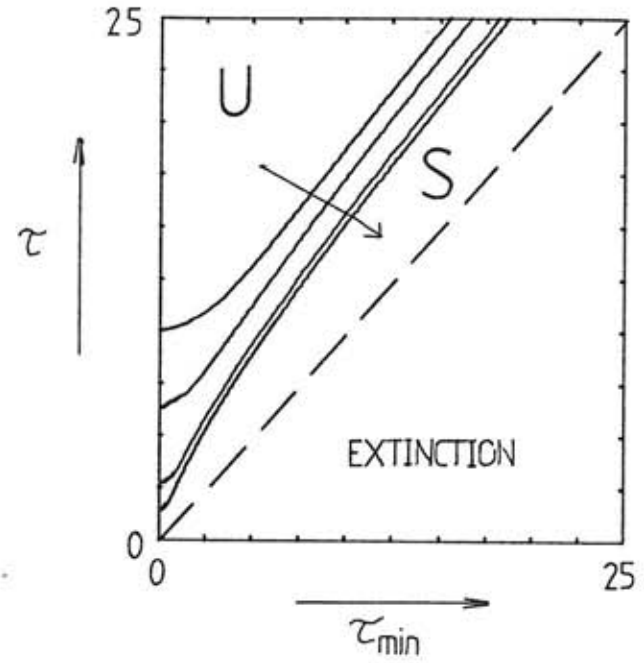

(a) $\phi' = 1$

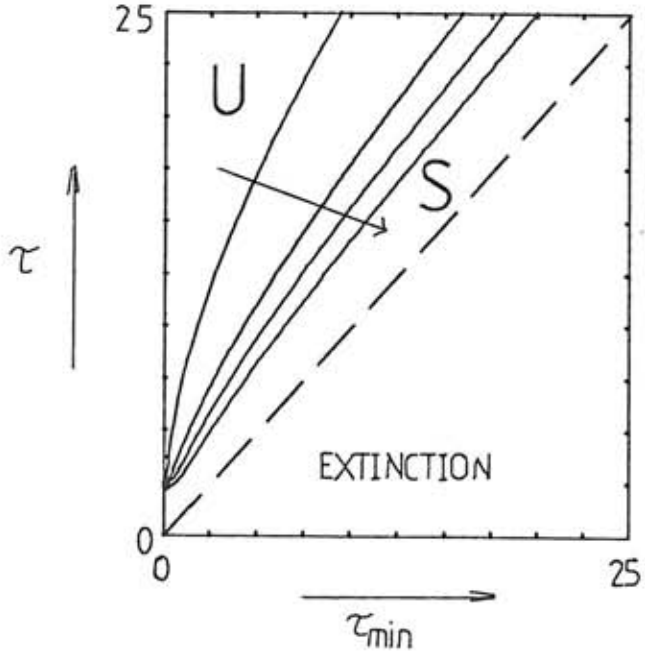

(b) L = 100

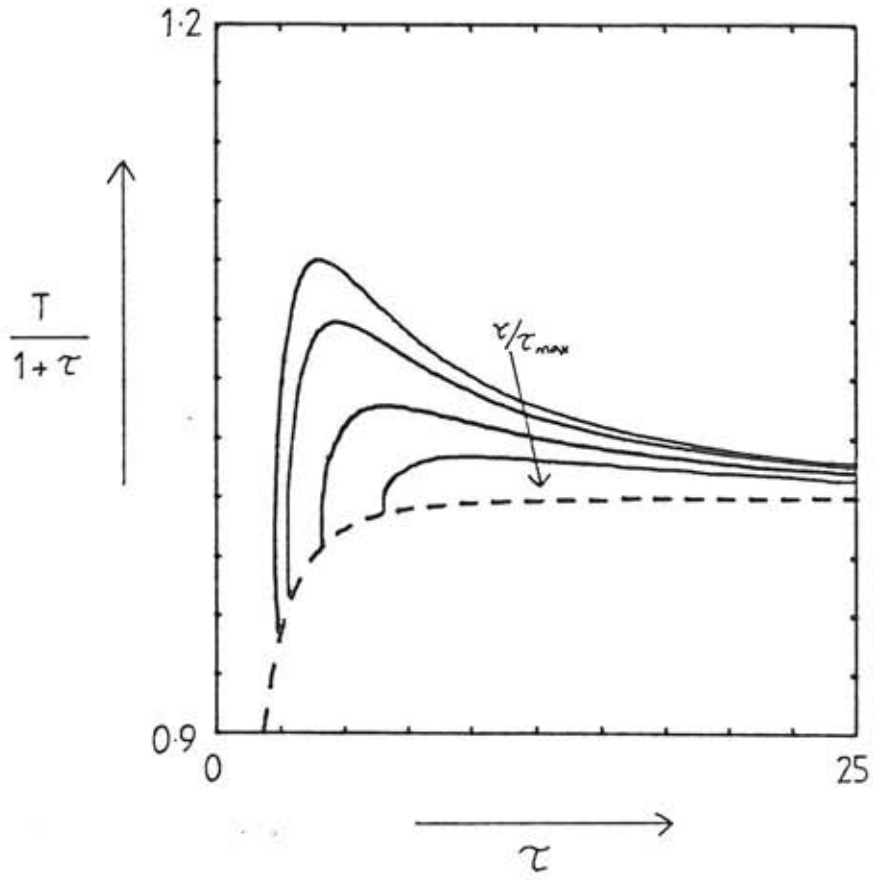

Figure 10.3. Range of period to delay ratios for the competition for food model when $q_N = 0$, found using p as a free parameter for L = 100 and $\tau/\tilde{\tau}_{max}$ = 0.0.1,0.3,0.5.

10.4 Competition via junk density

Lastly, we consider a model in which larvae compete solely by depositing junk. We assume there is no direct interference ($\tau_L = 0$), and again assume a constant density of food, $\rho_M(t) \equiv F$, to ensure no indirect competition for food. Equations governing the population dynamics are

$$\frac{d\rho_L}{dt} = L\rho_A(t) - M(t) - \delta\rho_L(t)$$

$$\frac{d\rho_A}{dt} = M(t) - \rho_A(t)$$

$$D_F \tau_F = \int_{t-\tau(t)}^{t} D(t')dt' \qquad (10.15)$$

$$\frac{d\rho_J}{dt} = \left[B + \frac{\epsilon I_F}{1+\gamma\rho_J(t)}\right] \rho_L(t) - h\rho_J(t)$$

$$M(t) = L\rho_A(t-\tau(t))e^{-\delta\tau(t)} \frac{D(t)}{D(t-\tau(t))}$$

$$D(t) = \frac{D_F}{1+\gamma\rho_J(t)}$$

where D_F, τ_F and I_F are respectively the maximum development rate, minimum maturation time, and maximum feeding rate at food density F, and the parameter γ is

given by

$$\gamma = \frac{\alpha_3}{\alpha + F}$$

As for our interference model, we shall consider only parameters $L > 1$ and $\tau > \tau_F$. For this range of values, the model has a single positive steady state, given by

$$\tau = \frac{\ell n(L)}{\delta}, \qquad \rho_J^* = \frac{1}{\gamma}\left[\frac{\tau}{\tau_F} - 1\right]$$

$$D^* = D_F \frac{\tau_F}{\tau}, \qquad \rho_L^* = \frac{h}{B\gamma} \frac{(\tau/\tau_F - 1)\tau/\tau_F}{\tau/\tau_F + \frac{\epsilon I_F}{B}}, \qquad (10.16)$$

$$\rho_A^* = \frac{\delta}{L-1} \rho_L^* .$$

This model is again of the general indirect competition type discussed in Chapter 9. For this model, the functions g, f and h of equations (9.8), (9.9) and (9.18) are given by

$$g(\rho_J) = \frac{D_F}{1+\gamma\rho_J}$$

$$f(\rho_J,\rho_L) = \left[B + \frac{\epsilon I_F}{1+\gamma\rho_J}\right] \rho_L - h\rho_J$$

$$h(\rho_J^*) = \frac{h\rho_J^*(1+\gamma\rho_J^*)}{B+\epsilon I_F+B\gamma\rho_J^*}$$

It follows from equation (9.18) that η is given by

$$\eta = \left[\frac{\gamma}{1+\gamma\rho_J^*}\right] \left[\frac{\rho_J^*(1+\gamma\rho_J^*)\left[1 + \frac{\epsilon I_F}{B} + \gamma\rho_J^*\right]}{(1 + \gamma\rho_J^*)^2 + \frac{\epsilon I_F}{B}(1+2\gamma\rho_J^*)}\right] \qquad (10.17)$$

and from equation (9.19) that p is given by

$$p = \frac{(1+\gamma\rho_J^*)\left[1 + \frac{\epsilon I_F}{B} + \gamma\rho_J^*\right]}{h[(1+\gamma\rho_J^*)^2 + \frac{\epsilon I_F}{B}(1+2\gamma\rho_J^*)]}$$

or using equations (10.16)

$$\eta = \frac{\left[(\tau/\tau_F - 1)(\tau/\tau_F + \frac{\epsilon I_F}{B})\right]}{(\tau/\tau_F)^2 + \frac{\epsilon I_F}{B}(2\tau/\tau_F - 1)} \qquad (10.18)$$

$$p = \frac{1}{h} \quad \frac{\tau/\tau_F\left[\tau/\tau_F + \frac{\epsilon I_F}{B}\right]}{(\tau/\tau_F)^2 + \frac{\epsilon I_F}{B}(2\tau/\tau_F - 1)}$$

and the characteristic equation is given by

$$\frac{\ell n(L)}{(L-1)\tau}\,\eta\,(\lambda+1-L)\,\frac{(1-e^{-\lambda\tau})}{\lambda} = (1 + p\lambda)(\lambda+1-e^{-\lambda\tau})$$

where η and p are given by equations (10.18).

Thus, local stability of the steady state and cycle period near stability boundaries depend on the values of the parameters L, τ, τ_F, h and $\epsilon I_F/B$. We note that it is not the <u>amount</u> of junk deposited per individual (measured by the parameters B and ϵI_F), but rather the relative dominance of the two ways in which junk may be deposited which influences stability and cycle period. For this reason we consider separately two special cases - that where $\epsilon = 0$ and that where $B = 0$.

(i) <u>$\epsilon = 0$</u>

When $\epsilon = 0$, it follows from equations (10.18) η and p take values

$$\eta = \eta_1 = 1 - \frac{\tau F}{\tau}, \qquad p = p_1 = \frac{1}{h},$$

so that the characteristic equation is given by

$$\frac{\ell n(L)}{(L-1)\tau}\left(1-\frac{\tau_F}{\tau}\right)(\lambda+1-L)\frac{(1-e^{-\lambda\tau})}{\lambda} = \left(1+\frac{\lambda}{h}\right)(\lambda+1-e^{-\lambda\tau}).$$

It can be seen that by allowing $h \to \infty$, this equation becomes identical to the characteristic equation (10.10) of our interference competition model.

Fig. 10.4 shows the local stability boundaries for this model. It can be seen that increasing the junk removal rate h decreases the stability of the steady state, and that as $h \to \infty$, the local stability boundaries approach those of the interference competition model (c.f. Fig 10.1). Thus, when larvae compete by depositing junk in this way, with a finite junk removal rate, the steady state is more stable than when larvae compete directly.

As the parameter p may take any positive value, and η may take any value between 0 and 1, it follows that Fig 9.3 shows the range of possible values of the period to generation time ratio for this model.

(ii) <u>B = 0</u>

When B = 0, it follows from equations (10.20) that the parameter groups η and p are given by

$$\eta = \eta_2 = \frac{\tau/\tau_F - 1}{2\tau/\tau_F - 1}, \qquad p = p_2 = \frac{\tau/\tau_F}{h(2\tau/\tau_F - 1)}$$

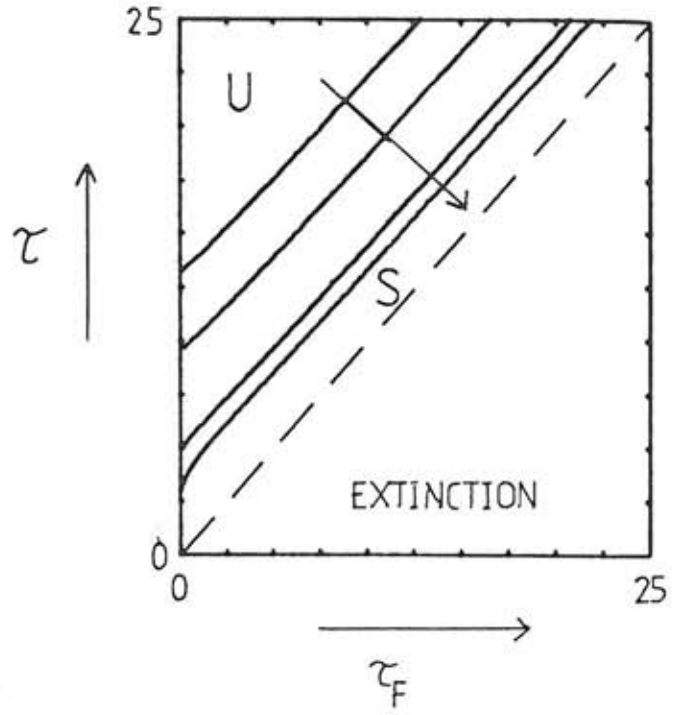

(a) h=1

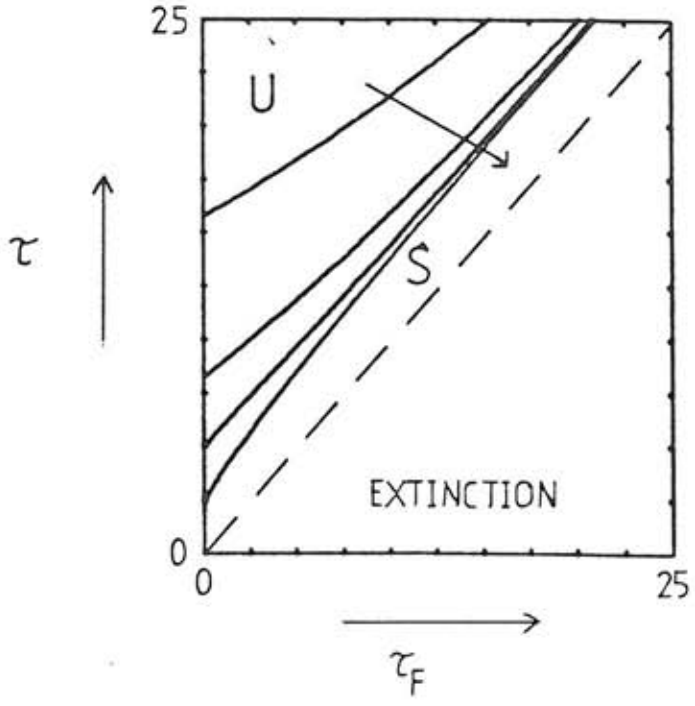

(b) L=100

so that p_2 may, by varying the junk removal rate h, take any positive value, but η_2 may only take values lying in the interval (0,0.5).

Fig. 10.5 shows the local stability boundaries for this model. Again, increasing the junk removal rate h decreases the stability of the steady state. However, for any particular values of the parameters L and h, it can be seen (c.f. Fig. 10.4) that the steady state is stable for a larger range of parameters than for the model with $\epsilon = 0$.

We use h (or p_2) as a free parameter to estimate the period to generation time ratio for this model. As the maximum value of η_2 is 0.5, it follows that $T/1+\tau$ is bounded above by the curve $\eta_2 = 0.5$. Fig. 10.6 shows the range of possible values of $T/1+\tau$ for L = 100,200,300. As expected, this range of values is far smaller than when $\epsilon = 0$.

For the full model given by equations (10.15), when η is given by equation (10.18), it can be shown that

$$\eta_1 \geq \eta \geq \eta_2.$$

That is, the period to generation time ratio $T/1+\tau$, calculated using p as a free parameter, will always lie between the corresponding values of $T/1+\tau$ for each of the

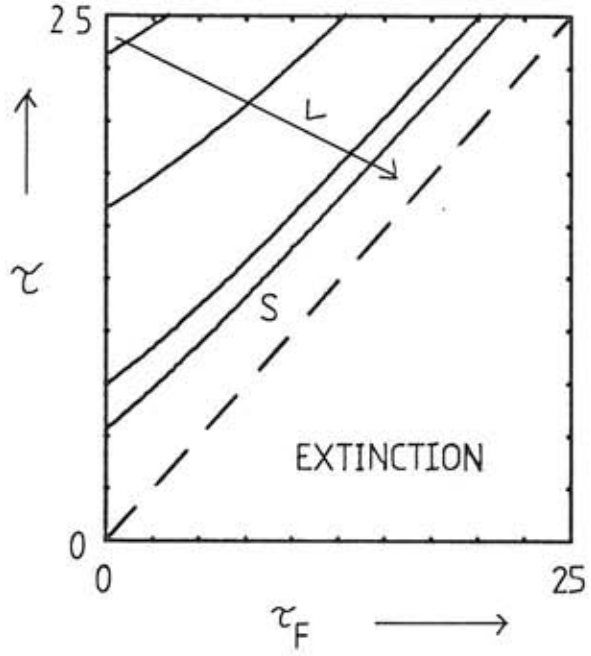

(a) h=1

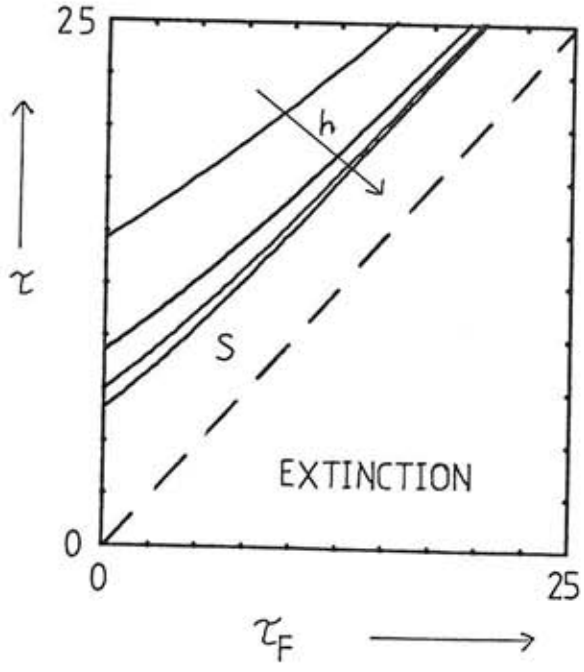

(b) L=100

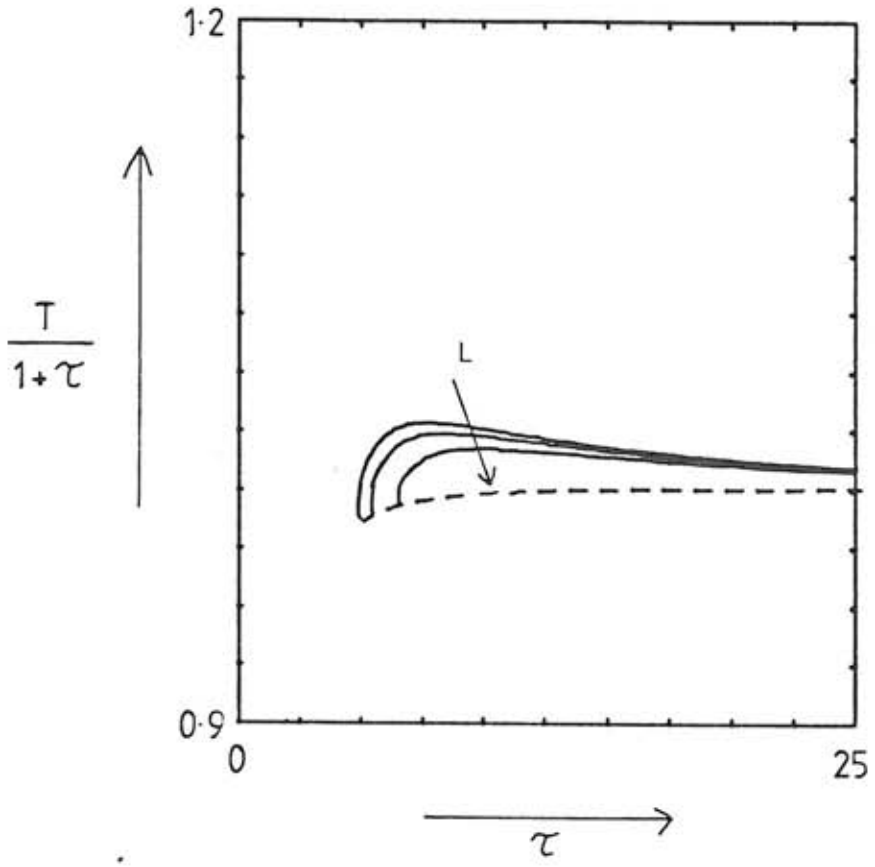

Figure 10.6. Range of values of $T/1+\tau$ for the competition via junk density model when B = 0, for values L = 100, 200, 300 with L increasing as shown. For each L, $T/1+\tau$ can only take values lying between this curve and the curve p = 0 (----).

above special cases. Fig 10.7 shows $T/1+\tau$ for L = 300 and τ/τ_F = 10, as the parameter

$$\sigma = \frac{\epsilon I_F}{B}$$

is increased. σ = 0 corresponds to our first special case ϵ = 0, and $\sigma \to \infty$ corresponds to our second case B = 0. It can be seen that increasing σ decreases the size of the period to generation time ratio. σ is a measure of which method of junk deposition dominates, and we note that an increase in σ results in greater regulation - a greater proportion of junk is deposited at a rate proportional to the feeding rate, which itself varies as junk density varies.

10.5 Discussion.

For all our models, parameters measuring the intensity of competition do not appear in the relevant characteristic equation and cannot therefore influence local stability of the steady state or cycle period near stability boundaries. Specifically, the parameter β of the interference competition model, which is a direct measure of the intensity of competition does not appear in the characteristic equation (10.10). The parameter I_{max} of the competition for food model, which is a measure of by how much an individual depletes the food density thereby competing with other larvae, is absent from

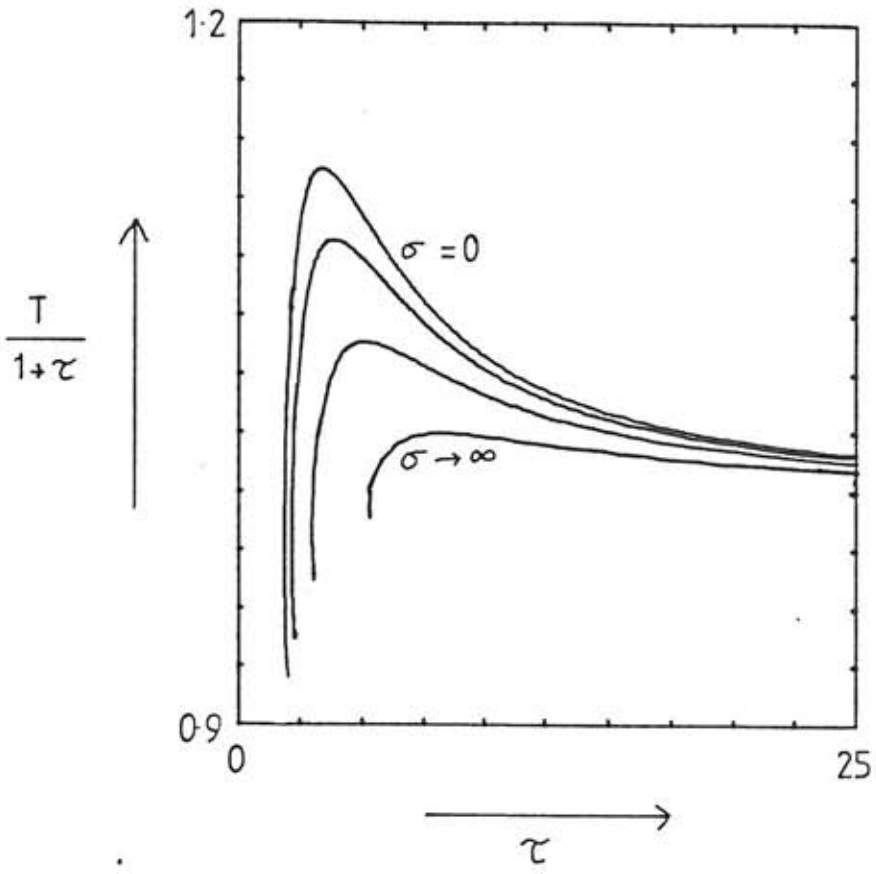

Figure 10.7. Period to generation time ratio for L = 100 and $\frac{\tau}{\tau_F} = 10$, for $\sigma = 0, 1, 5, \infty$.

equation (10.14). In each of the two special cases of the junk model ($\epsilon = 0$ or $B = 0$), the parameter B or ϵ - again a measure of the quantity of junk an individual can deposit - is absent from the characteristic equation. For all our models, it is the 'external' parameters - the constant food density F which determines the minimum delay for both interference and competition via junk density models, the minimum delay τ_{min}, the amount of food supplied per unit handling time Φ', and the junk removal rate h - which determine stability and cycle period.

As all models are particular examples of the general variable maturation time model of Chapter 9, it follows that stability is decreased as fecundity is increased, and that increasing the delay parameter τ ultimately destabilizes the steady state - this is confirmed by Figs. 10.1, 10.2, 10.4, 10.6.

For the models considered, it can be seen from Figs. 9.2, 9.3, 10.3, 10.6, 10.7 that the period to generation time ratio $T/1+\tau$ is always close to unity for moderate values of the parameters, with the cycle period approaching the generation time for large values of the delay. The period to generation time ratio is always less than unity when competition is direct (Fig. 9.2), with values of $T/1+\tau$ significantly less than 1 only occurring at large values of the parameter L ($T/1+\tau > 0.87$ for $L < 500$). All

our other models can have cycle periods which are both greater than and less than the generation time, although values significantly greater or less than 1 again only occur at large values of L. For the models of sections 10.2 - 10.4, we have shown that $T/1+\tau$ is, for given values of L and τ, least when competition is by direct interference and greatest when larvae compete for food with a development index which is weight gained in the stage.

The models of sections 10.3 and 10.4 give an indication of two factors which may be important in determining the size of the period to generation time ratio. Our competition for food model (section 10.3) shows that $T/1+\tau$ decreases as the development rate becomes less sensitive to changes in food density (as q_N is increased). That is for this model the size of the change in maturation time due to competition affects the period to generation time ratio, with small values of $T/1+\tau$ occurring when $\tau(t)$ may only take a small range of values.

Our competition via junk density model (section 10.4) shows that $T/1+\tau$ is smallest when junk is deposited at a rate proportional to the individual feeding rate - the special case B = 0. We note that the extent of regulation is greatest in this case, with regulation occurring both via changes in maturation time and through the rate of

junk deposition itself - that is, at high junk densities, no junk is deposited. As the parameter σ is decreased, thereby decreasing the extent of regulation, the period to generation time ratio is increased, taking its maximum value when the only means of regulation is via the maturation time (the case $\epsilon = 0$).

CHAPTER ELEVEN

Chapter 11 : Conclusions

The work covered in Section II was motivated by two problems which may commonly arise in the study of laboratory maintained populations: namely, whether the detail of the manner in which larvae compete, or the factor triggering pupation, may significantly affect the dynamics of a population in culture. As discussed in Chapter 7, we wish to know whether either of these may affect the size of any population cycle periods; indeed, we wish to know which parameters will influence cycle periods.

A prerequisite of such a study was the development of an analytic technique for evaluating period to delay ratios. We have, in Chapter 8, developed a method for evaluating period to delay ratios near stability boundaries for non-linear single delay systems, which may be easily adapted to systems in which the delay itself is a dynamic variable. Although our method applies only to parameter values near stability boundaries, Gurney & Nisbet (1985) found that such an estimate is a good approximation to the period of limit cycle solutions which occur when parameters take values in the locally unstable region of parameter space.

All models we have considered throughout Section II are of the type given by equations (7.1), namely, models of a

population in which larval competition is responsible for regulation of the population by inducing changes in the larval maturation period and therefore in larval survival. By considering two general classes of such models - those in which competition is either 'direct' or 'indirect' (i.e. mediated through variations in a second unspecified variable), we have shown that the period to generation time ratio is always smallest when competition is direct.

We have shown that when competition is direct, the single factor determining the period to generation time ratio is the size of the (steady state) larval maturation period. When competition is indirect, both the larval maturation time and adult fecundity will influence the size of this ratio; we have obtained bounds on the period to generation time ratio for the whole class of models considered in Chapter 9. Thus, although the manner of competition (i.e. direct or indirect) CAN result in different period to delay ratios, the differences only become significant when the fecundity parameter L becomes very large (e.g. for $L \leq 100$, $T/1+\tau$ always lies between 0.94 and 1.15). These differences become negligible as the delay is increased, with cycle periods close to the generation time occurring at large values of the delay. As the class of models considered in Chapter 9 do not consider any particular functional form of development rate, they by implication allow for the choice of a

variety of larval development indices. Thus we conclude that the choice of larval development index will NOT significantly influence the period to generation time ratio.

In Chapter 10, we considered three specific models, each of which represented one of the types of competition we believe occur in Plodia. As expected (given the result of the work in Chapter 9) we found broadly similar period to generation time ratios for all models. We find that both of the indirect competition models we consider yield greater stability of the steady state than the direct competition model, and that a significant shift in the position of the stability boundary is only found at extreme values of the parameters (the parameters Φ and h). We also find that parameters measuring the intensity of competition serve only to determine the size of the steady state (larva and adult) populations and do not affect either stability or cycle period. We find that it is the 'external' parameters related to the food replacement regime (the food supply rate Φ or food density F, the junk removal rate h) which may affect stability.

Although it is widely believed that 'junk' production may exert 'negative influences' on larval development and survival (Peters & Barbosa, 1977), we know of no models which have included such an effect. We have represented

competition via the deposition of junk in a, perhaps unrealistic, manner by assuming competition by increased time-wasting due to the presence of junk. However a brief calculation (along the lines indicated in Chapter 9) shows that a competition via food density model in which larvae also 'spoil' food items (at a rate $\propto \rho_M(t)\rho_L(t)$) yields the same range of period to generation time ratios as given by Fig. 9.3.

As a result of the work presented in Section II, we conclude it is unlikely that either the manner of competition or larval development index will significantly affect stability or cycle period. We have not yet considered a model in which more than one type of competition occurs; evidently such a study would be necessary before reaching any firm conclusions.

We have considered models in which the only means of regulation is through larval competition and have not found significant differences in models which consider different competition mechanisms. In models of the type developed in Section I, where larval competition is only one of several mechanisms which contribute towards regulation of the population, we might expect the detail of competition to be even less important.

We note that one of the reasons for investigating cycle periods was the failure of our Plodia model to produce

cycle periods which match those of the experimental populations. Values of parameters of the strategic models in Section II which are appropriate to Plodia are $L \simeq 18.75$ and $\tau \simeq 5$; these models would give population oscillations with a cycle period very close to the generation time. Thus, we must look elsewhere for the reason for the failure of our (Section I) Plodia MODELS to give cycle periods close to the generation time. One possibility is the functional form of the larval per capita death rate; as shown in Chapter 5 this can affect the dynamics of the model. A similar strategic study to that of Chapter 9, in which the larval maturation period is taken to be constant and density-dependence is incorporated into the per capita death rate would show how changes in the functional form of the death rate could affect the cycle period. Other factors present in the Plodia models which our strategic models fail to consider are the finite egg and pupa development periods and the effect of egg cannibalism, and it is probable that each of these may influence cycle periods.

We conclude that the excessively large period to generation time ratios of our Plodia models are NOT due to the failure of the model to properly reflect larval competition and development. Although these factors need to be investigated experimentally in order to obtain an accurate model of the dynamics of Plodia, we do not believe their inclusion would produce fluctuations of a

different type to those of the existing models.

APPENDIX A

Appendix A: Distributed Maturation

The data of the AE experiments show a distribution of egg-to-adult maturation periods - a cohort of newly laid eggs emerge into adults after a development period of 22-40 days (BGYF data). Evidently such an effect should be incorporated into our model.

The Outline Model of Chapter 2 shows that egg and pupa maturation periods do not vary, so that the observed maturation distribution must originate in the larval stage of the life-cycle. We use a stage-structured model which assumes all individuals in a given stage have identical (time-dependent) vital rates; thus as a cohort of larvae will all develop at the same rate, it follows that to incorporate a distribution of maturation periods into our model we must allow for maturation at different development indices. Thus, we consider a mortality-corrected maturation distribution $\psi(q)$ which is the distribution of development indices at maturation which would be observed for a cohort if all survived (see Gurney et al, 1986). In this Appendix, we show how $\psi(q)$ may be estimated for Plodia larvae.

The AE experiment began by introducing a small number of newly-laid eggs into a large container of plentiful food. We shall estimate the shape of the maturation distribution $\Psi(q)$ by making the following assumptions

about the vital rates during the AE experiment :-

(a) during the larval stage, all larvae were developing at the maximum possible rate, D_{max} (i.e. we shall assume the effects of interference and competition for food are negligible).

(b) we assume the larval per capital death rate was the minimum possible, c

(c) we assume that the recruitment rate to the larval stage may be approximated by a delta-function. W.L.O.G. we take this to be a delta-function at t=0 and write

$$\int_{-\infty}^{\infty} R(t)dt = R$$

It follows from the above, that at time t (>0) all larvae who have not yet matured have development index

$$q = D_{max}t \qquad (A.1)$$

The maturation rate out of the larval stage at time t is given by

$$M(t) = D(t) \int_o^t R(x) \exp\left[- \int_x^t \delta(t')dt' \right] \psi\left[\int_x^t D(t')dt' \right] dx$$

which, given our assumptions and equation (A.1), reduces to

$$M(t) = R\, D_{max}\, e^{-ct}\, \psi(D_{max} t) \qquad (A.2)$$

The data of the AE experiment give the number of adults to emerge each day. That is after correcting for times spent in egg and pupa stages, and fitting a curve to the data, we may obtain the maturation rate out of the larval stage. As we wish to be able to express M(t) in terms of variables which satisfy ordinary differential equations, we fit a curve of the form $t^n \exp(-t/a)$ to the data of the AE experiment. Fig. A.1. shows the curve we use, which is of the form

$$M(t) = \begin{cases} 0 & t \leq \tau_{min} \\ p(t-\tau_{min})^5 \exp(-(t-\tau_{min})/a) & t \geq \tau_{min} \end{cases} \qquad (A.3)$$

where τ_{min} is the minimum possible maturation period (we use τ_{min} = 10.5 days, a = 0.725214) and p is a constant.

It follows from (A.1) (A.2) and (A.3) that the mortality-corrected maturation distribution $\psi(q)$ will be given by

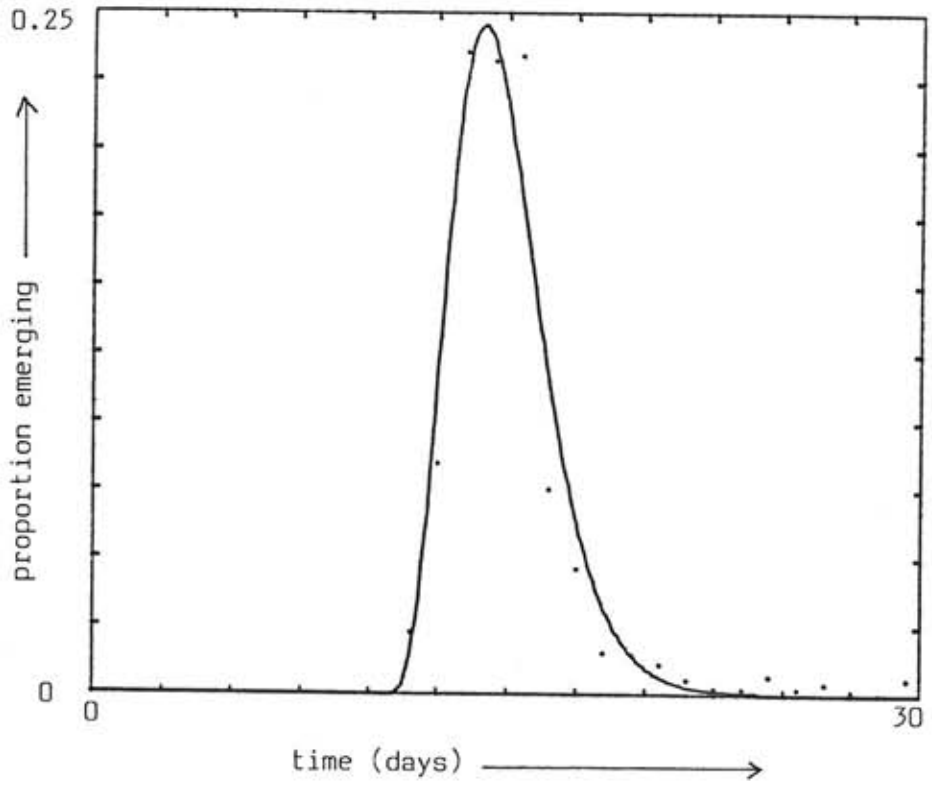

Figure A.1. Curve fitted to the data of the AE experiment. The solid line is of the form given by equation (A.3) with parameters

$a = 0.725214,$

$\tau_{min} = 10.5,$

$p = 0.0581226.$

$$\Psi(q) = \begin{cases} 0 & q \leq Q \\ P(q-Q)^5 \exp(-(q-Q)/q_o) & q \geq Q \end{cases} \qquad (A.4)$$

where

$$Q = D_{max}\tau_{min} \qquad (A.5)$$

is the minimum index at which maturation may occur, and

$$q_o = \frac{D_{max}}{1/a - c} \qquad (A.6)$$

where a is given above and c is the minimum larval per capita death rate. P is a constant which is determined by the requirement that if there are no larval deaths all larvae must eventually mature

i.e $$\int_o^\infty \Psi(q)dq = 1$$

or $$P = \frac{1}{5!\ q_o^6} \qquad (A.7)$$

Thus, it can be seen that for any choice of development index (i.e. in our case, weight or age), evaluating the parameters D_{max} and c will give the maturation distribution $\Psi(q)$.

It may be shown that it follows from our assumptions ((a),(b),(c)), that larval survival during this experiment will be given by the equation

$$S_L = \frac{\exp(-c\,\tau_{min})}{\left[\frac{c}{1/a - c} + 1\right]^6} \qquad (A.8)$$

We now estimate the size of the minimum larval per capita death rate, c, by considering the data of Podoler (1974), who found the maximum larval survival to be

$$S_L = 0.905 \qquad (A.9)$$

Thus, using our estimates of a = 0.725214 and τ_{min} = 10.5, it follows from equations (A.8) and (A.9) that we may take the minimum larval per capita death rate to be

$$c = 0.006717 \quad \text{days}^{-1}.$$

APPENDIX B

APPENDIX B: ESTIMATION OF THE PARAMETERS FOR THE PLODIA MODELS

In this Appendix, we give estimations of the parameters of our Plodia models, which were used to obtain the simulations (Chapter 5, Figs. 5.1 - 5.4) of the CTS experiments. We choose our unit of population to be the number of individuals per full-size cage, our unit of time to be 1 day, and our unit of weight to be 1 dry-mg. We shall use the following conversion factors (Lawton, 1984, pers. comm.)

$$c_1 = \frac{\text{dry weight of adult Plodia}}{\text{wet weight of adult Plodia}} = 0.4$$

$$c_2 = \frac{\text{dry weight of food}}{\text{wet weight of food}} = 0.74$$

B.1. PARAMETERS COMMON TO ALL MODELS

The following parameter estimates are used in each of our four models.

(i) e

e denotes the number of eggs laid per adult per day. As discussed in the text, we shall assume each adult lays 37.5 eggs over 6 days (Chapters 2 and 3), giving

$$e = 6.25 \text{ eggs adult}^{-1} \text{ day}^{-1}.$$

(ii) τ_E, τ_p, τ_A.

As discussed in Chapter 2, we assume a constant development period for eggs, pupae and Young Adults, which are taken to be

$$\tau_E = 3.5 \text{ days}$$

$$\tau_p = 7.0 \text{ days}$$

$$\tau_A = 6.0 \text{ days}$$

respectively.

(iii) Φ

We have simplified our model by assuming that food is supplied at a constant rate, Φ. BGYF food was supplied to the CTS population experiments at a rate of 7 (wet) g per week. Thus, we may take

$$\Phi = c_2 \times \frac{7000}{7} \text{ dry-mg day}^{-1}$$

$$\Phi = 740 \text{ dry-mg day}^{-1}$$

(iv) δ_A.

We estimate the per capita death rate δ_A of the Old Adult stage from the data of the AS experiment (Fig. 2.1) and estimate

$$\delta_A = 0.5 \text{ days}^{-1}.$$

(v) c, τ_{min}, r_o.

We use the estimations for c and τ_{min} which we found in Appendix A, viz

$$c = 0.006717 \text{ days}^{-1},$$

$$\tau_{min} = 10.5 \text{ days}.$$

We shall also be using a parameter r_o which we define to be

$$r_o = \frac{q_o}{D_{max}}$$

which will, given equation (A.6) and our Appendix A estimate of the parameters and a and c, take a value

$$r_o = 0.7288 \text{ days}$$

(vi) ϵ, κ

ϵ (cf equation (4.9)) is the efficiency with which larvae convert food eaten into weight gained, and κ denotes the weight lost during pupation. We shall assume the values of these parameters are

$$\epsilon = 0.1$$

$$\kappa = 0.8$$

(Lawton, 1984, pers. comm.).

B.2. PARAMETERS OF MODELS I and III

In this section, we give estimates of parameters used in Models I and III. We shall make use of the following equations.

It can be shown that if the larval per capita death rate is a constant, δ, and the larval development index is taken to be 'time-in-stage', then larval survival is given by

$$S_L = \frac{\exp(-\delta\ \tau_{min})}{(r_o\ \delta + 1)^6} \qquad (B.1)$$

and the mean larval development period is

$$\tau = \tau_{min} + \frac{6\ r_o}{\delta r_o + 1} \qquad (B.2)$$

where the parameters r_o and τ_{min} are given above.

B.2.1 PARAMETERS RELATING TO FEEDING/DEATH RATES

In this sub-section we estimate the maximum feeding rate I_{max}, and two quantities δ_o and I_{MO} (which we shall make use of later) which we define to be:-

δ_o = larval per capita death rate at the steady state food density in the absence of interference

I_{MO} = larval per capita food uptake rate at the steady state food density in the absence of interference.

(i) I_{max}

Most of the available data of adult weights is of adult weight after death, the sole exception being the data of the OB experiments. Accordingly, we shall estimate the parameter I_{max} from Podoler's (1974) observation that the maximum adult female weight at emergence is 14.5 (wet)mg; we assume this figure represents the resulting adult weight when larvae feed at their maximum rate.

At maximum feeding rate, the per capita death rate is the minimum possible, c (c.f. Fig. 4.1); it follows from equation (B.2) that the mean development period is 14.85 days. Thus, we estimate

$$I_{max} = \frac{14.5}{14.85} \times \frac{c_2 \kappa}{\epsilon} \text{ dry-mg day}^{-1}$$

$$= 4.8871 \text{ dry-mg day}^{-1}.$$

where we have allowed for weight lost during pupation, the efficiency with which larvae convert food eaten into weight gained, and converted from wet-weight to dry-weight.

(ii) δ_o.

In Chapter 3, we estimated that larval survival at the steady state food density would be 0.35 if there were no interference. From our definition of δ_o, it follows we may estimate this quantity by substituting $\delta = \delta_o$ and $S_L = 0.35$ into equation (B.1) and solving for δ_o. We find

$$\delta_o = 0.07111 \text{ days}^{-1}.$$

(iii) I_{MO}.

We shall estimate I_{MO} from the data of the CTS experiment. Fig. 2.8 shows the mean weight versus adult density; we shall take the weight at the intercept (i.e. zero density) to represent the resulting mean adult weight of a cohort feeding at a rate I_{MO}. We estimate this weight to be 2.45 dry mg. We shall take the mean larval development period to be 14.66 days (found from equation (B.2) with $\delta = \delta_o$), which gives

$$I_{MO} = \frac{2.45}{14.66} \times \frac{1}{\epsilon\kappa} \text{ dry-mg day}^{-1}$$

$$I_{MO} = 2.089 \text{ dry-mg day}^{-1}.$$

B.2.2 PARAMETERS OF δ_A.

The per capita death rate δ_A, which is used in Model I, is related to the feeding rate I_M by equation (4.7), viz.

$$\delta_A = \frac{\eta}{I_M} \qquad (B.3)$$

It follows from sections B.2.1, B.2.2 that we may take either

$$\eta = \delta_o \, I_{MO} = 0.1485$$

or $$\eta = c \, I_{max} = 0.0328$$

The disparity between these figures shows that the functional form given by equation (B.3) is not ideal.

A brief calculation shows that taking $\eta = 0.1485$ gives a mean steady state adult weight of $\simeq$ 1.3 dry-mg over the working range of steady states, whereas taking $\eta = 0.0328$ gives a mean adult weight $\simeq$ 0.3 dry-mg! Thus, while both figures are lower than the observed adult weight, we shall take

$$\eta = 0.1485.$$

B.2.3 PARAMETERS OF δ_B.

The per capita death rate δ_B used in Model III is related to the feeding rate by the equation

$$\delta_B = \begin{cases} \delta_{max} & I_M \leq I_o \\ \dfrac{\eta}{I_M - K} & I_M \geq I_o \end{cases} \qquad \text{(B.4)}$$

(c.f. equation (4.8) and Fig. 4.1(b)).

It can be seen that the following equations must hold :-

$$\delta_o = \frac{\eta}{I_{MO} - K} \quad \text{and} \quad c = \frac{\eta}{I_{max} - K}$$

which implies η and K take values

$$\eta = 0.0207$$

$$K = 1.798.$$

We, somewhat arbitrary, choose $\delta_{max} = 0.32$ days^{-1} which gives a mean larval lifetime of just over 3 days for feeding rates below the threshold. The continuity of δ at $I_M = I_o$ gives the threshold feeding rate

$$I_o = K + \frac{\eta}{\delta_{max}} = 1.86 \quad \text{dry-mg day}^{-1}.$$

B.2.4 ESTIMATING α, β GIVEN STEADY STATE SURVIVALS

As discussed in Chapter 5, we wish to assign values to the parameters α and β which will result in steady state survivals which lie at a chosen point on our working range of steady states. For a given point, and therefore for given values of S^*_L and S^*_E, we use the following procedure to calculate α and β.

We begin by noting that it follows from equation (4.12) that the steady state food density ρ^*_M is given by

$$\rho^*_M = -\frac{\Phi \tau_E}{\ell n(2S^*_E)} \qquad (B.5)$$

which may now be found for any given S^*_E. Furthermore it may be seen from equation (B.1) that δ^* may be calculated for any given value of S^*_L; δ^* in turn yields, via equation (B>3) or (B>4), the value of I^*_M which in turn gives the steady state larval density ρ^*_L via equation (4.11), or

$$\rho^*_L = \frac{\Phi}{I^*_M} \qquad (B.6)$$

Thus, for any given values of S^*_L and S^*_E on our working range, we may estimate ρ^*_M and ρ^*_L. It follows from our definition of I_{MO} that

$$I_{MO} = \frac{I_{max}\rho^*_M}{\alpha+\rho^*_M} \qquad (B.7)$$

and from the definition of I^*_M that

$$I^*_M = \frac{I_{max}\rho^*_M}{\alpha+\beta\rho^*_L+\rho^*_M} \qquad (B.8)$$

Thus we are now able, via the above equations, to calculate values of the parameters α and β for any given point on our working range of steady states.

We use the above procedure to calculate values of α and β for the simulations given in Figs. 5.1 and 5.3. The values used are as follows:

Model I (Fig. 5.1)

(a) S^*_L = 13.8% S^*_E = 19.3% α = 3641.05 β = 8.7737

(b) S^*_L = 9.62% S^*_E = 27.7% α = 5872.2 β = 16.104

(c) S^*_L = 7.21% S^*_E = 37.0% α = 11460.8 β = 34.287

Model III (Fig. 5.3)

(a) S^*_L = 9.62% S^*_E = 27.9% α = 5872.2 β = 2.2447

(b) S^*_L = 7.21% S^*_E = 37.0% α = 11476.3 β = 4.7772

(c) S^*_L = 6.25% S^*_E = 42.7% α = 21897.1 β = 9.4371.

B.3 PARAMETERS OF MODELS II AND IV

Both Model II and Model IV assume that the weight of a larva is a measure of its state of development. It may be shown that, for these models, when the larval per capita death rate is a constant, δ, and the per capita feeding rate is a constant, I_M, the larval survival will be given by

$$S_L = \frac{\exp(-x\tau_{min})}{(r_o x+1)^{\delta}} \qquad (B.9)$$

where

$$x = \delta \frac{I_{max}}{I_M}$$

B.3.1 PARAMETERS RELATING TO FEEDING/DEATH RATES

(i) I_{max}

As these models assume that weight is a measure of larval development, implying that mean larval weight upon maturation does not vary, it follows that Models II and IV cannot reflect the range of adult weights of *Plodia*. Thus, we estimate I_{max} from the data of the CTS experiments.

We suppose that when larvae are feeding at the maximum rate, the resulting mean adult weight will be the maximum

found during the CTS experiment - 2.6 dry-mg. We further assume that the mean larval development period is the minimum possible - 14.85 days. Thus, after again allowing for the conversion efficiency and weight lost during pupation, we obtain

$$I_{max} = 2.104 \text{ dry-mg day}^{-1}$$

(ii) δ_o, I_{MO}.

We estimate I_{MO} by considering the weight/density data of the OB experiment (Fig. 2.13). We estimate the mean adult weight at emergence to be $W_o \propto 3.6$ dry-mg at an effective zero density of larvae; we assume we may use this estimate to obtain I_{MO} (the feeding rate at the steady state food density in the absence of interference). The mean larval maturation period during the OB experiments was $\tau_o \propto 28$ days. Thus, we take

$$I_{MO} = \frac{W_o}{\tau_o} \cdot \frac{1}{\epsilon\kappa}$$

$$\propto 1.6 \text{ dry-mg day}^{-1}.$$

We shall again estimate δ_o by taking larval survival to be 35% at the steady state food density. This implies, via equation (B.9), that

$$x = \delta_o \frac{I_{max}}{I_{MO}} = 0.07111 \text{ days}^{-1}$$

which, given our estimates (above) of δ_o and I_{MO}, yields

$$\delta_o = 0.054 \text{ days}^{-1}.$$

B.3.2 PARAMETERS OF δ_A.

For consistency (c.f. section B.3.2) we shall take the parameter η of the functional form of the death rate δ_A to be given by

$$\eta = \delta_o \, I_{MO}$$

or $$\eta = 0.0865$$

B.3.3 PARAMETERS OF δ_B.

The parameters of the functional form of δ_B are found in the same way as for our Models I and III (section B.2.3), i.e. we find η and K from the equations

$$\delta_o = \frac{\eta}{I_{MO}-K} \qquad c = \frac{\eta}{I_{max}-K}$$

where $\delta_o = 0.054$, $I_{MO} = 1.6$ dry-mg and $I_{max} = 2.104$ dry-mg day^{-1}, and we shall again take

$$\delta_{max} = 0.32 \text{ days}^{-1}.$$

We find

$$\eta = 0.003867$$

$$K = 1.5284.$$

B.3.4 ESTIMATING α, β GIVEN STEADY STATE SURVIVALS

The method we use for estimating the α and β parameters of the feeding rate for a given point on our working range is fundamentally the same as that outlined in section B.2.4, which we applied to models I and III.

We note that for a given value of S^*_L, the quantity

$$x^* = \delta^* \frac{I_{max}}{I^*_M}$$

may be found from equation (B.9). For each functional form of the death rate (i.e. δ_A or δ_B) it follows that the steady state feeding rate I^*_M may be calculated from the above equation. That is, for Model II in which the relationship between δ^* and I^*_M is given by equation (B.3), I^*_M will be given by

$$(I^*_M)^2 = \eta \frac{I_{max}}{x^*}$$

and may be found for any given value of x^*. For Model IV, where δ^* is related I^*_M by equation (B.4), I^*_M may be found from the equation

$$(I^*_M)^2 - KI^*_M - \eta \frac{I_{max}}{x^*} = 0.$$

Having estimated I^*_M, the steady state larval density ρ^*_L and the parameters α and β may be found from equations (B.6) - (B.8).

We use the following values for the simulations given in Figs. 5.2 and 5.3 :

Model II (Fig. 5.2)

(a) $S^*_L = 13.8\%$ $S^*_E = 19.3\%$ $\alpha = 858.54$ $\beta = 2.2568$

(b) $S^*_L = 9.62\%$ $S^*_E = 27.7\%$ $\alpha = 1384.6$ $\beta = 4.1644$

(c) $S^*_L = 7.21\%$ $S^*_E = 37.0\%$ $\alpha = 2706.1$ $\beta = 9.0698$

Model IV (Fig. 5.4)

(a) $S^*_L = 11.43\%$ $S^*_E = 23.3\%$ $\alpha = 1070.8$ $\beta = 0.2195$

(b) $S^*_L = 7.69\%$ $S^*_E = 34.7\%$ $\alpha = 2232.3$ $\beta = 0.5256$

(c) $S^*_L = 6.29\%$ $S^*_E = 42.4\%$ $\alpha = 4857.6$ $\beta = 1.2021$

B.4 PARAMETERS OF MODEL III INCORPORATING VARIABLE FECUNDITY.

With the exception of adult fecundity parameters and the α and β parameters, all parameters we use are as given for Model III (Sections B.1 and B.2). For a given value of S^*_L, the procedure outlined in Section 6.1 is followed to estimate S^*_E and I^*_M, and the steady state adult fecundity E^* (eggs per adult lifetime). We then estimate the α and β parameters in the same way as given in Section B.2.4. We use the following values for the simulations given in Figs. 6.2 :

(a) $S^*_L = 12.8\%$ $S^*_E = 19.75\%$ $(E^* = 39.55\%)$
$\alpha = 3726.85$ $\beta = 1.26201$

(b) $S^*_L = 7.21\%$ $S^*_E = 35.5\%$ $(E^* = 39.1)$
$\alpha = 10081.4$ $\beta = 4.1966$

(c) $S^*_L = 6.25\%$ $S^*_E = 41.0\%$ $(E^* = 39.02)$
$\alpha = 17046.7$ $\beta = 7.5211$

APPENDIX C

Appendix C: A Source of Zero Eigenvalues

Linearization about the single positive steady state of the model in Chapter 8 yields a characteristic equation (8.12) which has a zero solution for all values of the parameters. We show that a linear system having a zero eigenvalue cannot have a unique steady state.

Consider the n^{th} order linear system.

$$\dot{\underline{x}}(t) = A\,\underline{x}(t) + B\,\underline{x}(t-\tau) \qquad (C.1)$$

where A and B are n x n constant matrices; this system has the trivial steady state solution

$$\underline{x}^* = \underline{0}$$

and characteristic equation

$$\det\,(A + B\,e^{-\lambda\tau} - \lambda I) = 0 \qquad (C.2)$$

which has a zero eigenvalue if and only if

$$\det\,(A + B) = 0$$

Now if $\underline{x}(t) = \underline{x}^*$ is a steady state of (C.1), then

$$(A + B)\,\underline{x}^* = \underline{0}$$

and so it can be seen that the linear system given by equations (C.1) has a zero eigenvalue if and only if $\underline{x}^*$ is an eigenvector (eigenvalue zero) of A + B, and as such $\underline{x}^*$ can, at best, only be determined to within a scalar multiple (see, for example, Hildebrand 1952 p 31). Thus, if the linear system (C.1) has a zero eigenvalue, this implies a non-unique steady state solution - there must exist an infinite number of non-zero steady states.

It can be shown (Bellman & Cooke, 1963), that (C.1) has the solution

$$\underline{x}(t) = \sum_{\lambda_i} \underline{C}_i \, e^{\lambda_i t}$$

where the λ_i are the roots of equation (C.2) and the C_i are constant vectors. In the case of a zero eigenvalue this becomes

$$\underline{x}(t) = \underline{C}_o + \sum_{\lambda_i \neq 0} C_i \, e^{\lambda_i t}$$

and so it can be seen that it is the size of the real parts of non-zero eigenvalues which determine whether the solution will converge to or diverge from one of the steady states. In the case of convergence, the steady

state ultimately reached will depend on the initial history.

Zero eigenvalues are relevant to the model considered in Chapter 8. To investigate the (local) stability of the model steady state, we consider a small deviation

$$\rho_L(t) = \rho_L^* + \ell(t)$$
$$\rho_A(t) = \rho_A^* + a(t)$$
$$\tau(t) = \tau^* + q(t)$$

Substituting these expressions into equations (7.1) and (8.11) and neglecting terms higher than first order yields the equations

$$\frac{d\ell}{dt} = La(t) - a(t-\tau^*) + \delta\rho_A^* q(t) + D^*\rho_A^*[\ell(t) - \ell(t-\tau^*)] - \delta\ell(t) \qquad (C.3)$$

$$\frac{da}{dt} = a(t-\tau^*) - \delta\rho_A^* q(t) - D^*\rho_A^*[\ell(t) - \ell(t-\tau^*)] - a(t) \qquad (C.4)$$

$$q(t) = D^* \int_{t-\tau^*}^{t} \ell(t')\, dt' \qquad (C.5)$$

The characteristic equation (8.12) is obtained by writing this last equation in differential equation form as

$$\frac{dq}{dt} = D^* \left[\ell(t) - \ell(t-\tau^*)\right] \qquad (C.6)$$

By seeking constant solutions $\ell(t) = \ell_0$, $a(t) = a_0$ and $q(t) = q_0$, it can be shown that equations (C.3), (C.4) and (C.6) admit the non-trivial constant solution

$$\begin{bmatrix} \ell(t) \\ a(t) \\ q(t) \end{bmatrix} = k \begin{bmatrix} 1 \\ \frac{\delta}{L-1} \\ 0 \end{bmatrix}$$

where k is an arbitrary constant, and so this system will have a characteristic equation with a zero eigenvalue. It can be shown that the characteristic equation is given by

$$\Gamma(\lambda + 1 - L)(1 - e^{-\lambda\tau^*}) = \lambda(\lambda + 1 - e^{-\lambda\tau^*})$$

However, by seeking constant solutions to equations (C.3),(C.4) and (C.5), it can be shown that these equations have only the trivial constant solution,

$$\begin{bmatrix} \ell(t) \\ a(t) \\ q(t) \end{bmatrix} = \begin{bmatrix} 0 \\ 0 \\ 0 \end{bmatrix}$$

and that the corresponding characteristic equation is

$$\Gamma(\lambda + 1 - L)\,\frac{(1-e^{-\lambda\tau^*})}{\lambda} = \lambda + 1 - e^{-\lambda\tau^*}$$

which does not have a zero eigenvalue. We conclude that it is the conversion of the integral equation (C.5) into the differential equation (C.6) which 'produces' the zero eigenvalue (see also Busenberg & Cooke 1980), and as (C.5) is a proper statement of the model, the $\lambda = 0$ solution of equation (8.12) is of no significance.

APPENDIX D

APPENDIX D : Other work

During the period of my studentship, I also collaborated with Dr. R. Bain of the Department of Applied Physics in the solution of a problem in the design of high order magnetic gradiometers with shaped near-source response, which involves the simultaneous solution of N algebraic equations in m (>N) variables. As a result of this work, the following papers have been submitted.

SOLUTION OF A PROBLEM IN MAGNETIC GRADIOMETRY IN TERMS OF ORTHOGONAL POLYNOMIALS.

A.E.JONES and R.J.P.BAIN

Department of Applied Physics
University of Strathclyde,
Glasgow, Scotland.

AMS Classification No. 33A65

Submitted to Mathematical Methods in the Applied Sciences

1. Introduction

A common problem in magnetometry is the detection of weak magnetic signal sources (such as magnetic or current dipoles) located near a measuring instrument, in the presence of large noise fields from distant sources ([4]). An N-th order magnetic-field gradiometer is an arrangement of pickup loops designed primarily to have zero net flux coupled to it by the first N terms of a Taylor expansion of the magnetic field threading the gradiometer, thus discriminating against distant sources.

One type of gradiometer (see Fig.1) consists of a series of adjacent rectangular pickup loops, wired in series with an insulated cross-over between each pair of loops. The positions of the cross-overs determine not only the order of the gradiometer, but also the detailed response to nearby sources ([2],[4]). This paper addresses the problem of selection of cross-over positions to achieve a given order N when one or more cross-over positions have been pre-selected to achieve a given near-source response. Denoting the cross-over positions as x_s, s=1,2,...,m, we require that

$$
\begin{aligned}
x_1 - x_2 + x_3 - \ldots - (-1)^m x_m &= \tfrac{1}{2}\,(1+(-1)^m) \\
x_1^2 - x_2^2 + x_3^2 - \ldots - (-1)^m x_m^2 &= \tfrac{1}{2}\,(1+(-1)^{m+1}) \\
&\cdots\cdots\cdots\cdots\cdots \\
x_1^N - x_2^N + x_3^N - \cdots - (-1)^m x_m^N &= \tfrac{1}{2}\,(1+(-1)^{m+N-1})
\end{aligned}
\qquad (1)
$$

where $N \leqslant m$, and that the x_s's also satisfy the inequalities

$$(2) \qquad -1 \leqslant x_m < x_{m-1} < \ldots < x_2 < x_1 \leqslant 1$$

([2],[3],[4]).

We define a solution set, $\{x_s\}$, to be a set of values which satisfy both equations (1) and the inequalities (2).

When $N = m$, it can been shown ([3],[6]) that equations (1) may be solved to give the single solution set

$$\left\{x_s = \cos\left[\frac{s\pi}{m+1}\right]\right\}$$

When N is less than m there is, of course, no unique solution set; for any solution set, N of the x_s's will depend on m-N of the x_s's. Values $x_1, x_2, \ldots, x_m$ satisfying equations (1) may be found by assigning values to m-N of the x_s's and solving (1) to obtain the remaining x_s's - although algebraic solution of equations (1) proves intractable for large m. If the set of values so obtained also satisfies (2), it is a solution set.

For x_s's satisfying (1), the obvious interchangability of x_{2i-1} with x_{2j-1}, and x_{2i} with x_{2j}, leads us to examine two polynomial equations with roots $\{x_{2i-1}\}$ and $\{x_{2i}\}$. We give these polynomial equations, which take different forms for $m = 2n-1$ and $m = 2n$ ($n \in \mathbb{N}$) : these cases are treated separately. As expected, the coefficients of these equations depend upon the values of m-N constants. Thus, we reduce the problem of finding solutions for equations (1) to that of obtaining the roots of two polynomial equations.

We illustrate the use of this formalism by examining the behaviour of the x_s's for N = m-1, when m-1 of these depend on the value of one x_s; we show when it is possible to solve equations (1) to give a valid solution set, and obtain bounds for each x_s.

2. Solution sets when m = 2n-1.

For a solution set $\{x_s\}$, we consider the polynomial equations

$$X^n + p_1 X^{n-1} + \quad \ldots\ldots \quad + p_{n-1} X + p_n = 0$$

and

$$X^{n-1} + q_1 X^{n-2} + \quad \ldots\ldots \quad + q_{n-2} X + q_{n-1} = 0$$

which have roots $x_1, x_3, \ldots, x_{2n-1}$ and $x_2, x_4, \ldots, x_{2n-2}$ respectively. We write these equations in the form

$$(3) \quad T_n(X) + k_1 T_{n-1}(X) + \quad \ldots\ldots \quad + k_{n-1} T_1(X) + k_n = 0$$

and

$$(4) \quad U_{n-1}(X) + m_1 U_{n-2}(X) + \quad \ldots\ldots \quad + m_{n-2} U_1(X) + m_{n-1} = 0$$

where $T_1, T_2, \ldots, T_n$ are Chebyshev polynomial of the first kind, and $U_1, U_2, \ldots, U_{n-1}$ are Chebyshev polynomials of the second kind (see [1]). As the roots of these equations are to be a solution set, the constants k_i and m_j are real and are such that the n roots of (3) and the n-1 roots of (4) all lie in the interval $[-1,1]$.

We now show that

$$k_i = m_i \quad \text{for all } i = 1,2,\ldots,N$$

when $N \in \{1,2,\ldots,n-1\}$

and $\quad k_i = m_i \quad$ for $i = 1,2,\ldots,n-1$

with $\quad k_i = 0 = m_i \quad$ for $i = 2n-N, 2n-N+1, \ldots, n$

when $N \in \{n, n+1, \ldots, 2n-1\}$

so that (3) and (4) are two polynomial equations with m-N

independent coefficients.

As $x_i \in [-1,1]$, we begin by defining new variables

$$x_{2i-1} = \cos\theta_i \qquad (i = 1,2,\ldots,n)$$

and $$x_{2i} = \cos\alpha_i \qquad (i = 1,2,\ldots,n-1).$$

By considering

$$W_r = \sum_{i=1}^{n} \cos\, r\theta_i \; - \sum_{i=1}^{n-1} \cos\, r\alpha_i$$

$$= \sum_{i=1}^{n} T_r(\cos\theta_i) \; - \sum_{i=1}^{n-1} T_r(\cos\alpha_i)$$

$$= \frac{r}{2} \sum_{j=0}^{[r/2]} (-1)^j \frac{(r-1-j)!}{j!(r-2j)!} 2^{r-2j} \left[\sum_{i=1}^{n} x_{2i-1}^{r-2j} - \sum_{i=1}^{n-1} x_{2i}^{r-2j} \right]$$

(see [1]) for r = 1,2,...,N, it can be seen from equations (1) that

$$W_r = \begin{cases} T_r(0) & \text{when } r = 1,3,5,\ldots \\ T_r(1) & \text{when } r = 2,4,6,\ldots \end{cases}$$

and so the θ_i and α_i must satisfy the equations

$$\begin{aligned}
&\cos\theta_1+\cos\theta_2+ \ldots +\cos\theta_n = \cos\alpha_1+\cos\alpha_2+ \ldots+\cos\alpha_{n-1} \\
&\cos2\theta_1+\cos2\theta_2+ \ldots +\cos2\theta_n = \cos2\alpha_1 + \cos2\alpha_2+ \ldots +\cos2\alpha_{n-1}+ 1 \\
&\qquad\qquad \ldots\ldots\ldots\ldots \\
&\cos N\theta_1+\cos N\theta_2+ \ldots +\cos N\theta_n = \cos N\alpha_1+ \cos N\alpha_2+ \ldots +\cos N\alpha_{n-1} \\
&\qquad\qquad + \frac{1}{2}\left[1+(-1)^N\right]
\end{aligned} \tag{5}$$

With the transformation X = cosθ, equation (3) may be written (see [1]) as

(6) $\cos n\theta + k_1 \cos (n-1)\theta + \ldots\ldots + k_{n-1} \cos \theta + k_n = 0$

which has roots $\cos\theta_1, \cos\theta_2, \ldots, \cos\theta_n$. With $X = \cos\alpha$, equation (4) may be written as

(7) $$\frac{\sin n\alpha}{\sin\alpha} + m_1 \frac{\sin (n-1)\alpha}{\sin\alpha} + \ldots\ldots + m_{n-2} \frac{\sin 2\alpha}{\sin\alpha} + m_{n-1} = 0$$

which has roots $\cos\alpha_1, \cos\alpha_2, \ldots, \cos\alpha_{n-1}$.

Consider the complex variable

$$z = \cos\theta + i \sin\theta$$

so that

$$z^r + z^{-r} = 2 \cos r\theta \qquad \forall\ r \in \mathbb{N}.$$

Using this substitution, (6) may be written as

$$z^n + \frac{1}{z^n} + k_1\left[z^{n-1} + \frac{1}{z^{n-1}}\right] + \ldots. + k_{n-1}\left[z + \frac{1}{z}\right] + 2k_n = 0$$

or

$$z^{2n} + k_1 z^{2n-1} + \ldots. + k_{n-1} z^{n+1} + 2k_n z^n$$

(8) $$+ k_{n-1} z^{n-1} + \ldots. + k_1 z + 1 = 0.$$

The 2n complex roots of this equation occur as the complex conjugate pairs :

(9) $$z_{2i-1} = \cos\theta_i + i \sin\theta_i; \qquad z_{2i} = \overline{z_{2i-1}} = \cos\theta_i - i \sin\theta_i$$
$$(i = 1, 2, \ldots, n)$$

where the $\cos\theta_i$ are self-evidently the n roots of (6). Moreover, it can be seen from (9) that

$$z_{2i-1}^r + z_{2i}^r = 2 \cos r\theta_i \qquad \forall\ r \in \mathbb{N}$$

so that the $\cos\theta_i$ roots of (6) and the z_i roots of (8) are such that

$$(10) \qquad 2\sum_{i=1}^{n} \cos r\theta_i = \sum_{i=1}^{2n} z_i^r \qquad \forall\ r \in \mathbb{N}\ .$$

Now consider equation (7). With

$$z = \cos\alpha + i\sin\alpha$$

so that

$$z^r - z^{-r} = 2i\sin r\alpha \qquad \forall\ r \in N$$

equation (7) may be written as

$$\frac{1}{z^{n-1}}\left[\frac{z^{2n}-1}{z^2-1} + m_1\frac{z(z^{2n-2}-1)}{z^2-1} + \ldots + m_{n-2}\frac{z^{n-2}(z^4-1)}{z^2-1} + m_{n-1}z^{n-1}\right] = 0. \qquad (11)$$

It can be seen that the equation

$$z^{2n} + m_1 z^{2n-1} + \ldots + m_{n-1}z^{n+1} - m_{n-1}z^{n-1} - \ldots - m_1 z - 1 = 0 \qquad (12)$$

has the same roots as equation (11), together with two additional roots at $z^2 = 1$. The complex roots of (12) again occur as complex conjugate pairs, and the 2n roots of (12) are given by

$$z_{2i-1} = \cos\alpha_i + i\sin\alpha_i \qquad z_{2i} = \cos\alpha_i - i\sin\alpha_i$$

$$(i = 1,2,\ldots,n-1)$$

$$z_{2n-1} = -1 \qquad z_{2n} = 1$$

where again the $\cos\alpha_i$ are the (n-1) roots of equation (7). Hence the $\cos\alpha_i$ roots of (7) and the z_i roots of (12) are such that

$$2\sum_{i=1}^{n-1} \cos r\alpha_i = \sum_{i=1}^{2n-2} z_i^r = \sum_{i=1}^{2n} z_i^r \qquad \text{when } r = 1,3,5,\ldots$$

and

$$2\sum_{i=1}^{n-1} \cos r\alpha_i = \sum_{i=1}^{2n-2} z_i^r = \left[\sum_{i=1}^{2n} z_i^r\right] - 2 \qquad \text{when } r = 2,4,6,\ldots$$

(13)

It follows from (5),(10) and (13) that the sums of the r^{th} powers of the roots of (8) and (12) must be equal for $r = 1,2,\ldots,N$.

Newton's Formula ([5]) state that for a polynomial equation

$$z^{2n} + p_1 z^{2n-1} + \ldots + p_{2n-1} z + p_{2n} = 0$$

the sums of the r^{th} powers of the roots

$$S_r = \sum_{i=1}^{2n} z_i^r$$

are related to the coefficients $p_1, p_2, \ldots, p_{2n}$ by the relationships

$$\begin{aligned}
&S_1 + p_1 = 0 \\
&S_2 + p_1 S_1 + 2p_2 = 0 \\
&S_3 + p_1 S_2 + p_2 S_3 + 3p_3 = 0 \\
&\qquad \ldots\ldots\ldots\ldots \\
&S_{2n} + p_1 S_{2n-1} + \ldots + p_{2n-1} S_1 + 2n\, p_{2n} = 0
\end{aligned}$$

and so for two such polynomial equations, the sums of the r^{th} powers of the roots will be equal for all $r = 1,2,\ldots,N$, $(N \leq 2n)$ if and only if the first N coefficients of the polynomials are equal.

Hence, as the $\cos\theta_i$ roots of (6) and the $\cos\alpha_i$ roots of (7) satisfy (5) it follows that the first N coefficients of (8) and (12) are equal, which implies

$$k_i = m_i \qquad \text{for } i = 1,2,\ldots,N$$

when $N \in \{1,2,\ldots,n\}$

and $$k_i = m_i \qquad \text{for } i = 1,2,\ldots,n-1$$

with $$k_i = 0 = m_i \qquad \text{for } i = 2n-N, 2n-N+1, \ldots, N$$

when $N \in \{n, n+1, \ldots, 2n-1\}$.

3. Solutions when m = 2n.

When m = 2n, and $\{x_s\}$ is a solution set, the x_{2i-1} $(i=1,2,\ldots,n)$ and the x_{2i} $(i=1,2,\ldots,n)$ of a solution set $\{x_s\}$ will be the roots of two polynomial equations of degree n which we write as

$$(14) \qquad R_n(X) + k_1 R_{n-1}(X) + \ldots + k_{n-1} R_1(X) + k_n = 0$$

and

$$(15) \qquad Q_n(X) + m_1 Q_{n-1}(X) + \ldots + m_{n-1} Q_1(X) + m_n = 0$$

respectively. $\{R_n\}$ and $\{Q_n\}$ are two families of orthogonal polynomials with $\deg[R_n] = n = \deg[Q_n]$. These polynomials are described fully in the Appendix. Again, as the roots of these equations are a solution set, which satisfy (2), the constants k_i and m_j are real and are such that the roots of (14) and (15) lie in the interval [-1,1].

With variables

$$x_{2i-1} = \cos\theta_i \qquad (i = 1,2,\ldots,n)$$

and

$$x_{2i} = \cos\alpha_i \qquad (i = 1,2,\ldots,n),$$

equations (1) may be written as

$$\begin{aligned}
&\cos\theta_1+\cos\theta_2+ \ldots +\cos\theta_n = \cos\alpha_1+\cos\alpha_2+ \ldots+\cos\alpha_n + 1\\
&\cos2\theta_1+\cos2\theta_2+ \ldots +\cos2\theta_n= \cos2\alpha_1 + \cos2\alpha_2+ \ldots +\cos2\alpha_n\\
&\qquad\qquad \ldots\ldots\ldots\ldots\ldots\\
&\cos N\theta_1+\cos N\theta_2+ \ldots +\cos N\theta_n = \cos N\alpha_1+ \cos N\alpha_2+ \ldots +\cos N\alpha_n\\
&\qquad\qquad + \tfrac{1}{2}\left[1+(-1)^{N-1}\right] .
\end{aligned} \tag{16}$$

With the transformation $X = \cos\theta$, equation (14) may be written (see the Appendix) as

$$\frac{\cos\left[n+\frac{1}{2}\right]\theta}{\cos\frac{\theta}{2}} + k_1\frac{\cos\left[n-\frac{1}{2}\right]\theta}{\cos\frac{\theta}{2}} + \ldots + k_{n-1}\frac{\cos\frac{3\theta}{2}}{\cos\frac{\theta}{2}} + k_n = 0 \qquad (17)$$

which has roots $\cos\theta_1, \cos\theta_2, \ldots, \cos\theta_n$, and with the transformation $X = \cos\alpha$, (15) may be written as

$$\frac{\sin\left[n+\frac{1}{2}\right]\alpha}{\sin\frac{\alpha}{2}} + m_1\frac{\sin\left[n-\frac{1}{2}\right]\alpha}{\sin\frac{\alpha}{2}} + \ldots + m_{n-1}\frac{\sin\frac{3\alpha}{2}}{\sin\frac{\alpha}{2}} + m_n = 0 \qquad (18)$$

which has roots $\cos\alpha_1, \cos\alpha_2, \ldots, \cos\alpha_n$.

We now show that

$k_i = m_i \qquad i = 1,2,\ldots,N$ when $N \leq n$

and $k_i = m_i \qquad i = 1,2,\ldots,n$

with $k_i = 0 = m_i$ for $i = 2n-N+1, 2n-N+2, \ldots, n$

when $N \in \{n+1, n+2, \ldots, 2n\}$

We consider the complex variable

$$z = \cos\frac{\theta}{2} + i\sin\frac{\theta}{2}$$

so that

$$z^r + z^{-r} = 2\cos\frac{r\theta}{2} \qquad \text{for all } r \in \mathbb{N}.$$

Substituting for $\cos r\theta/2$ in (17) gives

$$\frac{1}{z^{2n}}\left[\frac{z^{4n+2}+1}{z^2+1} + k_1 z^2\frac{z^{4n-2}+1}{z^2+1} + \ldots + k_{n-1}z^{2n-2}\frac{z^6+1}{z^2+1} + k_n z^{2n}\right] = 0 \qquad (19)$$

It can be seen that the equation

$$z^{4n+2} + k_1 z^{4n} + \ldots + k_n z^{2n+2} + k_n z^{2n} + \ldots + k_1 z^2 + 1 = 0 \qquad (20)$$

has the same roots as (19), together with two additional roots at $z^2=-1$. Writing $\omega = z^2$, (20) becomes

$$(21) \quad \omega^{2n+1} + k_1\omega^{2n} + \ldots + k_n\omega^{n+1} + k_n\omega^n + \ldots + k_1\omega + 1 = 0.$$

Hence, the 2n+1 roots of this equation are

$$\omega_{2i-1} = \cos\theta_i + i\sin\theta_i, \quad \omega_{2i} = \cos\theta_i - i\sin\theta_i, \qquad (i = 1,2,\ldots,n)$$

$$\omega_{2n+1} = -1$$

where the $\cos\theta_i$ are the n roots of (17). It follows that the $\cos\theta_i$ are related to the roots ω_i of (21) by

$$2\sum_{i=1}^{n}\cos r\theta_i = \sum_{i=1}^{2n}\omega_i^r = \left[\sum_{i=1}^{2n+1}\omega_i^r\right] + 1 \qquad \text{when } r = 1,3,5,\ldots.$$

(22)

$$2\sum_{i=1}^{n}\cos r\theta_i = \sum_{i=1}^{2n}\omega_i^r = \left[\sum_{i=1}^{2n+1}\omega_i^r\right] - 1 \qquad \text{when } r = 2,4,6,\ldots.$$

Similarly, by considering the complex variables

$$z = \cos\frac{\alpha}{2} + i\sin\frac{\alpha}{2}$$

and $$\omega = z^2$$

it can be shown that the 2n+1 roots of the equation

$$(23) \quad \omega^{2n+1} + m_1\omega^{2n} + \ldots + m_n\omega^{n+1} - m_n\omega^{n} - \ldots - m_1\omega - 1 = 0$$

are $$\omega_{2i-1} = \cos\alpha_i + i\sin\alpha_i, \quad \omega_{2i} = \cos\alpha_i - i\sin\alpha_i,$$

and $$\omega_{2n+1} = 1, \qquad (i = 1,2,\ldots,n)$$

where the $\cos\alpha_i$ are the n roots of (18), so that these roots and

the 2n+1 roots of (23) are such that

$$(24)\quad 2\sum_{i=1}^{n}\cos r\alpha_i = \sum_{i=1}^{2n}\omega_i^r = \left[\sum_{i=1}^{2n+1}\omega_i^r\right] - 1 \qquad \text{for all } r \in \mathbb{N}$$

The relationships (16),(22) and (24) show that the first N coefficients of (21) and (23) must be equal.

Thus, $k_i = m_i$ for $i = 1,2,\ldots,N$ when $N \leq n$

and $k_i = m_i$ for $i = 1,2,\ldots,n$

with $k_i = 0 = m_i$ for $i = 2n-N+1, 2n-N+2, \ldots, n$

when $N \in \{n+1, n+2, \ldots, 2n\}$.

4. Solution Sets.

We have shown that the roots of equations (3) and (4), or (14) and (15), will satisfy equations (1). In each case the polynomial equations contain an 'unknown' m-N constants.

By assigning values, $b_1, b_2, \ldots, b_{m-N}$ say, to an arbitrary m-N of the x_s's, $y_1, y_2, \ldots, y_{m-N}$ say, and substituting these values into the appropriate equations (i.e. (3) or (14) if we wish to specify $x_{2i-1} = b_r$, (4) or (15) if we wish to specify $x_{2i} = b_s$), we obtain m-N linear equations which may be solved to find the values of the constants k_i, m_j in terms of the known values b_j. Thus, by examining the roots of these polynomial equations, it is possible to determine whether or not a solution set $\{x_s\}$, satisfying both equations (1) and the inequalities (2) can be found in which m-N of the x_s's take their assigned values. For certain combinations of y_i and b_j, solutions satisfying (2) cannot be found, and no solution set exists.

We now consider what restrictions must be placed on the b_i's to ensure that a solution set can be found for the case N = m-1.

Suppose that m = 2n-1 and N = m-1 = 2n-2 ($n \in \mathbb{N}$). Then equations (3) and (4) are

$$T_n(X) + k_1 T_{n-1}(X) = 0 \tag{25}$$

and

$$U_{n-1}(X) + k_1 U_{n-2}(X) = 0 \tag{26}$$

where k_1 is an arbitrary constant whose value is found by assigning a value to one of the x_s's. If x_{2i-1} is to take the value b, say, then

$$k_1 = - \frac{T_n(b)}{T_{n-1}(b)} ,$$

and if x_{2i} is to take the value b then

$$k_1 = - \frac{U_{n-1}(b)}{U_{n-2}(b)} .$$

We now look at the behaviour of the roots of equations (25) and (26) as k_1 varies. If $X = \cos\theta$, where $\theta \epsilon [0,\pi]$, satisfies equation (25), it can be shown that

$$\frac{dk_1}{d\theta} = \frac{1}{2} \sec^2(n-1)\theta \, [\, (2n-1) \sin\theta + \sin(2n-1)\theta \,]$$

so that

$$\frac{dk_1}{dX} = - \frac{1}{2} \sec^2(n-1)\theta \left[\, (2n-1) + \frac{\sin(2n-1)\theta}{\sin\theta} \, \right]$$

$$= - \frac{1}{2} \frac{\left[\, (2n-1) + U_{2n-2}(X) \, \right]}{\left[\, T_{n-1}(X) \, \right]^2}$$

It can be shown that

$$\frac{dk_1}{dX} < 0 \quad \text{for all } n \text{ and } X \epsilon [-1,1].$$

Hence, if $X = x_s$ is a solution of (25), then x_s decreases monotonically with k_1. Similarly, it can be shown that if $X = x_s$ is a solution of (26), then x_s decreases monotonically with k_1.

Thus, all roots $x_1, x_2, \ldots, x_{2n-1}$ decrease as k_1 increases. As we are seeking solutions which satisfy (2), we now consider the two limiting cases in which we specify either $x_1 = 1$ or $x_{2n-1} = -1$.

Suppose $x_1 = 1$ is a solution. Then $X = 1$ must be a root of (24), so that

$$T_n(1) + k_1 T_{n-1}(1) = 0$$

which implies $k_1 = -1$.

With $k_1 = -1$, the roots of (25) are given by

$$(27) \qquad \begin{aligned} x_1 &= 1 \\ x_{2s+1} &= \cos\left[\frac{2s\pi}{2n-1}\right] \qquad s = 1,2,\ldots,n-1 \end{aligned}$$

and the roots of (26) are

$$(28) \qquad x_{2s} = \cos\left[\frac{(2s-1)\pi}{2n-1}\right] \qquad s = 1,2,\ldots,n-1$$

and it can be seen that these are a solution set.

Now suppose that $x_{2n-1} = -1$ is a solution. Then $X = -1$ will be a root of (25) and

$$T_n(-1) + k_1 T_{n-1}(-1) = 0$$

which implies $k_1 = 1$.

With $k_1 = 1$, the roots of (25) are given by

$$(29) \qquad x_{2s-1} = \cos\left[\frac{(2s-1)\pi}{2n-1}\right] \qquad s = 1,2,\ldots,n$$

and the roots of (26) are

$$(30) \qquad x_{2s} = \cos\left[\frac{2s\pi}{2n-1}\right] \qquad s = 1,2,\ldots,n-1.$$

and these again are a solution set.

Hence, as all roots decrease monotonically with k_1, it follows that $k_1 \epsilon [-1,1]$ for all roots to lie in the interval $[-1,1]$, and furthermore it can be seen from (27)-(30), that for any k_1 lying in this interval,

$$(31) \qquad \cos\left[\frac{s\pi}{m}\right] \leq x_s \leq \cos\left[\frac{(s-1)\pi}{m}\right]$$

for all $s = 1,2,\ldots,m$, and a solution set exists. Figure 2 illustrates the behaviour of the x_s for $m = 5$ and $N = 4$.

Thus, if we specify $x_s = b$, a solution set will exist if and only if

$$\cos\left[\frac{s\pi}{m}\right] \leqslant b \leqslant \cos\left[\frac{(s-1)\pi}{m}\right] . \tag{32}$$

Similarly, when $m = 2n$, it can be shown that all roots $x_1, \ldots, x_{2n}$ decrease monotonically with k_1, solution sets exist if and only if $k_1 \epsilon [-1,1]$, and that (31) and (32) hold in this case too.

Acknowledgements.

We would like to thank Steve Blythe and Gordon Donaldson for their contributions to this work, and Peter Maas and Roger Nisbet for comments on earlier drafts of this paper. We wish to register our gratitude to the Department of Applied Physics where the spirit of interdisciplinary co-operation made this work possible.

Appendix : Properties of the polynomials R_n and Q_n.

1. The polynomials R_n are orthogonal on the interval [-1,1] with respect to the weight function

$$w_R(X) = \left[\frac{1 + X}{1 - X} \right]^{\frac{1}{2}}$$

with

$$\int_{-1}^{1} w_R(X)\, R_m(X)\, R_n(X)\, dX = \begin{cases} \pi & \text{if } m = n \\ 0 & \text{if } m \neq n. \end{cases}$$

The polynomials Q_n are orthogonal on [-1,1] with respect to the weight function

$$w_Q(X) = \left[\frac{1 - X}{1 + X} \right]^{\frac{1}{2}}$$

with

$$\int_{-1}^{1} w_Q(X)\, Q_m(X)\, Q_n(X)\, dX = \begin{cases} \pi & \text{if } m = n \\ 0 & \text{if } m \neq n. \end{cases}$$

2. R_n and Q_n satisfy the recurrence relationships

$$R_{n+1}(X) = 2X\, R_n(X) - R_{n-1}(X) \qquad n = 1,2,3...$$

$$Q_{n+1}(X) = 2X\, Q_n(X) - Q_{n-1}(X) \qquad n = 1,2,3...$$

with $R_0(X) = 1$, $R_1(X) = 2X - 1$,
$Q_0(X) = 1$, $Q_1(X) = 2X + 1$.

3. R_n and Q_n satisfy the differential equations

$$(1 - X^2)\, R_n''(X) + (1 - 2X)\, R_n'(X) + n(n+1) R_n(X) = 0$$

$$(1 - X^2)\, Q_n''(X) - (1 + 2X)\, Q_n'(X) + n(n+1) Q_n(X) = 0.$$

4. R_n and Q_n are given explicitly by

$$R_n(X) = \sum_{m=0}^{n} (-1)^{n-m}\, 2^m\, \frac{2n+1}{2m+1}\, {}^{n+m}C_{n-m}\, (1+X)^m$$

$$Q_n(X) = \sum_{m=0}^{n} (-1)^{n-m}\, 2^m\, {}^{n+m}C_{n-m}\, (1+X)^m .$$

5. R_n and Q_n are related to the Chebyshev polynomials by

$$X\, R_n(2X^2-1) = T_{2n+1}(X)$$

$$Q_n(2X^2-1) = U_{2n}(X)$$

and it can be seen that

$$R_n(\cos\theta) = \frac{T_{2n+1}\left[\cos\frac{\theta}{2}\right]}{\cos\frac{\theta}{2}} = \frac{\cos\left[n+\frac{1}{2}\right]\theta}{\cos\frac{\theta}{2}}$$

$$Q_n(\cos\theta) = U_{2n}\left[\cos\frac{\theta}{2}\right] = \frac{\sin\left[n+\frac{1}{2}\right]\theta}{\sin\frac{\theta}{2}} .$$

6. R_n and Q_n are related to the Jacobi polynomials

$$P_n^{(-\frac{1}{2},\frac{1}{2})}(X) \quad \text{and} \quad P_n^{(\frac{1}{2},-\frac{1}{2})}(X)$$

by

$${}^{2n}C_n\; R_n(X) = 2^{2n}\; P_n^{(-\frac{1}{2},\frac{1}{2})}(X)$$

$${}^{2n}C_n\; Q_n(X) = 2^{2n}\; P_n^{(\frac{1}{2},-\frac{1}{2})}(X).$$

References

[1] Abramowitz,M.; Stegum,J.A.: Handbook of Mathematical Functions. New York: Dover Publications 1965 (Chapter 22).

[2] Bain,R.J.P.;Jones,A.E.;Donaldson,G.B.: Design of High-order Superconducting Planar Gradiometers with Shaped Asymmetric Near-source Response. Submitted to IEEE Transactions on Magnetics.

[3] Donaldson,G.B.;Bain,R.J.P.: An Improved Design of High Order Superconducting Gradiometer Coils for Magnetic Monopole Detection. Applied Physics Letters 45 (1984) 990-992.

[4] Donaldson,G.B.;Pegrum,C.M.;Bain,R.J.P.: Integrated Thin Film SQUID Instruments. In: SQUID '85 - Superconducting Quantum Interference Devices and their Applications.: Editors Hahlbohm,H.D.;Lubbig,H. Berlin: W.de Gruyter and Co. 1985.

[5] Durell,C.V.;Robson,A.: Advanced Algebra Vol. 2. London: G.Bell and Sons 1958;p302-303.

[6] Tesche,C.D.: The IBM Monopole Experiments. In: Fourth Workshop on Grand Unification. Editors: Weldon,H.A.; Langacker,P.;Steinhardt,P.J. New York: Birkhauser 1983.

Fig.1: Example of a planar gradiometer geometry. Insulated crossovers exist at x_1 and x_2 ; thus the only continuous current-carrying path is ABGFCDEFCBGHA. The structure is fabricated with wires or thin-film metal tracks, and any electric current induced by magnetic flux is monitored.

Fig.2: x_s as a function of k_1 for an m = 5, N = 4 gradiometer.

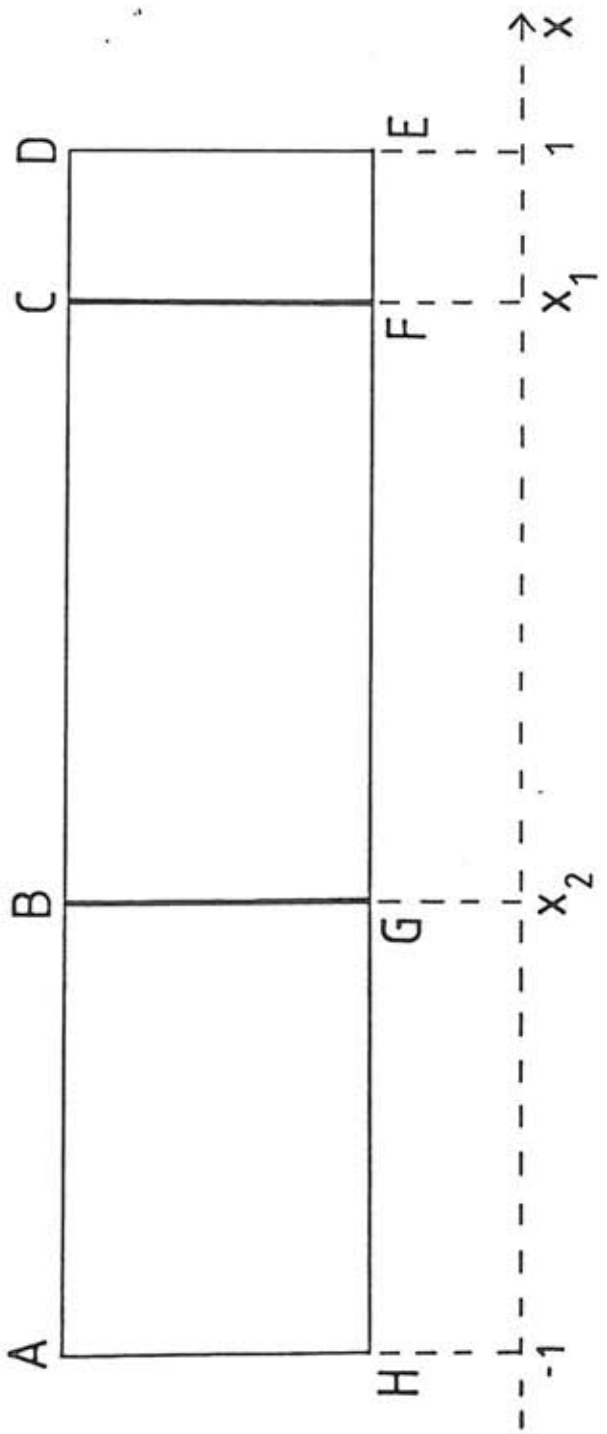

Figure 1.

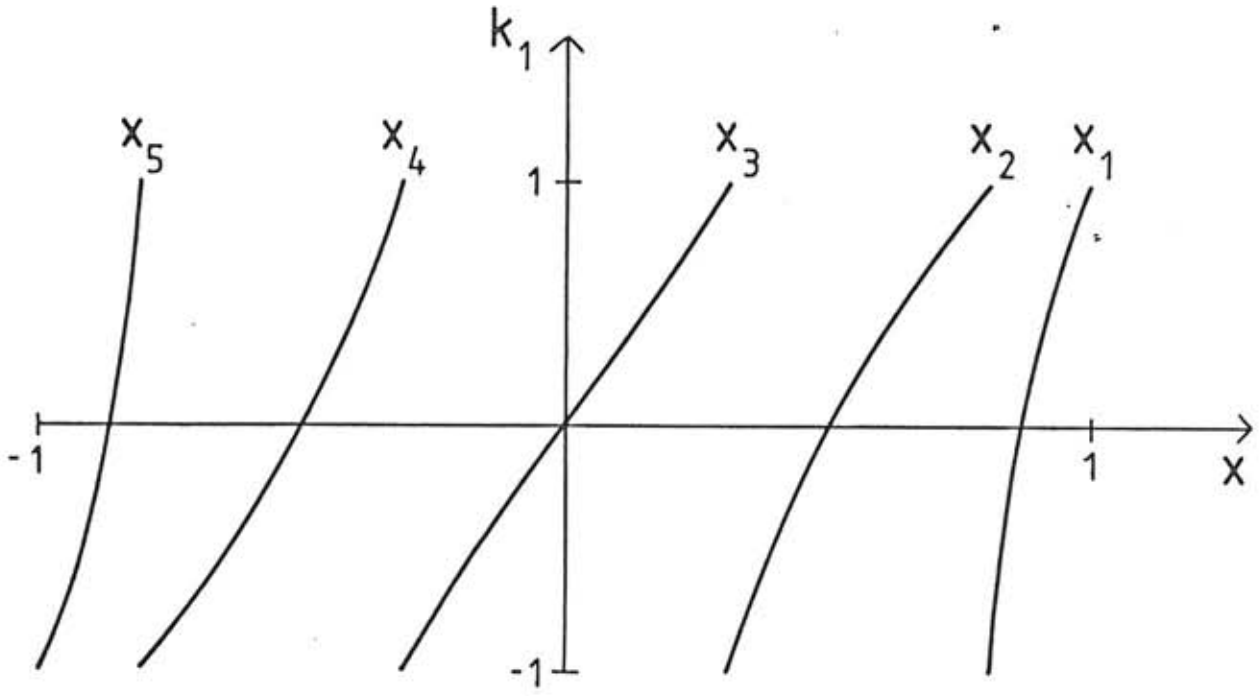

Figure 2

DESIGN OF HIGH-ORDER SUPERCONDUCTING PLANAR GRADIOMETERS WITH SHAPED ASYMMETRIC NEAR-SOURCE RESPONSE

R.J.P. Bain, A.E. Jones and G.B. Donaldson
Department of Physics and Applied Physics
University of Strathclyde
Glasgow G4 ONG, Scotland.

Abstract

We describe the solution of the general problem of designing an N-th order planar gradiometer with m > N crossovers, where the position of (m-N) of these crossovers is selected on near-source response criteria. The ability to pre-select certain crossover positions is valuable in many applications (e.g. biomedical, NDT) because it allows us to control specific properties of the near-source response such as (i) response peaking at specified locations (ii) zero-response at certain locations (iii) minimal coupling to near-sources, at each end of a gradiometer of arbitrary order. Examples are given for the important cases m = N+1 and m = N+2.

Introduction

In recent years there has been growing interest in thin-film planar gradiometers, often integrated with thin-film d-c SQUIDs[1]. In comparison with the more traditional wire-wound gradiometer designs, they offer the possibility of high-volume low-cost manufacture in a state of repeatedly high intrinsic balance, making them especially suitable for multi-gradiometer arrays for magnetic-field mapping. A significant limitation in current planar gradiometer designs is that the geometry of any given type is uniquely determined by the gradiometer order chosen. This means one has little flexibility in selecting the detailed near-source response to match the application; for example if the gradiometer is to be used to detect sources located near one end of it, one might wish to couple maximum flux from sources near that end and simultaneously couple minimum flux from interference sources at the other end.

Karp and Duret[2] demonstrated that wirewound gradiometers of first and second order could be designed to have "unidirectional" responses by suitable choice of the turns-area product and position of the gradiometer coils. Their approach cannot be simply applied to planar gradiometers, however.

In this paper we show how the modifications in geometry necessary to control external response may be accommodated in a planar gradiometer of arbitrary order.

Design Procedure

We consider a geometry of the form illustrated in Fig. 1 consisting of a series of (m+1) adjacent rectangular pickup loops, wired in series with an insulated crossover between each pair of loops. Current due to any net flux threading the structure is monitored by a SQUID (not shown). We use the usual [3] approach that a N-th order gradiometer is defined as one coupling zero net flux from all components of a Taylor expansion of magnetic field about the

Manuscript received 30 September, 1986.

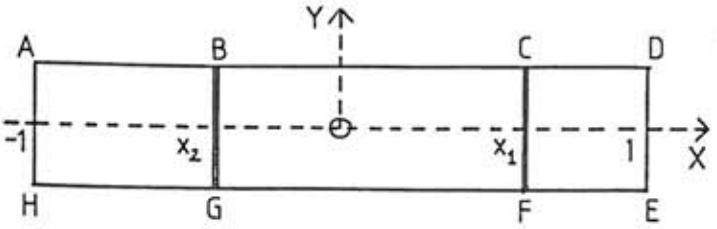

Figure 1. Example of a planar gradiometer geometry. Insulated crossovers exist at x_1 and x_2; thus the only continuous current-carrying path is ABGFCDEFCBGHA.

gradiometer, up to and including terms of the form $\partial^{N-1}B_z/\partial x^{N-1}$. Then to form a N-th order gradiometer, the crossover positions x_s, s = 1,2,...m must satisfy the following N equations in m unknowns,

$$x_1 - x_2 + x_3 - \ldots\ldots - (-1)^m x_m = \tfrac{1}{2}\,(1+(-1)^m)$$

$$x_1^2 - x_2^2 + x_3^2 - \ldots\ldots - (-1)^m x_m^2 = \tfrac{1}{2}\,(1+(-1)^{m+1}) \qquad (1)$$

$$x_1^N - x_2^N + x_3^N - \ldots\ldots - (-1)^m x_m^N = \tfrac{1}{2}\,(1+(-1)^{m+N-1})$$

where $N \leq m$ and

$$-1 \leq x_m < x_{m-1} < \ldots\ldots < x_2 < x_1 \leq 1 \qquad (2)$$

We define a solution set $\{x_s\}$ to be a set of values $x_1, x_2, \ldots, x_m$ which satisfy both equations (1) and the inequalities (2). It can be shown[3,4] that in the case N=m the unique solution of equations (1) is a solution set and is given by

$$\{\, x_s = \cos\,[s\pi/(N+1)]\,\}$$

To adjust the gradiometer external response we choose positions for (m-N) of the crossovers and solve (1) to obtain the remaining N crossover positions (assuming the resultant x_s's also satisfy (2)). While it is possible to solve (1) algebraically for low order gradiometers, the problem rapidly becomes algebraically intractable as N rises. The problem could be tackled by numerical iteration procedures but again becomes increasingly expensive in computation time as N rises.

We now describe how the problem of obtaining solutions to (1) may be reduced to the trivial one of obtaining the roots of two polynomial equations. The polynomials have different forms for an even (m=2n) or odd (m=2n-1) number of crossovers; we will treat

these separately. A proof of the following results will be published elsewhere[5].

Solutions for m=2n-1

We separate the crossover positions x_s into even- and odd- indexed groups. We write the n-th order polynomial equation having roots $x_1, x_3, \ldots, x_{2n-1}$ as

$$T_n(X)+k_1T_{n-1}(X)+\ldots\ldots+k_{n-1}T_1(X)+k_n = 0 \qquad (3)$$

and the (n-1)-th order equation having roots $x_2, x_4, \ldots, x_{2n-2}$ as

$$U_{n-1}(X)+m_1U_{n-2}(X)+\ldots\ldots+m_{n-2}U_1(X)+m_{n-1} = 0 \qquad (4)$$

where $T_1, T_2 \ldots T_n$ are Chebyshev polynomials of the first kind, $U_1, U_2 \ldots\ldots U_{n-1}$ are Chebyshev polynomials of the second kind[6] and k_i and m_j are coefficients to be determined.

We have shown[5] that if $x_1, x_2, \ldots\ldots, x_{2n-1}$ are to satisfy (1), then the coefficients k_i and m_j must be such that

$$k_i = m_i \quad \text{for all } i = 1,2,\ldots\ldots,\min(n-1,N) \qquad (5)$$

$$\text{with } k_i = 0 \quad \text{for } i = 2n-N,\ 2n-N+1,\ldots\ldots,n \qquad (6)$$

when $n \leq N \leq 2n-1$.

Solutions for m = 2n

We again separate the crossover positions x_s into even and odd-indexed groups. We write the equation with roots $x_1, x_3, \ldots\ldots x_{2n-1}$ as

$$R_n(X)+k_1R_{n-1}(X)+\ldots\ldots+k_{n-1}R_1(X)+k_n = 0 \qquad (7)$$

and the equation with roots $x_1, x_3, \ldots x_{2n}$ as

$$Q_n(X)+m_1Q_{n-1}(X)+\ldots\ldots\ldots+m_{n-1}Q_1(X)+m_n = 0 \qquad (8)$$

In this case $R_1, R_2 \ldots\ldots, R_n$ and $Q_1, Q_2 \ldots\ldots, Q_n$ are two families of orthogonal polynomials (R_n and Q_n are of degree n). We describe their full properties elsewhere[5]; for present purposes their essential features are that they follow the same recursion formulae as the Chebyshev polynomials, i.e.

$$R_{n+1}(X) = 2X\,R_n(X) - R_{n-1}(X)$$

$$Q_{n+1}(X) = 2X\,Q_n(X) - Q_{n-1}(X)$$

but with $R_o(X) = 1$, $R_1(X) = 2X-1$

and $Q_o(X) = 1$, $Q_1(X) = 2X+1$

As before the k_i and m_j are coefficients to be determined.

We have shown[5] that if $x_1, x_2, \ldots, x_{2n}$ are to satisfy (1), then the coefficients k_i and m_j must be such that

$$k_i = m_i \quad \text{for all } i = 1,2,\ldots,\min(n,N) \qquad (9)$$

$$\text{with } k_i = 0 \quad \text{for } i = 2n-N+1, 2n-N+2, \ldots, n \qquad (10)$$

when $n+1 \leq N \leq 2n$.

Solutions in specific cases

The roots of equations (3) and (4) for an odd number of crossovers, or (7) and (8) for an even number, will always satisfy equations (1) and provided they may be arranged in such a way that they also satisfy the inequalities (2), will form a solution set. In either case, as a result of equations (5), (6), or (9), (10), we have a pair of polynomial equations with (m-N) independent coefficients to be evaluated. These coefficients are simply determined; (m-N) "fixed" crossover positions are chosen on near-source response (or other) criteria and inserted into the equations appropriate to their index number. The resulting (m-N) linear equations are then solved to obtain the required coefficients. The complete solution is then simply the roots of the resulting polynomials, easily determined to arbitrary precision by (in our case) a Newton-Raphson algorithm. Provided the inequalities (2) are satisfied, the gradiometer is physically realisable in the form of Fig. 1.

For near-source response shaping, one would normally choose to "fix" the crossovers at one or both ends of the gradiometer. Since the gradiometer inductance, which we normally wish to minimise, scales approximately with m for a given gradiometer area[3], we would normally choose m = N+1 with x_1 "fixed" or m = N+2 with x_1 and x_m fixed, depending on whether response must be controlled at one or both ends of the gradiometer.

Example 1: N even, m = N+1. Setting m = 2n-1, equations (3) and (4) become

$$T_n(X) + k_1\,T_{n-1}(X) = 0 \qquad (11)$$

and $$U_{n-1}(X) + k_1\,U_{n-1}(X) = 0 \qquad (12)$$

Choosing $x_1 = b$, say, sets the value of k_1 :-

$$k_1 = -\frac{T_n(b)}{T_{n-1}(b)}$$

and it may be shown[5] that provided b is such that

$$\cos\left[\frac{\pi}{N+1}\right] \leq b \leq 1$$

then the roots of equations (11) and (12) form a solution set.

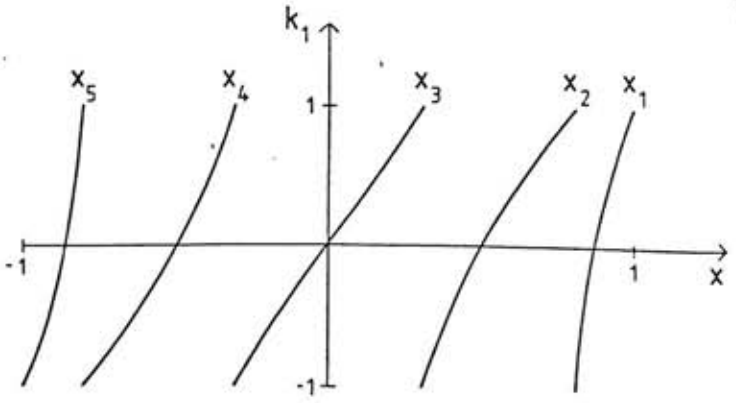

Figure 2. Position of crossovers x_s as a function of k_1.

Fig. 2 illustrates how the crossover positions x_s vary as a function of k_1 for an N = 4, m = 5 gradiometer. Selecting one of the x_s positions (normally, though not necessarily, x_1) determines k_1 and thus the other 4 crossover positions. Note that $k_1 = 0$ gives the optimal 5-th order design (N = 5, m = 5), while $k_1 = \pm 1$ effectively gives the optimal 4-th order design.

Example 2: N even, m = N+2. Setting m = 2n, equations (7) and (8) become

$$R_n(X) + k_1 R_{n-1}(X) + k_2 R_{n-2}(X) = 0 \qquad (13)$$

and

$$Q_n(X) + k_1 Q_{n-1}(X) + k_2 Q_{n-2}(X) = 0 \qquad (14)$$

Choosing $x_1 = b$ and $x_m = c$, say, then we obtain k_1 and k_2 from the equations

$$R_n(b) + k_1 R_{n-1}(b) + k_2 R_{n-2}(b) = 0$$

$$Q_n(c) + k_1 Q_{n-1}(c) + k_2 Q_{n-2}(c) = 0$$

and it may be shown that provided b and c are such that

$$\cos\left[\frac{\pi}{N+1}\right] \leq b \leq 1 , \qquad -1 \leq c \leq \cos\left[\frac{N\pi}{N+1}\right] ,$$

then the roots of equations (13) and (14) will form a solution set.

Gradiometer Response Curves

We illustrate some of the near-source response curves obtainable by an example. The coordinate system and units of length are as indicated by Fig. 1. For clarity we restrict our attention to a magnetic dipole source, with moment directed along the z-axis, positioned along the x-axis. The example is a 4-th order gradiometer with 6 crossovers; we have selected $x_1 = 0.94$ and $x_6 = -0.99$, and calculated the required positions x_s, s = 2,3,4,5 of the other crossovers by the method described above. The gradiometer width in the y-direction is 1 unit.

Figs. 3a and 4a (solid lines) show the responses to a magnetic dipole at either end of the gradiometer. Fig. 3b (dotted line) is the response to an optimal 4-th order (N = 4, m = 4) gradiometer while Fig. 4b is the response to an optimal 6-th order (N = 6, m = 6) gradiometer. "Response" in these Figs. is proportional to the net gradiometer flux; the exact signal detected by a coupled SQUID would depend on both the gradiometer inductance (approximately proportional to m) and the SQUID inductance, as well as the dipole strength.

The following general features are noteworthy:

(a) the sharp negative peak in respnose near $x \approx -1.03$ in Fig. 3a. The position (and existence) of this peak may be adjusted by suitable crossover positioning; thus at the other end of the gradiometer (Fig. 4a) we have a much smaller, broader negative peak at $x \approx 1.30$,

(b) the existence of zero-response "dead" points in the response at $x \approx -1.02$ (Fig. 3a) and $x \approx 1.24$ (Fig. 4a); the exact locations can obviously be varied as for the peaks. These locations are "dead" to dipoles of any orientation; such "dead" points do not generally exist out of the gradiometer (x-y) plane,

(c) comparing Figs. 4a and 4b, we note that while the far-field response of the optimal N = 6 gradiometer will clearly fall off much faster than that of Fig. 4a (as x^{-9} for Fig. 4b but as x^{-7} for Fig. 4a), the near-source resonse is significantly smaller.

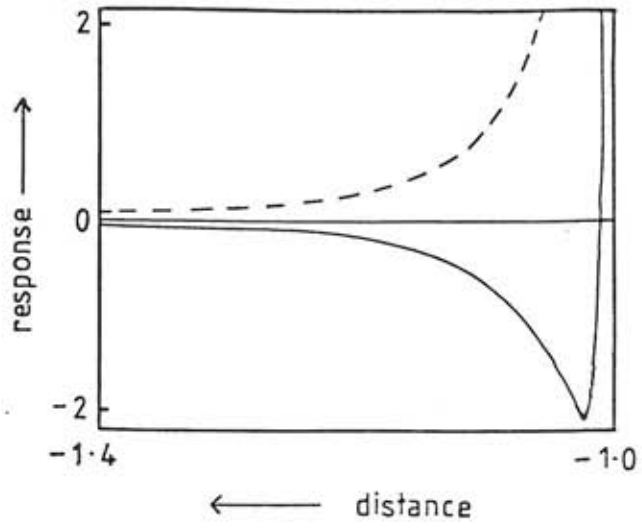

Figure 3. Gradiometer response (see text) versus magnetic dipole distance from the gradiometer centre for
(a) (solid line) a N = 4, m = 6 design
(b) (dashed line) a N = 4, m = 4 design.

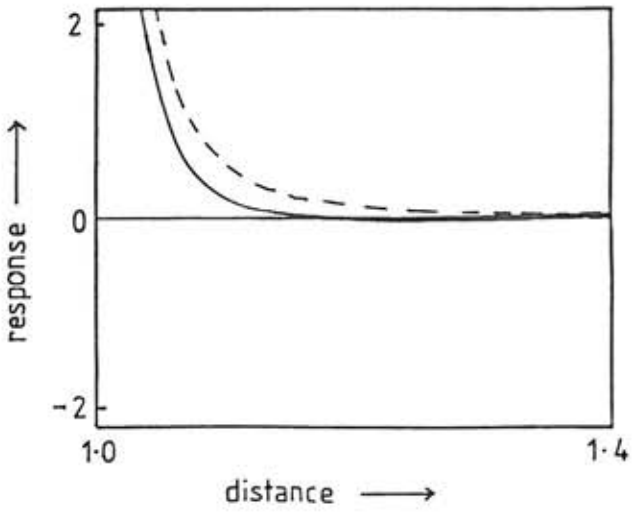

Figure 4. Gradiometer response (see text) versus magnetic dipole distance from the gradiometer centre for
(a) (solid line) a N = 4, m = 6 design, as in Fig. 3a but from the opposite end of the gradiometer
(b) (dashed line) a N = 6, m = 6 design.

We emphasise that Figs. 3 and 4 are simply representative of these features, and not optimised by any one. For specific features in a design, we first make a rough calculation of response based only on the chosen crossovers nearest the gradiometer boundary, (i.e. x_1 and x_m) then iterate through the design procedure/response calculation.

We also note that while the above example covers only the response to magnetic dipoles in the gradiometer plane, a similar procedure may be followed for current-dipole sources and for out-of-plane sources.

Applications

Modification of near-source resonse may be useful in the following experimental situations:-

(a) The negative peak in response may be used to determine the location of a given source such as a magnetic-dipole or current-dipole source, relative to the gradiometer. Distance of the peak from the gradiometer is widely adjustable although at the expense of sensitivity.

(b) Small magnetic-dipole interference sources which necessarily must be placed in close proximity to the gradiometer may be placed at the zero-reponse "dead" points of the gradiometer. Such sources might include superconducting components (for example SQUIDs) which distort the environmental magnetic field.

(c) The effect of extended magnetic interference sources near the gradiometer may be minimised by designing for a rapid fall in near-source response with distance. This situation arises for example in magnetic monopole detection where the necessary magnetic shielding may itself be a significant interference source[3]. It is noteworthy from Fig. 4 that an N = 4, m = 6 design has a superior performance to an "optimal" N = 6, m = 6 design from this point of view.

Conclusions

We have described in detail an important simplification of the design procedure for asymmetric planar gradiometers and illustrated some of the useful features of such gradiometers. Current work includes fabrication of prototypes and more detailed investigation of responses to sources out of the gradiometer plane.

References

1. G.B. Donaldson, C.M. Pegrum and R.J.P. Bain "Integrated thin film SQUID instruments", SQUID '85 - Superconducting Quantum Interference Devices and their Applications, p. 729-759, Ed. H.D. Hahlbohm and H. Lubbig, W. de Gruyter, Berlin, 1985.

2. P, Karp and D. Duret, "Unidirectional magnetic gradiometers", J. Appl. Phys., 51, 1267-1272, 1980.

3. G.B. Donaldson and R.J.P. Bain, "An improved design of high order superconducting gradiometer coils for magnetic monopole detection", Appl. Phys. Letts. 45, 990-992.

4. C.D. Tesche in Fourth Workshop on Grand Unification, p. 121, Ed. H.A. Weldon, P. Langscker and P.J. Steinhardt, Birkhauser, 1983.

5. A.E. Jones and R.J.P. Bain, "Solution of a problem in magnetic gradiometry in terms of orthogonal polynomials". Submitted to Mathematical Methods in the Applied Sciences.

6. M. Abramowitz and J.A. Stegun, Chapter 22 in "Handbook of Mathematical Functions", Dover Publications, New York, 1965.

REFERENCES

ADLER, V.E. 1960. Effects of low temperature on eggs of the Angoumois grain moth, the Indian meal moth, and the confused flow beetle. J. Econ. Ent. 53, 973-4.

BAKKER, K. 1961. An analysis of factors which determine success in competition for food larvae of Drosophila melanogaster Archs neerl. Zool. 14. 200-281.

BEDDINGTON, J.R., HASSELL, M.P., and LAWTON, J.H., 1976. The components of arthropod predation II. The predator rate of increase. J. Anim. Ecol. 45, 115-185.

BELLMAN, R. and COOKE, K.L. 1963. Differential-Difference Equations, Academic Press, New York.

BENSON, J.F. 1973. The biology of Lepidoptera infesting stored products, with special reference to population dynamics. Biol. Rev. 4. 1-26.

BLYTHE, S.P., NISBET, R.M. and GURNEY, W.S.C. 1984. The dynamics of population models with distributed maturation period. Th. Pop. Biol. 25, 289-311.

BORROR, D.J. and DE LONG, D. 1954. An Introduction to the study of insects Holt Reinhart. Chapter 3.

BUSENBERG, S. and COOKE, K.L. 1980. The effect of integral conditions in certain equations modelling epidemics and population growth. J. Math. Biol. 10, 13-32.

CHITTENDEN, F.H. 1894. The more important insects injurious to stored grain. Yearbook of the USDA 277-94.

CLINE, L.D. 1970. Indian meal moth egg hatch and subsequent larval survival after short exposures to low temperature. J. Econ. Ent. 63, 1081-3.

COOKE, K.L. and GROSSMAN, Z. 1982. Discrete delay, distributed delay and stability switches. J. Math. Anal. and Applic. 86, 592-627.

COOKE, K.L. and van den DRIESSCHE, P. 1986. On zeros of some transcendental equations. Funkcialaj Ekvacioj. In press.

CROWLEY, P.H., NISBET, R.M., GURNEY, W.S.C. and LAWTON, J.H. Population Regulation in animals with complex life-histories: formulation and analysis of a damselfly model. Adv. Ecol. Res. to appear 1987.

CUSHING, J.M. 1977. Integrodifferential equations and delay models in population dynamics. Springer-Verlag, New York.

DARWIN, C. 1859. The origin of species by means of natural selection. Reprinted by The Modern Library, Random House, New York, Chapter 3.

GURNEY, W.S.C., NISBET, R.M. and LAWTON, J.H. 1983. The systematic formulation of tractable single-species population models incorporating age structure. J. Anim. Ecol. 52, 479-495.

GURNEY, W.S.C. and NISBET, R.M. 1985. Fluctuation periodicity, generation separation, and the expression of larval competition. Theo. Pop. Biol.

GURNEY, W.S.C., NISBET, R.M. and BLYTHE, S.P. 1986. The systematic formulation of models in stage-structured populations in 'The dynamics of physiologically structured populations' (O. Diekmann. Ed.) Springer-Verlag.

HASSELL, M.P., LAWTON, J.H. and BEDDINGTON, J.R. 1977. Sigmoid functional responses by invertebrate predators and parasitoids. J. Anim. Ecol. 46, 249-262.

HASSELL, M.P. 1978. The dynamics of arthropod predator-prey systems. Princeton, New Jersey: Princeton University Press.

HILDEBRAND, F.B. 1952. Methods of applied mathematics. Prentice-Hall, New Jersey.

HILL, G.F. 1959. An ecological study of the Indian meal-moth Plodia interpunctella (Hubner) with emphasis on diapause. J. Coun. Sci. Industr. Res. 1, 330.

HOLLING, C.S. 1959. Some characteristics of simple types of predation and parasitism. Can. Ent. 91, 385-398.

HOLLING, C.S. 1966. The functional response of invertebrate predators to prey density. Mem. Ent. Soc. Can. 48, 1-86.

MAAS, P., NISBET, R.M. and GURNEY, W.S.C. 1982. Solver, an adaptable program template for initial value problem solving. Applied Physics Industrial Consultants, University of Strathclyde, Glasgow.

MACDONALD, N. 1978. Time lags in biological models, Springer-Verlag (Lecture notes in Biomathematics, Vol. 27).

MAHAFFY, J.M. 1982. A test for stability of linear differential delay equations. Quart. App. Math. 40, 193-202.

MUKERJI, M.K. and GUPPY, J.C. 1970. A quantitative study of food consumptions and growth in Pseudaletia unipunctata (Lepidoptera: Noctuidae). Can. Ent. 102, 1179-88.

NICHOLSON, A.J. 1954. An outline of the dynamics of animal populations, Australian Journal of Zoology, 2, p9-65.

NISBET, R.M. and GURNEY, W.S.C. 1983. The systematic formulation of population models with dynamically varying instar duration. Theor. Pop. Biol., 23, 114-135.

NISBET, R.M. and GURNEY, W.S.C. 1986. The formulation of age-structure models in Biomathematics, Vol. 17, Mathematical Ecology (Hallam, T.G. and Levin, S.A. Eds.).

NISBET, R.M., BLYTHE, S.P., GURNEY, W.S.C. and METZ, J.A.J. 1985. Stage-structure models of populations with distinct growth and development processes. IMA Journal of mathematics Applied in Medicine & Biology, 2, 57-68.

PETERS, T.M. and BARBOSA, P. 1977. Influence of population density on size, fecundity and developmental rate of insects in culture. Ann. Rev. Entomol. 22, 431-50.

PODOLER, H. 1974. Effects of intraspecific competition in the Indian meal-moth (Plodia interpunctella, Hubner) (Lepidoptera: Phycitidae) on populations of the moth and its parasite Nemeritis canescens (Gravenhorst) (Hymenoptera: Ichneymonidae). J. Anim. Ecol. 43, 641-651.

REYES, A.V. 1969. Biology and host range of Plodia interpunctella, Hubner (Pyralididae: Lepidoptera). Phillipp. Entomol. 1, 301-11.

SNYMAN, A. 1949. The influence of population densities on the development and oriposition of Plodia interpunctella, Hubn. (Lepidoptera). J. Ent. Soc. Sth. Afr. 12, 137-71.

SOUTHWOOD, T.R.E. 1966. Ecological methods, with particular reference to the study of insect populations. Chapman and Hall, London, Chapter 11.

TZANAKAKIS, M.E. 1959. An ecological study of the Indian meal-moth Plodia interpunctella (Hubner) with emphasis on diapause. Hilgardia, 29, 205.

ULLYETT, G.C. 1933. The mass rearing of Microbracon brevicornis, Wesm. S.A. Jrnl. of Science, 30, 426-432.

ZACHER, F. 1939. Die Dorrobstmotte als Schadling in Lebensmittelhandel und Industrie Dtsch. Lebensmitt-Rdsch., 9. (Cited by Snyman 1949 and Williams 1964.)